UNIVERSITY OF CALIFORNIA
RIVERSIDE

The Influence of Landscape Position on Soil Respiration and Urban Microclimate

A Dissertation submitted in partial satisfaction
of the requirements for the degree of

Doctor of Philosophy

in

Ecology, Evolution & Organismal Biology

by

Steven M Crum

June 2017

Dissertation Committee:
Dr. G. Darrel Jenerette, Chairperson
Dr. Michael Allen
Dr. James Sickman

The Dissertation of Steven M Crum is approved:

_____

_____

_____

Committee Chairperson

University of California, Riverside

Acknowledgements

To start, I would like to thank my advisor, Darrel Jenerette, for his tireless support and encouragement for the past five years. I would like to extend my gratitude to members of my dissertation committee, Michael Allen and James Sickman, for their support and feedback on my research. Finally, for field help and consultation I would like to thank Lindy Allsman, Liyin Liang, Sheri Shiflett, Kyle Ricio, Holly Andrews, and Peter Ibsen.

The studies in this dissertation were supported by National Aeronautics and Space Administration through grant NNX12AQ02G and the US National Science Foundation through grant DEB-0919006. The text in Chapter 1 of this dissertation is a reprint of the work published in the Journal of Geophysical Research Biogeosciences, October 2016 (Crum, S.M; Liang, L.L.; Jenerette, G.D. 2016. Landscape position influences soil respiration variability and sensitivity to physiological drivers in mixed-use lands of Southern California, USA. Geophysical Research Biogeosciences, 121, doi:10.1002/2016JG003469). The co-authors Liyin L. Liang and G. Darrel Jenerette, listed in this publication aided in field work, analysis, and writing of this paper.

ABSTRACT OF THE DISSERTATION

The Influence of Landscape Position on Soil Respiration and Urban Microclimate

by

Steven M Crum

Doctor of Philosophy, Graduate Program in Ecology, Evolution & Organismal Biology
University of California, Riverside, June 2017
Dr. G. Darrel Jenerette, Chairperson

Linking variation in ecosystem functioning to landscape drivers has become an important research need for understanding ecosystem responses to global change. Due to extensive land use and land cover changes many regions have variable distributions of landscape drivers and ecosystem processes. Furthermore, changes in local- to regional-scale climate may impact ecosystem variation and sensitivity to physiological drivers. This dissertation investigates how contrasting scale-dependent drivers of soil temperature, moisture and substrate levels influence soil respiration (R_s), a key ecosystem process, using in-situ landscape surveys and experimental subsidies of water and labile carbon. Furthermore, to improve understanding of scale-dependent sources of variation of urban microclimate this dissertation investigates how land cover and vegetation influences local distributions of air temperature (T_a), land surface temperature (LST), and relative humidity (RH), using intensive and widely distributed networks of microclimate sensors. Finally, vital in estimates of urban warming, this dissertation examines the relationships between T_a and LST among common urban land covers.

I found R_s in intensively managed urban land uses has increased rates, decreased spatial variation, and decreased sensitivity to environmental conditions. Furthermore, among common urban land uses spatial variation in R_s was positively correlated with soil temperature, and negatively correlated with soil moisture and substrate. Landscape position, or land use and climate distributions, influenced R_s by altering both levels and R_s sensitivity of physiological drivers. Next, in my first microclimate study I found negative T_a and positive RH correlations with vegetation intensity. Vegetation cooling effects were greater in more arid climates and in the evening hours. Furthermore, increasing city-scale mean T_a was associated with higher spatial variation of T_a in coastal cities, and lower variation in more arid cities. In my final study I observed vertical height-dependent T_a-LST relationships associated with land cover composition. Furthermore, I observed decreased nighttime T_a-LST differences among land covers. These findings can help city planners identify potential heat risk reductions strategies associated with urban vegetation and land cover composition. Together, these systematic evaluations of landscape effects on R_s and microclimate provide a framework of understanding the effects of interactive global change drivers on urban ecosystem processes.

Table of Contents

List of Figures

List of Tables

Introduction

Metropolitan regions contain a mosaic of distinct land uses, and consequently have highly variable ecosystem functioning and structure (Kaye et al. 2005, Jenerette et al. 2006). Patterns in land use, land cover, and vegetation are directly linked to microenvironmental conditions and biogeochemical cycles (Kaye et al. 2005, Brazel et al. 2007, Tayyebi and Jenerette 2016). Additionally, changes in meso- and regional-scale climate can lead to large differences in ecosystem functioning and structure (Groffman et al. 2009). Identifying the different and interactive effects of landscape position, which includes land use and climate distributions, on urban ecosystems has become a pressing need for understanding responses to multiple global change drivers. In addressing these challenges, a multiple scale perspective is necessary. At fine scales, ecosystem functioning is regulated by organismal responses to microenvironmental conditions including temperature, moisture, and substrate levels (Xu and Qi 2001, Davidson et al. 2012). While at regional scales variation in land cover and mesoclimate may regulate ecosystem processes (Kaye et al. 2005, Chatterjee and Jenerette 2011, Zhang et al. 2012). Bridging fine- and regional-scale drivers of ecosystem functioning are needed to improve understanding of ecosystem responses to rapidly changing environmental conditions (Jenerette et al. 2006, Zhang et al. 2012). The objective of this dissertation is to explore the effects of interactive global change drivers on urban ecosystem processes of soil respiration (R_s) and vegetation cooling of urban microclimate.

R_s is an important process describing ecosystem functioning and is a critical component of the carbon cycle within ecosystems and globally (Canadell et al. 2000). R_s is an integrative variable of ecosystem metabolism, representing interactions between plant and microbial dynamics (Ryan and Law 2005). From an ecosystem or physiological scale, R_s is primarily regulated by soil temperature, moisture, and substrate levels. Temperature is a fundamental ecosystem property driving chemical, physical and biological processes (Davidson et al. 2006). However, R_s temperature sensitivity depends on enzymatic processes that are also regulated by soil moisture and substrate availability. At low levels, soil moisture regulates R_s directly by limiting biological activity or indirectly by limiting diffusion of substrates, while high soil moisture levels constrain R_s by limiting soil oxygen diffusion (Xu and Qi 2001, Davidson et al. 2012, Oikawa et al. 2014). Regional-scale patterns in land use and climate may also have direct influences on soil temperature, moisture, and substrate levels (Raich and Schlesinger 1992, Zhou et al. 2009). R_s in urban and agricultural systems is often decoupled with seasonal precipitation patterns and instead respond more to warming (Kaye et al. 2005). In contrast, arid and semi-arid wildland ecosystems experience R_s pulses several orders of magnitude higher than baseline levels following precipitation (Jarvis et al. 2007, Sponseller 2007). While much effort has been directed towards understanding physiological regulation of R_s (e.g. Davidson et al. 2006, Oikawa et al. 2014), landscape heterogeneity in R_s dynamics is noted as a major uncertainty (Koerner and Klopatek 2009, Riveros-Iregui et al. 2012, Zhang et al. 2012, Du et al. 2015).

Landscape heterogeneity in urban land cover and vegetation distributions is also directly linked to patterns in air temperature (T_a), land surface temperature (LST), and relative humidity (RH, Brazel et al. 2007, Jenerette et al. 2016, Hall et al. 2016). Since the mid-20th century, large cities in the United States are warming twice as fast as surrounding rural areas (Stone et al. 2012), especially in the southwestern United States (Brazel et al. 2000). Urban warming is created by increasing impervious surfaces and decreasing vegetation cover, which warms temperatures in the urban core (Oke 1973, Santamouris 2015). Regionally, the magnitude of vegetation cooling is influenced by patterns in climate, where, particularly in dryland regions, urbanization may increase vegetation intensity compared to rural and wildland areas. However, locally the distribution of urban vegetation and built surfaces may magnify temperature inequities within a city, resulting in unequal vegetation cooling benefits and health consequences for residents (Jenerette et al. 2016). Potentially offsetting cooling benefits, increases in RH associated with highly-vegetated residential areas of arid and semi-arid regions may increase human-perceived temperatures (Steadman 1979, Hall et al. 2016). Vegetation moderation of microclimate may also depend on mesoclimate and meteorological conditions (Zhao et al. 2014). Mesoclimates, or city-scale climates, with relatively high mean daily temperatures may enhance vegetation cooling by increasing the effects of shading and potential transpiration rates (Jenerette et al. 2016, Tayyebi and Jenerette 2016, Ramamurthy and Bou-Zeid 2017). The negative feedback of vegetation cooling may result in greater T_a spatial variation in cities with warmer climates. Countering mean temperature effects within cities, wind and precipitation may reduce the negative

feedback of vegetation cooling due to increases in air convection and reductions in surface heating (Imhoff 2010, Zhao et al. 2014, Chow et al. 2014). Characterizing how vegetated and built land covers influence microclimate—including T_a, LST, and RH—and their interrelationships is an important research challenge for reducing and predicting the impacts of urban warming.

To improve understanding of scale-dependent sources of variation and sensitivity of R_s, in chapter 1 I evaluate the roles of soil temperature, moisture, and substrate levels in three land use types and at three climate positions along the coastal to desert gradient in southern California, USA. I find, from a combination of surveys and manipulative experiments, that interactive physiological, landscape, and seasonal factors are drivers of R_s. Furthermore, at the interface between landscape and physiological regulation of R_s, I find regional-scale coordination between physiological drivers and meter-scale spatial variability in R_s. This evaluation of physiological and landscape level effects on R_s expands understanding of the impacts of interactive global change drivers on urban ecosystem processes.

To improve understanding of the sources of variation in urban microclimate, for chapter 2 I evaluated the roles of vegetation, mesoclimate, and meteorology on spatiotemporal patterns of summertime T_a and RH. I found, using a widely distributed observational network of T_a and RH sensors across a coastal to desert climate gradient, increasing local-scale cooling effects positively correlated with levels of vegetation intensity. Furthermore, I observed increased spatial variation with increasing mean city-wide temperature in coastal cities, however, there was a gradient toward decreased

variation with increased mean temperature across the gradient, likely the result of patterns in wind velocity. Expanding upon this question, for chapter 3 I evaluated the importance of land cover in shaping microscale spatial distributions of T_a, LST, and RH and their interactions. Through the use of thermal imagery and micrometeorological measures I find land cover specific T_a-LST relationships that may help improve estimates of urban T_a using LST, important in predicting atmospheric urban warming effects using remote sensing techniques that capture land surface warming. Understanding the scale-dependent drivers of microclimate across urban landscapes could help city planners better identify land cover and vegetation impacts on urban cooling and heat vulnerabilities.

Literature Cited

Brazel, A., P. Gober, S. Lee, S. Grossman-Clark, J. Zehnder, B. Hedquist, and E. Comparri. 2007. Determinants of change in the regional urban heat island in metropolitan Phoenix (Arizona, USA) between 1990 and 2004. Climate Research **33**:171-182.

Canadell, J. G., H. A. Mooney, D. D. Baldocchi, J. A. Berry, J. R. Ehleringer, C. B. Field, S. T. Gower, D. Y. Hollinger, J. E. Hunt, R. B. Jackson, S. W. Running, G. R. Shaver, W. Steffen, S. E. Trumbore, R. Valentini, and B. Y. Bond. 2000. Carbon metabolism of the terrestrial biosphere: A multitechnique approach for improved understanding. Ecosystems **3**:115-130.

Chatterjee, A., and G. D. Jenerette. 2011. Spatial variability of soil metabolic rate along a dryland elevation gradient. Landscape Ecology **26**:1111-1123.

Chow, W. T. L., T. J. Volo, E. R. Vivoni, G. D. Jenerette, and B. L. Ruddell. 2014. Seasonal dynamics of energy balance in Phoenix, AZ. International Journal of Climatology **34**:3863-3880.

Davidson, E. A., I. A. Janssens, and Y. Luo. 2006. On the variability of respiration in terrestrial ecosystems: moving beyond Q_{10}. Global Change Biology **12**:154-164.

Davidson, E. A., S. Samanta, S. S. Caramori, and K. Savage. 2012. The Dual Arrhenius and Michaelis-Menten kinetics model for decomposition of soil organic matter at hourly to seasonal time scales. Global Change Biology **18**:371-384.

Du, Z., D. A. Riveros-Iregui, R. T. Jones, T. R. McDermott, J. E. Dore, B. L. McGlynn, R. E. Emanuel, and L. Xu. 2015. Landscape position influences microbial composition and function via redistribution of soil water across a watershed. Applied Environmental Microbiology **81**:8457-8468.

Groffman, P. M., J. P. Hardy, M. C. Fisk, T. J. Fahey, and C. T. Driscoll. 2009. Climate variation and soil carbon and nitrogen cycling processes in a Northern Hardwood Forest. Ecosystems **12**:927-943.

Hall, S. J., J. Learned, B. Ruddell, K. L. Larson, J. Cavender-Bares, N. Bettez, P. M. Groffman, J. M. Grove, J. B. Heffernan, S. E. Hobbie, J. L. Morse, C. Neill, K. C. Nelson, J. P. M. O'Neil-Dunne, L. Ogden, D. E. Pataki, W. D. Pearse, C. Polsky, R. R. Chowdhury, M. K. Steele, and T. L. E. Trammell. 2016. Convergence of microclimate in residential landscapes across diverse cities in the United States. Landscape Ecology **31**:101-117.

Imhoff, M. L., P. Zhang, R. E. Wolfe, and L. Bounoua. 2010. Remote sensing of the urban heat island effect across biomes in the continental USA. Remote Sensing of Environment **114**:504-513.

Jarvis, P., A. Rey, C. Petsikos, L. Wingate, M. Rayment, J. Pereira, J. Banza, J. David, F. Miglietta, M. Borghetti, G Manca, and R. Valentini. 2007. Drying and wetting of Mediterranean soils stimulates decomposition and carbon dioxide emission: The "Birch effect". Tree Physiology **27**:929-940.

Jenerette, G. D., J. Wu, N. B. Grimm, and D. Hope. 2006. Points, patches, and regions: scaling soil biogeochemical patterns in an urbanized arid ecosystem. Global Change Biology **12**:1532-1544.

Jenerette, G. D., S. L. Harlan, A. Buyantuev, W. L. Stefanov, J. Declet-Barreto, B. L. Ruddell, S. W. Myint, S. Kaplan, and X. Li. 2016. Micro-scale urban surface temperatures are related to land-cover features and residential heat related health impacts in Phoenix, AZ USA. Landscape Ecology **31**:745-760.

Kaye, J. P., R. L. McCulley, and I. C. Burke. 2005. Carbon fluxes, nitrogen cycling, and soil microbial communities in adjacent urban, native and agricultural ecosystems. Global Change Biology **11**:575-587.

Koerner, B. A., and J. M. Klopatek. 2009. Carbon fluxes and nitrogen availability along an urban-rural gradient in a desert landscape. Urban Ecosystems **13**:1-21.

Oikawa, P. Y., D. A. Grantz, A. Chatterjee, J. E. Eberwein, L. A. Allsman, and G. D. Jenerette. 2014. Unifying soil respiration pulses, inhibition, and temperature hysteresis through dynamics of labile soil carbon and O_2. Journal of Geophysical Research: Biogeoscience doi: 10.1002/2013JG002434.

Oke, T. R. 1973. City size and the urban heat island. Atmospheric Environment **7**:769-779.

Raich, J. W., and W. H. Schlesinger. 1992. The Global carbon dioxide flux in soil respiration and its relationship to vegetation and climate. Tellus Series B **44**:81-99.

Ramamurthy, P., and E. Bou-Zeid. 2017. Heatwaves and urban heat islands: A comparative analysis of multiple cities. Journal of Geophysical Research: Atmospheres **122**:168-178.

Riveros-Iregui, D. A., B. L. McClynn, R. E. Emanuel, and H. E. Epstein. 2012. Complex terrain leads to bidirectional responses of soil respiration to inter-annual water availability. Global Change Biology **18**:749-759.

Ryan, M. G., and B. E. Law. 2005. Interpreting, measuring, and modeling soil respiration. Biogeochemistry **48**:7-20.

Santamouris, M. 2015. Analyzing the heat island magnitude and characteristics in one hundred Asian and Australian cities and regions. Science of the Total Environment **512**:582-598.

Sponseller, R. 2007. Precipitation pulses and soil CO_2 flux in a Sonoran Desert ecosystem. Global Change Biology **13**:426-436.

Steadman, R. G. 1979. The assessment of sultriness. Part I: A temperature-humidity index based on human physiology and clothing science. American Meteorological Society **18**:861-873.

Stone, B., J. Vargo, and D. Habeeb. 2012. Managing climate change in cities: Will climate action plans work? Landscape and Urban Planning **107**:263-271.

Tayyebi, A., and G. D. Jenerette. 2016. Increases in the climate change adaptation effectiveness and availability of vegetation across a coastal to desert climate gradient in metropolitan Los Angeles, CA, USA. Science of the Total Environment **548-549**:60-71.

Xu, M., and Y. Qi. 2001. Soil-surface CO_2 efflux and its spatial and temporal variations in a young ponderosa pine plantation in northern California. Global Change Biology **7**:667-677.

Zhang, C., H. Tian, G. Chen, A. Chappelka, X. Xu, W. Ren, D. Hui, M. Lui, C. Lu, S. Pan, and G. Lockaby. 2012. Impacts of urbanization on carbon balance in terrestrial ecosystems of the Southern United States. Environmental Pollution **164**:89-101.

Zhao, L., X. Lee, R. B. Smith, and K. Oleson. 2014. Strong contributions of local background climate to urban heat islands. Nature **511**:216-219.

Zhou, X., M. Talley, and Y. Luo. 2009. Biomass, litter, and soil respiration along a precipitation gradient in Southern Great Plains, USA. Ecosystems **12**:1369-1380.

Chapter 1: Landscape position influences soil respiration variability and sensitivity to physiological drivers in mixed-use lands of southern California, USA

Abstract

Linking variation in ecosystem functioning to physiological and landscape drivers has become an important research need for understanding ecosystem responses to global changes. I investigate how these contrasting scale dependent ecosystem drivers influence soil respiration (R_s), a key ecosystem process, using in-situ landscape surveys and experimental subsidies of water and labile carbon. Surveys and experiments were conducted in summer and winter seasons and were distributed along a coastal to desert climate gradient and among the dominant land use classes in southern California, USA. I found R_s decreased from lawn to agricultural and wildland land uses for both seasons and along the climate gradient in the summer while increasing along the climate gradient in the winter. R_s variation was positively correlated with soil temperature, and negatively to soil moisture and substrate. Water additions increased R_s in wildland land uses, while urban land uses responded little or negatively. However, most land uses exhibited carbon limitation, with wildlands experiencing largest responses to labile carbon additions. These findings show intensively managed land uses have increased rates, decreased spatial variation, and decreased sensitivity to environmental conditions in R_s compared to wild lands while increasing aridity has the opposite effect. In linking scales, physiological drivers were correlated with R_s but landscape position influenced R_s by altering both the physiological drivers and the sensitivity to the drivers. Systematic evaluation of

physiological and landscape variation provides a framework for understanding the effects of interactive global change drivers to ecosystem metabolism across multiple scales.

Introduction

Because of extensive land use changes, many regions include a mosaic of urban, agriculture and wild land uses, and consequently have highly variable rates of ecosystem functioning and structure (Kaye et al. 2005, Jenerette et al. 2006). Similarly, increases in aridity, both within and among regions, can also lead to large differences in ecosystem functioning and structure (Groffman et al. 2009). Identifying the different and interactive effects of land use and climate on ecosystems has become a pressing need for understanding ecosystem responses to multiple global change drivers. In addressing this challenge, a multiple scale perspective is necessary. At fine scales, ecosystem functioning is regulated by plant and soil physiological responses to local environmental conditions including moisture, temperature, and substrate availability (Vargas et al. 2011, Davidson et al. 2012). While at regional scales, variation in land use and climate may regulate rates of ecosystem functioning (Kaye et al. 2005, Chatterjee and Jenerette 2011, Zhang et al. 2012). Reconciling and linking the variation in ecosystem functioning due to physiological and landscape level drivers has become a valuable research approach (Riveros-Iregui et al. 2012). Bridging fine and regional-scale drivers of ecosystem functioning are needed to improve understanding of ecosystem dynamics and prediction

of ecosystem responses to rapidly changing environmental conditions (Jenerette et al. 2006, Zhang et al. 2012).

Soil respiration (R_s), commonly measured as CO_2 efflux, is an important process describing ecosystem functioning and is a critical component of the carbon (C) cycle within ecosystems and globally (Canadell et al. 2000). R_s is an integrative variable of ecosystem metabolism, representing interactions between plant and microbial dynamics and sensitivities to above and belowground biophysical conditions, and varies both within and among ecosystems by several orders of magnitude (Ryan and Law 2005, Vargas et al. 2011). While much effort has been directed towards understanding physiological regulation of R_s (Davidson et al. 2006), landscape heterogeneity is noted as a major uncertainty for this flux (Koerner and Klopatek 2009, Riveros-Iregui et al. 2012, Zhang et al. 2012, Du et al. 2015). Spatial variation in soil biogeochemical processes are frequently explained using "hotspot" theory, where spatial variation in ecosystem processes are dominated by patches of high reaction rates (McClain et al. 2003, Chatterjee and Jenerette 2011, Kuzyakov and Blagodatskya 2015). These patches vary in size from field-scale microsites to regional-scale land use types. Along with hot spots, hot moments are periods of time that have relatively higher biogeochemical reaction rates (McClain et al. 2003). Similar to hot spots, hot moments influence temporal variability, as well as temporally dependent spatial variability, highlighting the importance for seasonal assessments of biogeochemical processes (Jenerette and Chatterjee 2012). An understanding of the terrestrial C cycle that can better account for these non-linear

ecosystem dynamics requires measures of how soil physiological drivers, landscape position, and season shape patterns in R_s.

From a soil physiological hypothesis, which encompasses responses in both heterotrophic and autotrophic communities, R_s is primarily regulated by soil temperature, soil moisture, and substrate availability (Table 1.1). One attempt to describe the interactions among these individual hypotheses has been the Dual Arrhenius Michaelis Menten (DAMM) model (Davidson et al. 2012, Oikawa et al. 2014). Temperature is a fundamental ecosystem property driving chemical, physical and biological processes (Davidson et al. 2006). However, R_s temperature sensitivity depends on enzymatic processes that are also regulated by soil volumetric water content (VWC) and substrate availability. Soil moisture regulates R_s at low VWC directly by limiting microbial and root activity or indirectly by limiting diffusion of substrates, while high VWC limits soil oxygen concentration thereby constraining R_s. Peak rates of R_s levels typically occur at intermediate VWC (Skopp et al. 1990, Xu and Qi 2001, Austin et al. 2004, Davidson et al. 2012, Oikawa et al. 2014). The relationships of R_s with substrate availability have been described with models using Michaelis-Menten enzyme kinetics that express R_s as a saturating function of substrate concentration (Davidson et al. 2006, Oikawa et al. 2014, Eberwein et al. 2015). The biogeochemical explanations of these physiological drivers predict that sites with higher soil temperature and substrate availability and intermediate soil moisture levels, will have higher rates of R_s (Xu and Qi 2001, Larionova et al. 2007, Davidson et al. 2012). However, substrate diffusion covaries with temperature and VWC to create a dynamic environment where each driver can cancel or work synergistically

with the effects of other drivers (Davidson et al. 1998). Furthermore, while the activation energy of enzymatic reactions is always positive, at low VWC temperature becomes virtually irrelevant in predicting fluxes (Davidson et al. 2012). These effects have consequences on biogeochemical hotspots. At the local ecosystem scale, increasing availability of soil moisture and substrate may lead to reduced importance of hotspots while increasing temperature positively influence hotspot distributions (Jenerette et al. 2006, Chatterjee and Jenerette 2011). These relationships are further complicated by higher level controls such as climate and land use.

Landscape position, which includes climate and land use distributions (Zhang et al. 2012, Lewis et al. 2014), also influences R_s variation (Table 1.1). Landscape regulation of R_s, which includes a mixture of climate and land use processes, occurs through a direct influence to the physiological drivers of R_s and may also have indirect effects by influencing the sensitivity of R_s to the physiological drivers (Jenerette and Chatterjee 2012). Regional scale climate patterns have direct influence on soil temperature and moisture conditions and are further associated with variation in soil organic matter (SOM) distributions (Raich and Schlesinger 1992, Zhou et al. 2009). Land use, and urbanization in particular, also has a major influence on R_s and soil C pools (Kaye et al. 2005, Pouyat and Carreiro 2006, Jenerette et al. 2006). Land cover and land use can influence physiological drivers through processes such as irrigation, resource amendments, and modification of local temperatures (Kaye et al. 2005, Hall et al. 2011, Jenerette et al. 2012). Additionally, long-term variation in soil environmental conditions associated with landscape patterns can alter sensitivities to environmental drivers,

through temperature acclimation (Luo et al. 2001), altered wetting sensitivity (Jarvis et al. 2007, Jenerette and Chatterjee 2012), or altered carbon use efficiency (Manzoni et al. 2012, Eberwein et al. 2015).

The interactions between land use and physiological regulation may further vary in response to changes in climate. Aridity may increase differences in soil temperature, VWC, and SOM between managed and wildland land uses (Table 1.1). As a consequence, in arid climates extensive irrigation may increase rates of R_s while in more mesic climates irrigation may reduce rates of R_s in urban sites compared to associated non-urban sites (Raich and Potter 1995, Chen et al. 2013, Lewis et al. 2014). Seasonal differences may further influence how variation in land use and climate affect R_s. R_s in urban and agricultural ecosystems is often decoupled with seasonal precipitation patterns and instead respond more to warming of the soil environment (Kaye et al. 2005). In contrast, arid and semi-arid wildland ecosystems experience R_s several orders of magnitude higher than baseline following precipitation (Jarvis et al. 2007, Sponseller 2007). Counteracting the reduced precipitation sensitivities in urban and agricultural systems, resource amendments, including top soil and fertilizers, may increase both recalcitrant and labile carbon availability (Jenerette et al. 2006, Lewis et al. 2014), which generally increases R_s in response to water amendments (Kaye et al. 2005, Hall et al. 2011). However, agricultural and urban land uses may decrease summer soil temperatures in arid systems (Kaye et al. 2004), which can then decrease R_s under optimal moisture and substrate conditions (Davidson et al. 2012).

While extensive work has been directed to evaluating the influence of physiological factors and landscape factors independently on ecosystem functioning, linking these two sources of ecosystem variation operating at greatly different scales remains an important need. To improve understanding of scale-dependent sources of variation and dynamics of R_s, I asked: what regulates the sensitivity of R_s among different land uses throughout the coastal to desert climate gradient of southern California, USA? In answering this question I evaluated the roles of soil temperature, moisture, and substrate availability in three land use types, lawn, agriculture, and wildland, and at three climate positions along the coastal to desert gradient (Figure 1.1). Climate position encompasses direct changes in soil temperature and moisture and has corresponding indirect effects to substrate availability and plant community composition. My study did not specifically evaluate any one climate factor on R_s, instead I evaluated overall climate gradient effects on physiological drivers and their sensitivities to R_s. The effects of physiological and landscape drivers on R_s were assessed using both landscape surveys and experimental additions of water and C substrates. At the physiological scale, the DAMM model framework predicts wetter, warmer, and higher substrate availabilities will have interactive nonlinear influences on R_s. At the landscape scale, the land use hypothesis predicts greater fluxes and lower variability in lawn and agricultural land uses where irrigation provides a consistent water source. Similarly, the climate hypothesis predicts greater fluxes with more water availability at coastal regions and higher variability in the hot and dry desert regions. Across scales, the landscape and physiological hypotheses suggests that landscape position influences the magnitude of the

physiological driver and the sensitivity of R_s to these drivers. Thus, while the physiological drivers remain important within all sites, I expect landscape regulation of the drivers and sensitivities to have a predominant influence on the magnitude of R_s fluxes and their heterogeneity throughout the region.

Methods

Study Sites

The study region is situated in the Los Angeles megacity of 18 million residents within southern California, USA. The area is characterized by a Mediterranean climate with hot-dry summers and cool-wet winters. A network of nine observational and experimental sites was established consisting of the three most common land use types in the greater Los Angeles area: lawn, agriculture, and wildland. These nine sites were distributed across an approximately 150 km transect from coastal Irvine to desert Palm Desert that encompassed a mild coastal to hot desert climate gradient (Figure 1.1). Given the large spatial extent of the study and extensive number of measurements full replication of this transect was not performed. Furthermore, unlike the lawn and agricultural sites, the wildland sites have dissimilar plant communities. Wildland sites in the coastal and inland sub-regions are characterized by coastal sage scrub communities dominated by *Eriogonum fasciculatm*, while the desert site is characterized as a desert scrub community dominated by *Larrea tridentata* (Table 1.2). Mean annual precipitation (MAP) varies between 300 mm at the coast and 103 mm in the desert; mean annual

temperature (MAT) varies between 17.0 °C at the coastal wildland site and 23.9 °C in the desert [http://cimis.water.ca.gov/WSNReportCriteria.aspx Accessed Jul/10/2015]. The climate gradient is more pronounced in summer when average maximum temperatures in August at the coastal wildland site are 28.4 °C, and 41.2 °C in the desert.

The 2012 to 2013 study period was unusually dry for southern California. Precipitation for the 2011 to 2012 hydrological year at the coastal wildland site was 184 mm, and 99 mm in the desert. For the 2012 to 2013 hydrological year precipitation at the coastal wildland site was 150 mm, and 45 mm in the desert. Air temperature remained within normal ranges. MAT at the coastal wildland site was 16.3 °C and 17.5 °C, and in the desert 23.5 °C and 22.9 °C for 2012 and 2013, respectively.

Landscape Surveys

To quantify fine-scale ecosystem variation within each site R_s, VWC, temperature, and SOM were measured at 2 m intervals replicated along three 50 m linear transects for a summer and winter sampling period (Figure 1.1). This sample size is consistent with previous work that found a sample size between 7 and 27 was needed to estimate the mean R_s within 20% and 10% accuracy, respectively, at a ponderosa pine plantation (Xu and Qi 2001). Each transect was a spatially independent replicate, separated by greater than 50 m. Sampling did not occur within 48 hours of rainfall, this precaution was important during the winter since most precipitation falls between the months of November through April. All measurements at each site were completed within 2.5 h and were collected between 11:00 to 16:00 local time. Consistent temporal

sampling is important because R_s measurements can change considerably throughout the day (Xu and Qi 2001).

R_s was measured using a 10 cm diameter surface sampling chamber attached to a CO_2 sensor (LI-8100, Li-Cor Biosciences, Lincoln, Nebraska, USA). Each sample was measured by calculating the slope of CO_2 accumulation in the chamber measured at 1 hz with an infra-red gas analyzer over an interval of one minute and a between measurement purge time of 45 s. The survey measurements include both autotrophic and heterotrophic components, and similar to many previous surveys I was not able to partition these different sources of R_s. Soil temperature and VWC were measured at 5 cm depth for each sample using hand-held probes (51II Thermometer, Fluke Corporation, Everett, Washington, USA and CS-620, Campbell Scientific, Logan, Utah, USA, respectively). Soil samples were collected at 5 cm depth and SOM content was measured by mass loss on ignition at 550 °C for 4 h in a muffle furnace.

Spatial heterogeneity of R_s was quantified with two measures of spatial variability. First, the mean of R_s was used to evaluate land use and climate differences in R_s among sites at regional scales. Second, the coefficient of variation (CV) was used as a measure of variation within patches, land uses and climates. The CV is a dimensionless quantity of variation standardized by the sample mean and commonly expressed as a whole-number percent.

Regression analysis was used to examine how variation in R_s is influenced by hypothesized physiological drivers of soil temperature, moisture, and organic matter. Relationships between spatial variability in R_s, measured by CV, and each physiological

driver were used to examine how spatial variability is functionally related to the hypothesized drivers. For both mean and CV in R_s I used the jackknife method to assess the significance of the relationships (Efron and Stein 1981). This method evaluates statistical significance by repeatedly selecting a subset of n-1 samples from the data. R_s data were log-transformed to meet homogeneity of variance requirements before analysis using a fixed-effect model ANOVA. Comparisons between unlike land uses among sub-regions were not included the post-hoc analysis. Alternatively, Tukey post-hoc comparisons within individual sub-regions and among land uses, and within individual land uses and across the climate gradient were included in the text for relevant comparisons.

Landscape Experiments

While my survey looks for correlations between land use and physiological variables, they do not provide direct evidence of causation. One goal of the growing field of experimental landscape ecology is to identify process variation within landscapes using networks of widely distributed experiments (Jenerette and Shen, 2012). Following such approaches, I also measured R_s following experimentally manipulated soil moisture and substrate levels by means of water additions and dextrose plus water additions, respectively. At each sub-region, sites were located on lawn, agriculture, and wildland land uses, for a total of nine locations throughout the study region. R_s measurements were performed using the same chamber based R_s system used for soil surveys. Soil temperature and VWC were measured adjacent to every R_s measurement at 5cm depth

using hand-held probes. Soil samples were collected at each experiment for analysis of SOM. At each site, fifteen 10 cm diameter polyvinyl chloride (PVC) collars, in five groups of three, were inserted in the soil to a depth of 5 cm, exposing the additional 5 cm aboveground. The groups of collars were installed at random locations in the lawn sites, and at random locations under the dominant plant species in the agriculture and wildland sites (see Table 1.2 for dominant plant species). The collars were inserted into the soil at least two weeks before measurements for conditioning. Vegetation within the collars was removed to exclude above ground autotrophic respiration. Approximately one hour before measurements, at five locations per site, 20 mL of deionized water was added to the water treatment collars, and 20 mL of a 60 g/L solution of dextrose and deionized water was added to the substrate treatment collars. All measurements were acquired between 11:00 and 15:00 local time. The experimental amendments allow more clear evaluation of heterotrophic responses independent of autotrophic emissions at the time scale investigated. These measurements were timed to quantify the maximum pulse response as assessed in previous arid environment pulse studies (Rey et al. 2005, Jenerette and Chatterjee 2012, Oikawa et al. 2014). Each site had two measurement dates, one in the summer, between July to September 2013, and one in the winter between November to December 2012. While this excludes many temporal aspects of R_s pulse dynamics, my goal was to evaluate potential differences between contrasting seasons. For standardization, experiments were performed at least 48 h after measurable precipitation.

For testing the effects of water and dextrose on R_s, I performed a two-way analysis of variance (ANOVA). The data were analyzed using a response ratio, calculated

as the treatment divided by the control (water / control and [dextrose + water] / water) commonly used in meta-analyses that evaluate multiple experiments (Elser et al. 2007). The control for the water treatment was no treatment and the control for the dextrose plus water treatment was the water treatment. This isolates the effects of dextrose outside the influence of the water addition. The response data were displayed using a log scale to represent the pulse effect as pulse magnitudes varied by several orders of magnitude. A log response ratio of zero indicates no treatment effect, and significance was evaluated using Student's *t*-test.

Results

Surveys: Physiological Drivers

Climate, land use, season, and their interactions had significant correlations with soil temperature, VWC, and SOM ($p < 0.001$, three-way ANOVA, Table 1.3). Season had the strongest effects on temperature, followed by land use and climate ($F_{2,1323}$ = 13265.66, $F_{1,1323}$ = 1058.71, and $F_{2,1323}$ = 173.08, respectively). Land use had the strongest effects on VWC, followed by season and climate ($F_{2,1323}$ = 1044.92, $F_{1,1323}$ = 355.47, and $F_{2,1323}$ = 71.41, respectively, Figure 1.2). Land use was correlated with SOM more strongly than climate ($F_{1,1323}$ = 164.18 and $F_{2,1323}$ = 94.34, respectively). Likewise, for both seasons, soil VWC was positively related to SOM. VWC was negatively correlated with temperature ($R^2 = 0.18$; $p < 0.0001$), and positively correlated

with SOM ($R^2 = 0.13$; $p < 0.0001$). SOM and temperature showed little correlation ($R^2 = 0.02$; $p < 0.0001$).

During the summer, soil temperatures increased from lawn to agricultural to wildland land uses in the coastal sub-region, while in the inland and desert sub-regions temperature increased from agricultural to lawn to wildland land uses (Table 1.2). For both lawn and agricultural land uses soil temperatures were the highest in the desert sub-region, while the inland sub-region had higher wildland temperatures (Table 1.2). During the winter, in all climates soil temperatures increased from lawn to agriculture to wildland land uses (Table 2). For both seasons, VWC increased from wildland to agriculture to lawn land uses. VWC decreased from coastal to desert during the winter for all land uses, but had no clear climate pattern during the summer (Table 1.2). SOM decreased from coastal to desert sub-regions in the wildlands, but had no clear climate pattern for the other land uses (Table 1.2).

Surveys: Soil R_s Sensitivity to Physiological Drivers

Across the study region, soil temperature was negatively correlated with R_s for both summer ($R^2 = 0.34$; $p < 0.0001$) and winter ($R^2 = 0.13$; $p < 0.0001$) measurement dates, with the summer exhibiting a higher magnitude and range of both R_s and temperature (Figure 1.3a). Generally, Soil VWC was positively related to R_s for both summer ($R^2 = 0.30$; $p < 0.001$) and winter ($R^2 = 0.20$; $p < 0.001$). Percent SOM was positively correlated with R_s for both summer and winter (Figure 1.3b; $R^2 = 0.14$, $p <$

0.001, and $R^2 = 0.28$; $p < 0.001$). Correlations were reported as log(R_s) to accommodate the wide range of flux rates.

The relative levels of soil physiological drivers were correlated with spatial variation of R_s ($p < 0.02$). The mean CV in R_s for each transect (Figure 1.4a) was positively linearly related to soil temperature for both seasons ($R^2 = 0.48$ and $R^2 = 0.46$, respectively). The CV in R_s (Figure 1.4b) was non-linearly negatively related to percent VWC for both seasons ($R^2 = 0.21$ and $R^2 = 0.56$, respectively). Percent SOM for both seasons (Figure 1.4c) was non-linearly negatively related to the CV in R_s ($R^2 = 0.48$ and $R^2 = 0.53$, respectively).

Surveys: Soil R_s Sensitivity to Landscape Influences

Climate, land use, season, and their interactions had significant correlations with R_s (Table 1.3; $p < 0.05$; three-way ANOVA); and was marginally significant for the interactive effects of all four factors and R_s ($p = 0.051$). Land use had the strongest effects on R_s, followed by season and climate ($F_{2,1323} = 466.56$, $F_{1,1323} = 267.37$, and $F_{2,1323} = 3.20$, respectively). Within each sub-region in the summer there was a decreasing R_s from lawn to agriculture and wildland land use types (Figure 1.5a; $p < 0.001$), with 14.26 μmol m^{-2} s^{-1} or 53 times higher fluxes in lawn compared to wildland land uses when averaged over the region (Figure 1.5c). During the winter the differences were less pronounced with lower R_s in the agriculture than the lawn land use type (Figure 1.5a and c; $p < 0.001$). Additionally, wildland land use types showed a clear downward trend in R_s from coastal to inland to desert sub-regions (Figure 1.5a; $p < 0.001$). R_s decreased from

summer to winter for all sub-regions (Figure 1.5b; $p < 0.001$). For land use effects, wildland sites had fluxes 12 times higher in the winter than the summer, contrasting that of lawn and agricultural land uses that had decreased fluxes from summer to winter (Figure 1.5c; $p < 0.001$).

Both landscape factors and seasonality had effects on the spatial variation of R_s ($p < 0.001$; three-way ANOVA), measured as the CV; land use had the strongest effects on variation, followed by season and climate when assessed using the jackknife method ($F_{2,1323} = 812.03$, $F_{1,1323} = 503.30$, and $F_{2,1323} = 15.08$, respectively). The coastal sub-region in summer had decreasing variation in R_s from lawn to agricultural to wildland land use types, while in inland and desert sub-regions the opposite trend was observed (Figure 1.6a; $p < 0.001$). The coastal and inland sub-regions in the winter had decreasing variation in R_s from agricultural to wildland to lawn land use types, while the desert sub-region had a similar trend to summer variation (Figure 1.6a; $p < 0.001$). Sub-region and land use variation in R_s decreased from summer to winter, except for the desert sub-region and two out of three agricultural sites (Figure 1.6b and c; $p < 0.001$). Overall during the summer, variation decreased from coastal to inland and desert sub-regions, with 115% more spatial variation in the coastal than the desert sub-region (Figure 1.6b). The opposite trend was observed in the winter sampling period with increasing variation from coastal to inland and desert sub-regions, with 144% more spatial variation in the desert than the coastal sub-region (Figure 1.6b). Variation in each land use was highest in the summer sampling period, with increasing variation from lawn to agricultural and wildland land use types, with 128% more spatial variation in the wildland than the lawn

land uses (Figure 1.6c). In the winter the most variation was found in agricultural land use types, with 229% more spatial variation than the lawn (Figure 1.6c). Variation in R_s did not correlate with variation in soil temperature, VWC, and SOM for both summer and winter samples ($p > 0.05$; regression analysis).

Landscape Experiments

Both water and substrate additions induced changes to R_s, although the response magnitude and direction were affected by landscape position and seasonality. For water and substrate treatments, summer land use had the strongest effects (Table 1.4; $F_{2,35} = 23.61$, $F_{2,35} = 20.53$, respectively; $p < 0.001$). For substrate treatments, summer interactive effects did not influence R_s (Table 1.4). All wildland sites positively responded to water additions in the summer, with 21.0 to 33.4 times higher flux than no treatment (Figure 1.7a and b); there were reduced positive water response for the winter (Figure 1.7a and b). Wildland land use types responded more to water additions than to substrate additions in summer, with marginally significant substrate responses over water ($p < 0.1$), while winter substrate response ranged from 2.0 to 3.0 times higher flux than water alone (Figure 1.7b). In summer, the coastal and inland lawn and desert agricultural land use patches had negative responses to water additions ($p < 0.05$), with 27 and 53% decreased fluxes than controls, respectively (Figure 1.7b). The inland agriculture and desert lawn responded to dextrose additions in summer ($p < 0.05$), all other managed sites except desert agriculture were marginally significant (Figure 1.7b). Furthermore, response ratios across sites were negatively non-linearly related to antecedent VWC for

both summer and winter (Figure 1.8, $R^2 = 0.74$, $p < 0.01$, $R^2 = 0.74$, $p < 0.01$, respectively).

Discussion

My findings, from a combination of observational surveys and manipulative experiments, show interactive physiological, landscape, and seasonal factors are important drivers of R_s, an ecosystem process central to terrestrial C cycling and metabolism. At regional scales, landscape position has important contributions to R_s rates, their physiological drivers, local variability, and sensitivities to environmental changes. Landscape position, reflecting a combination of land use and climate influences, lead to differences in both the direction and magnitude of responses to physiological drivers, with contrasting inhibition and pulsed R_s responses to water additions and varying responses to substrate addition. At the interface between landscape and physiological regulation of R_s, I found regional-scale coordination between physiological drivers and variability in R_s — higher temperatures, lower moisture, and lower organic matter all increased local variability. Together, these findings improve understanding of how interactions between landscape and physiological levels regulate ecosystem functioning — at regional scales climate, land use, and season alter biophysical drivers of R_s and sensitivities to these drivers. Furthermore, regional variability was consistent with an urban homogenization hypothesis (Groffman et al. 2014), as lawns had considerably less R_s variation than wildland land uses across all climates. Surprisingly, variation in soil

temperature, VWC, and SOM did not correlate with variation in R_s. Instead, I attribute these differences to biogeochemical hot spots. Sites with higher fluxes and lower pulse responses had lower spatial variation in R_s, consistent with the hypothesis that urban sites are less sensitive to changes in soil conditions. With increasing efforts directed to modeling ecosystem functioning and C fluxes in mixed land use regions that include urbanization (Churkina 2008, Zhang et al. 2012, Zhang et al. 2013), incorporating both the changes in physiological drivers and ecosystem sensitivities will become increasingly valuable.

Soil Physiological Drivers of Regional R_s

Using the DAMM model framework (Davidson et al. 2012) to evaluate hypotheses of soil physiological regulation of soil respiration, I observed interactive effects of soil temperature, moisture and substrate influences that are broadly consistent with physiological predictions of the interaction between drivers. While at the global scale soil temperature is the best predictor and positively correlated with R_s (Raich and Schlesinger 1992, Raich and Potter 1995), I found soil temperature to be negatively correlated with R_s. I interpret this finding as the confounding effect of soil moisture (Davidson et al. 1998), which was negatively correlated with temperature. This negative relationship was primarily influenced by wildland sites which were strongly limited by VWC. In contrast, irrigated sites were generally not limited by VWC and notably R_s increased in the summer in six of the nine sites, indicating positive temperature responses. The negative temperature – R_s relationships do not imply a negative activation

energy but rather that the activation energy becomes irrelevant at low VWC (Davidson et al. 2006) and the inhibition of R_s by low VWC was much stronger than the direct temperature effects. These interactions are consistent with R_s patterns in other arid and semiarid ecosystems and predictions from the DAMM model (Rey et al. 2002, Janssens and Pilegaard 2003, Davidson et al. 2006, Oikawa et al. 2014).

The confounding interactions of soil temperature, moisture, and substrate highlight the location and season specific importance of physiological regulation. All wildland locations were sensitive to experimental wetting in summer with strong pulse responses, consistent with findings in other unmanaged dryland ecosystems (Cable et al. 2008, Jenerette and Chatterjee 2012). However, in highly managed ecosystems this sensitivity to moisture addition was absent or resulted in R_s inhibition. The wetting induced inhibition is consistent with an oxygen (O_2) limitation hypothesis (Linn and Doran 1984, Davidson et al. 2012, Riveros-Iregui et al. 2012, Oikawa et al. 2014), where wetting of moist soils can inhibit diffusion of O_2 to sites of microbial and root activity and reduce R_s rates. The negative responses to water additions in lawn ecosystems suggest water saturation of the soil environment and subsequent anoxic soil conditions following wetting. Although these inhibitions were likely dominated by heterotrophic processes at the time scale investigated, a limitation to these experiments and most pulse studies in general, is the difficultly in partitioning autotrophic and heterotrophic contributions. In contrast to water availability, almost all ecosystems were substrate limited, also consistent with previous findings in diverse unmanaged and managed dryland ecosystems (Jenerette and Chatterjee 2012, Eberwein et al. 2015). The magnitude

of substrate amendment sensitivity varies throughout the region, however, in the highly managed lawn and agricultural land uses the substrate sensitivities are similar. These findings suggest that in highly managed sites, where moisture limitation has been overcome, substrate availability still imposes limits on R_s. New physiological models that account for interactions between C and O_2 as influenced by water and temperature, could be useful for reconciling the large variation in R_s responses to wetting (Oikawa et al. 2014). These findings are important for improving ecosystem models used at regional scales that increasingly rely on complex soil microbial and biophysical schemes (Zhang et al. 2012, Zhang et al. 2014).

Landscape Drivers of Regional R_s

Landscape variation in both land use and climate is an important factor influencing R_s. Landscape effects arise from an interaction between changes in the physiological drivers and changes in sensitivities to the physiological drivers (Davidson et al. 2006, Lewis et al. 2006, Lewis et al. 2014, Jenerette and Chatterjee 2012). These differences result from the combined changes in land use and climate, which lead to altered soil chemical and physical structure and soil trace gas fluxes (Jenerette et al. 2006, Hall et al. 2009, Lewis et al. 2014). My use of a climate gradient analysis is similar to much more widely used elevation gradients, which generally include large changes in community composition and do not solely represent the direct effects of changing temperature and precipitation on R_s (e.g. Conant et al. 2000, Smith et al. 2002, Groffman et al. 2009, Anderson-Teixeira et al. 2011, Lybrand and Rasmussen 2014). In these

studies climate is compounded with landscape position, or changes in ecosystem structure or land use. I extend the findings from such elevation gradients by using a different, though related, climate gradient. Furthermore, while there are studies investigating land use (Kaye et al. 2005, Koerner et al. 2009) and climate effects on R_s (e.g. Conant et al. 2000, Anderson-Teixeira et al. 2011), to my knowledge there are no studies that have investigated the interactive effects of land use and climate on R_s variation.

Consistent with previous studies, I found much higher soil VWC and SOM in highly managed land uses contrasting with wildland land use types (Jenerette et al. 2006, Hall et al. 2009). In the summer there was no difference among sub-regions for the wildland land use, while during the winter there was a clear gradient with higher fluxes towards the coast, likely a consequence of higher precipitation and reduced evaporative demand at the coast. The wildland land use in the summer for all sub-regions had very low fluxes, a consequence of near zero soil VWC. Irrigation for both lawn and agricultural land uses increased the differences between land uses, and I expect was more important for accounting for differences than the temperature variation between sub-regions. In the experimental study, substrate solubilization and microbial resurrection from dormancy likely accounted for larger seasonal effects in the wildland sites, where water additions induced a larger R_s response in the summer period when the soil was the driest (Fierer and Schimel 2003, Davidson et al. 2006, Jarvis et al. 2007, Jenerette and Chatterjee 2012). During the winter, seasonal precipitation inputs likely muted R_s sensitivity to further wetting events.

Changes in the sensitivity to physiological drivers creates considerably more complexity in understanding the sources of regional variation in ecosystem functioning. Notably, I found a decoupling of R_s from further moisture additions in highly managed land uses, and more sensitivity to changes in substrate. Conversely, R_s in drier soils was less sensitive to changes in substrate, and more sensitive to levels of soil moisture (Davidson et al. 2012). Differences in water and substrate response between managed and wildland ecosystems are predicted to result in alternate regulations of R_s. The management induced decoupling of dryland urban ecosystem functioning from precipitation has previously been observed from remotely sensed analyses (Buyantuyev and Wu 2009, Jenerette et al. 2013) and models (Zhang et al. 2013) and I provide a first experimental assessment of these ecosystem effects.

Toward a Synthesis of Physiological and Landscape Regulation of Ecosystem Processes in Mixed-use Regions

Variation in physiological drivers provides key information for linking patch and regional-scale patterns of R_s. Soil metabolic rates respond non-linearly to changes in drivers, which results in higher variability when conditions in general reduce flux rates. The importance of changing soil moisture and substrate levels is magnified in water and substrate scarce environments. In resource scarce environments biogeochemical hot spots create greater resource discontinuity and spatial variation in R_s. Conversely, fluxes in sites with saturated water and substrate levels are less sensitive to changes in resources. Additionally, fluxes in warmer environments have greater responses to spatial and

temporal changes in water and substrate, as resource availability regulates temperature sensitivity (Davidson et al. 2006). The variation in landscape induced sensitivities to water and C substrate addition highlight the differences in how physiological drivers influence R_s and how landscape variation modifies these sensitivities. Ecosystems with the highest responses to water and substrate additions also have the greatest spatial variability in surveyed R_s. This trend is particularly noticeable in the wildland sites, where flux responses to water additions are orders of magnitude higher than that of other locations. The physiological underpinnings of R_s variability have extensive nonlinear interactions. My data do not determine if landscape position changes the activation energy of enzymatic reactions, or the shape of the R_s response curve to VWC. Instead sensitivity is likely determined through where the sites fall within different positions of the non-linear Michaelis-Menton and substrate diffusion functions.

My findings, that variation in R_s is driven not only by landscape position but is a function of the absolute levels of soil physiological drivers, are consistent with previous findings where ecosystems with low VWC and SOM are also those that have more resource heterogeneity (Austin et al. 2004). However, my results suggest the connection between environmental variability and R_s variability is indirect. Fine-scale variation in soil physiological drivers did not correlate with variation or absolute levels of R_s. Alternatively, sites with mean VWC and SOM high enough to be on the flat part of the physiological saturating response functions, R_s will be less spatially variable, regardless of microsite variation in these drivers. In contrast, when substrates are low enough to fall within the dynamic ranges of the response functions, then microsite differences become

important in determining flux rates. This evidence supports a hypothesis that R_s spatial variability is a consequence of limitations in soil moisture or substrate supply. Xu and Qi (2001) found that in a ponderosa pine plantation spatial variation in R_s was the highest during the non-growing season (August to April) when soil moisture was the lowest. In these conditions, small changes in soil moisture may have large consequences on the sensitivity of R_s to other physiological drivers. Localized areas within these patches that have elevated levels of soil moisture and substrate represent biogeochemical hotspots.

Together both survey and experimental findings support an inverse-metabolic pulses hypothesis (Huxman et al. 2004), where ecosystems with higher fluxes before wetting are associated with reduced pulse sensitivities. The variation among patches in flux rates and local variability show an enhanced sensitivity to environmental conditions during unfavorable periods for plants and soil microbes. Some of the highest fluxes were observed in wildland plots that received water additions, despite having the lowest SOM. This is likely the result of labile soil C accumulation, a consequence of extensively reduced heterotrophic metabolism. Other studies show that relatively small rain events, as low as 2 mm (Austin et al. 2004, Huxman et al. 2004), can induce soil metabolic pulses, and that subsequent rain events have reduced pulse rates, likely resulting from of labile C depletion (Oikawa et al. 2014). While the inverse-metabolic pulse process has been observed in semiarid and arid wildland ecosystems (Reynolds et al. 2004, Huxman et al. 2004, Jenerette and Chatterjee 2012), these are the first results that extends such frameworks across mixed land use regions including urban and agricultural uses.

At regional scales, R_s variation is the consequence of both physiological and landscape patterns. These drivers are interrelated, as temperature, and inputs of water and substrate depend on landscape position. A key aspect of landscape effects is a combination of changes to both the physiological drivers and the ecosystem sensitivity to these drivers. Across scales these variables are coupled, as soil physiological drivers consistently influence the local variability in R_s. Strong interactions between land use and climate influence patterns of R_s at multiple scales through complex direct and indirect effects on physiological dynamics. Systematic evaluation of physiological and landscape variation provides a key framework for understanding the effects of interactive global change drivers to ecosystem metabolism.

Literature Cited

Anderson-Teixeira, K. J., J. P. Delong, A. M. Fox, D. A. Brese, and M. E. Litvak. 2011. Differential responses of production and respiration to temperature and moisture drive the carbon balance across a climatic gradient in New Mexico. Global Change Biology **17**:410-424.

Austin, A. T., L. Yahdjian, J. M. Stark, J. Belnap, A. Porporato, U. Norton, D. A. Ravetta, and S. M. Schaeffer. 2004. Water pulses and biogeochemical cycles in arid and semiarid ecosystems. Oecologia **141**:221-235.

Buyantuyev, A., and J. Wu. 2009. Urbanization alters spatiotemporal patterns of ecosystem primary production: A case study of the Phoenix metropolitan region. USA. Journal of Arid Environments **73**:512-520.

Cable, J. M., K. Ogle, D. G. Williams, J. F. Weltzin, and T. E. Huxman. 2008. Soil texture drives responses of soil respiration to precipitation pulses in the Sonoran Desert: Implications for climate change. Ecosystems **11**:961-979.

Canadell, J. G., H. A. Mooney, D. D. Baldocchi, J. A. Berry, J. R. Ehleringer, C. B. Field, S. T. Gower, D. Y. Hollinger, J. E. Hunt, R. B. Jackson, S. W. Running, G. R. Shaver, W. Steffen, S. E. Trumbore, R. Valentini, and B. Y. Bond. 2000. Carbon metabolism of the terrestrial biosphere: A multitechnique approach for improved understanding. Ecosystems **3**:115-130.

Chatterjee, A., and G. D. Jenerette. 2011. Spatial variability of soil metabolic rate along a dryland elevation gradient. Landscape Ecology **26**:1111-1123.

Chen, Y., S. D. Day, A. F. Wick, B. D. Strahm, P. E. Wiseman, and W. L. Daniels. 2013. Changes in soil carbon pools and microbial biomass from urban land development and subsequent post-development soil rehabilitation. Soil Biology and Biogeochemistry **66**:38-44.

Churkina, G. 2008. Modeling the carbon cycle of urban systems, Ecological Modeling **216**:107-113.

Conant, R. T., J. M. Klopatek, and C. C. Klopatek. 2000. Environmental factors controlling soil respiration in three semiarid ecosystems. Soil Science Society of America Journal **64**:383-390.

Davidson, E. A., E. B. Belk, and R. D. Boone. 1998. Soil water content and temperature as independent or confounded factors controlling soil respiration in a temperate mixed hardwood forest. Global Change Biology **4**:217-227.

Davidson, E. A., I. A. Janssens, and Y. Luo. 2006. On the variability of respiration in terrestrial ecosystems: moving beyond Q_{10}. Global Change Biology **12**:154-164.

Davidson, E. A., S. Samanta, S. S. Caramori, and K. Savage. 2012. The Dual Arrhenius and Michaelis-Menten kinetics model for decomposition of soil organic matter at hourly to seasonal time scales. Global Change Biology **18**:371-384.

Du, Z., D. A. Riveros-Iregui, R. T. Jones, T. R. McDermott, J. E. Dore, B. L. McGlynn, R. E. Emanuel, and L. Xu. 2015. Landscape position influences microbial composition and function via redistribution of soil water across a watershed. Applied Environmental Microbiology **81**:8457-8468.

Eberwein, J. R., P. Y. Oikawa, L. A. Allsman, and G. D. Jenerette. 2015. Carbon availability regulates soil respiration responses to nitrogen and temperature. Soil Biology and Biogeochemistry **88**:158-164.

Efron, B., and C. Stein. 1981. The jackknife estimate of variance. Annals of Statistics **9**:586-596.

Elser, J. J., M. E. S. Bracken, E. Cleland, D. S. Gruner, W. S. Harpole, H. Hillebrand, J. T. Ngai, E. W. Seabloom, J. B. Shurin, and J. E. Smith. 2007. Global analysis of nitrogen and phosphorus limitation of primary producers in fresh-water, marine and terrestrial ecosystems. Ecology Letters **10**:1135-1142.

Fierer, N., and J. P. Schimel. 2003. A proposed mechanism for the pulse in carbon dioxide production commonly observed following the rapid rewetting of a dry soil. Soil Science of America Journal **67**:798-805.

Groffman, P. M., J. P. Hardy, M. C. Fisk, T. J. Fahey, and C. T. Driscoll. 2009. Climate variation and soil carbon and nitrogen cycling processes in a Northern Hardwood Forest. Ecosystems **12**:927-943.

Groffman, P. M., J. Cavender-Bares, N. D. Bettez, J. M. Grove, S. J. Hall, J. B. Hefferman, S. E. Hobbie, K. L. Larson, J. L. Morse, C. Neill, K. Nelson, J. O'Neil-Dunne, L. Ogden, D. E. Pataki, C. Polsky, R. R. Chowdhury, and M. K. Steele. 2014. Ecological homogenization of urban USA. Frontiers in Ecology and the Environment **12**:74-81.

Hall, S. J., B. Ahmed, P. Ortiz, R. Davies, R. A. Sponseller, and N. B. Gimm. 2009. Urbanization alters soil microbial functioning in the Sonoran Desert. Ecosystems **12**: 654-671.

Hall, S. J., R. A. Sponseller, N. B. Grimm, D. Huber, J. P. Kaye, C. Clark, and S. L. Collins. 2011. Ecosystem response to nutrient enrichment across an urban airshed in the Sonoran Desert. Ecological Applications **21**:640-660.

Huxman, T. E., K. A. Snyder, D. Tissue, A. J. Leffler, K. Ogle, W. T. Pockman, D. R. Sandquist, D. L. Potts, and S. Schwinning. 2004. Precipitation pulses and carbon fluxes in semiarid and arid ecosystems. Oecologia **141**:254-268.

Janssens, I. A., and K. Pilegaard. 2003. Large seasonal changes in Q_{10} of soil respiration in a beech forest. Global Change Biology **9**:911-918.

Jarvis, P., A. Rey, C. Petsikos, L. Wingate, M. Rayment, J. Pereira, J. Banza, J. David, F. Miglietta, M. Borghetti, G Manca, and R. Valentini. 2007. Drying and wetting of Mediterranean soils stimulates decomposition and carbon dioxide emission: The "Birch effect." Tree Physiology **27**:929-940.

Jenerette, G. D., J. Wu, N. B. Grimm, and D. Hope. 2006. Points, patches, and regions: scaling soil biogeochemical patterns in an urbanized arid ecosystem. Global Change Biology **12**:1532-1544.

Jenerette, G. D., R. L. Scott, and T. E. Huxman. 2008. Whole ecosystems metabolic pulses following precipitation events. Functional Ecology **22**:924-930.

Jenerette, G. D., and A. Chatterjee. 2012. Soil metabolic pulses: water, substrate, and biological regulation. Ecology **93**:959-966.

Jenerette, G. D., and W. Shen. 2012. Experimental landscape ecology. Landscape Ecology doi: 10.1007/s10980-012-9797-1.

Jenerette, G. D., G. Miller, A. Buyantuev, D. E. Pataki, T. W. Gillespie, and S. Pincetl. 2013. Urban vegetation and income segregation in drylands: a synthesis of seven metropolitan regions in the southwestern United States. Environmental Research Letters **8** doi: 10.10888/1748-9326/8/4/044001.

Kaye, J. P., I. C. Burke, A. R. Mosier, and J. Pablo Guerschman. 2004. Methane and nitrous oxide fluxes from urban soils to the atmosphere. Ecological Applications **14**: 975-981.

Kaye, J. P., R. L. McCulley, and I. C. Burke. 2005. Carbon fluxes, nitrogen cycling, and soil microbial communities in adjacent urban, native and agricultural ecosystems. Global Change Biology **11**:575-587.

Koerner, B. A., and J. M. Klopatek. 2009. Carbon fluxes and nitrogen availability along an urban-rural gradient in a desert landscape. Urban Ecosystems **13**:1-21.

Kuzyakov, Y., and E. Blagodatskaya. 2015. Microbial hotspots and hot moments in soil: Concept & review. Soil Biology and Biochemistry **83**:184-199.

Larionova, A., I. Yevdokimov, and S. Bykhovets. 2007. Temperature response of soil respiration is dependent on concentration of readily decomposable C. Biogeosciences **4**:1073-1081.

Lewis, D. B., J. P. Kaye, C. Gries, A. P. Kinzig, and C. L. Redman. 2006. Agrarian legacy in soil nutrient pools of urbanizing arid lands. Global Change Biology **12**:703-709.

Lewis, D. B., J. P. Kaye, and A. P. Kinzig. 2014. Legacies of agriculture and urbanization in labile and stable organic carbon and nitrogen in Sonoran Desert soils. Ecosphere **5**: 1-18.

Linn, D. M., and J. W. Doran. 1984. Effects of water filled pore space on carbon dioxide and nitrous oxide production in tilled and non-tilled soils. Soil Science of America Journal **48**:1267-1272.

Luo, Y. Q., S. Q. Wan, D. F. Hui, and L. L. Wallace. 2001. Acclimatization of soil respiration to warming in a tall grass prairie. Nature **413**:622-625.

Lybrand, R.A., and C. Rasmussen. 2014. Quantifying climate and landscape position controls on soil development in semiarid ecosystems. Soil Science of America Journal **79**:104-116.

Ma, S., D. D. Baldocchi, J. A. Hatala, M. Detto, J. Curiel Yuste. 2012. Are rain-induced ecosystem respiration pulses enhanced by legacies of antecedent photodegradation in semi-arid environments? Agricultural and Forest Meteorology **154-155**:203-213.

Manzoni, S., P. Taylor, A. Richter, A. Porporato, and G. I. Ågren. 2012. Environmental and stoichiometric controls on microbial carbon-use efficiency in soils. New Phytologist **196**:79-91.

McClain, M. E., E. W. Boyer, C. L. Dent, S. E. Gergel, N. B. Grimm, P. M. Groffman, S. C. Hart, J. W. Harvey, C. A. Johnston, E. Mayorga, W. H. McDowell, and G. Pinay. 2003. Biogeochemical hot spots and hot moments at the interface of terrestrial and aquatic ecosystems. Ecosystems **6**:301-312.

Oikawa, P. Y., D. A. Grantz, A. Chatterjee, J. E. Eberwein, L. A. Allsman, and G. D. Jenerette. 2014. Unifying soil respiration pulses, inhibition, and temperature hysteresis through dynamics of labile soil carbon and O_2. Journal of Geophysical Research Biogeosciences doi: 10.1002/2013JG002434.

Pouyat, R. V., and M. M. Carreiro. 2006. Carbon storage by urban soils in the United States. Journal of Environmental Quality **35**:1566-1575.

Raich, J. W., and W. H. Schlesinger. 1992. The Global carbon dioxide flux in soil respiration and its relationship to vegetation and climate. Tellus Series B. 44:81-99.

Raich, J. W., and C. S. Potter. 1995. Global patterns of carbon dioxide emissions from soils. Global Biogeochemical Cycles **9**:23-36.

Rey, A., E. Pegoraro, V. Tedeschi, I. De Parri, J. G. Jarvis, and R. Valentini. 2002. Annual variation in soil respiration and its components in a coppice oak forest in Central Italy. Global Change Biology **8**:851-866.

Rey, A., C. Petsikos, P. G. Jarvis, and J. Grace. 2005. Effects of temperature and moisture on rates of carbon mineralization in a Mediterranean oak forest soil under controlled and field conditions. European Journal of Soil Science **56**:589-599.

Reynolds, J. F., P. R. Kemp, K. Ogle, R. J. Fernandez. 2004. Modifying the "pulse-reserve" paradigm for deserts of North America: precipitation pulses, soil water and plant responses. Oecologica doi: 10.1007/s00442-004-1524-4.

Riveros-Iregui, D. A., B. L. McClynn, R. E. Emanuel, and H. E. Epstein. 2012. Complex terrain leads to bidirectional responses of soil respiration to inter-annual water availability. Global Change Biology **18**:749-759.

Du, Z., D. A. Riveros-Iregui, R. T. Jones, T. R. McDermott, J. E. Dore, B. L. McGlynn, R. E. Emanuel, L. Xu. 2015. Landscape position influences microbial composition and function via redistribution of soil water across a watershed. Applied Environmental Microbiology **81**:8457-8468.

Ryan, M. G., and B. E. Law. 2005. Interpreting, measuring, and modeling soil respiration. Biogeochemistry **48**:7-20.

Skopp, J., M. D. Jawson, and J. W. Doran. 1990. Steady-state aerobic microbial activity as a function of soil water content. Soil Science of America Journal **54**:1619-1625.

Smith, J. L., J. J. Halvorson, and H. Bolton Jr. 2002. Soil properties and microbial activity across a 500 m elevation gradient in a semi-arid environment, Soil Biology and Biochemistry **34**:1749-1757.

Sponseller, R. 2007. Precipitation pulses and soil CO_2 flux in a Sonoran Desert ecosystem. Global Change Biology **13**:426-436.

Vargas, R., D. D. Baldocchi, M. Bahn, P. J. Hanson, K. P. Hosman, L. Kulmala, J. Pumpanen, and B. Yang. 2011. On the multiple-temporal correlation between photosynthesis and soil CO_2 efflux: reconciling lags and observations. New Phytologist **191**:1006-1017.

Xu, M., and Y. Qi. 2001. Soil-surface CO_2 efflux and its spatial and temporal variations in a young ponderosa pine plantation in northern California. Global Change Biology **7**:667-677.

Zhang, C., H. Tian, G. Chen, A. Chappelka, X. Xu, W. Ren, D. Hui, M. Lui, C. Lu, S. Pan, and G. Lockaby. 2012. Impacts of urbanization on carbon balance in terrestrial ecosystems of the Southern United States. Environmental Pollution **164**:89-101.

Zhang, C., J. Wu, N. B. Grimm, M. Mchale, and A. Buyantuyev. 2013. A hierarchical patch mosaic ecosystem model for urban landscapes: Model development and evaluation. Ecological Modeling **250**:81-100.

Zhang, X., G. Niu, A. S. Elshall, M. Ye, G. A. Barron-Gafford, and M. Pavo-Zuckerman. 2014. Assessing five evolving mirobial enzyme models against field measurements from a semiarid savannah—What are the mechanisms of soil respiration pulses? Geophysical Research Letters **41**:6428-6434.

Zhou, X., M. Talley, and Y. Luo. 2009. Biomass, litter, and soil respiration along a precipitation gradient in Southern Great Plains, USA. Ecosystems **12**:1369-1380.

Table 1.1 Soil physiological and landscape level hypotheses for patterns in soil respiration

	Hypothesis	Description
Physiological	(1)Temperature sensitivity	Activation energy requirements of enzymatic reactions are temperature sensitive
	(2) Water availability	Microbial functioning requires moisture and indirectly moisture influences substrate (C and O_2) diffusion
	(3) Substrate availability	Substrate availability and quality influences R_s as a primary limiting resource
Landscape	(4) Climate	Climate regulates R_s by altering soil temperature, substrate, and water availability
	(5) Land use	Land use regulates R_s by altering physical, chemical, and biological processes. Including soil temperature, substrate, and water availability

Table 1.2 Site descriptions including geographic location, soil conditions and properties of the coastal to desert study region in southern California, USA

Site	Location	Elev. (m)	Soil T (°C)[a] [b]	Soil VWC (%)[ab]	Soil texture[a]	SOM (%)[a]	Soil pH[a]	Dominant vegetation
Coastal Lawn	33.6492, -117.8499	36	28.6/ 11.6	14.8/ 37.7	Sandy loam	6.5	7.53	*Cynodon dactylon*
Coastal agriculture	33.6937, -117.7217	122	31.0/ 12.1	9.7/ 17.1	Loam	4.4	8.76	Varieties of Citrus
Coastal wildland	33.6342, -117.8462	85	33.7/ 15.0	0.8/ 9.2	Clay loam	11.6	5.85	*Eriogonum fasciculatm*
Inland lawn	33.9735, -117.3262	329	29.7/ 12.0	24.4/32.1	Sandy loam	16.5	7.06	*Cynodon dactylon*
Inland agriculture	33.9615, -117.3352	305	27.8/ 15.5	5.4/ 6.2	Loam	5.2	7.25	Varieties of Citrus
Inland wildland	33.9667, -117.3219	390	51.4/ 15.9	0.8/ 8.4	Sandy loam	3.7	7.30	*Eriogonum fasciculatm*
Desert lawn	33.7732, -116.3539	73	33.2/ 10.7	15.7/24.3	Sandy loam	7.5	6.72	*Cynodon dactylon*
Desert agriculture	33.5220, -116.1503	12	32.0/ 11.7	4.3/ 5.5	Sand	3.4	8.57	Varieties of Citrus
Desert wildland	33.6708, -116.3721	243	47.8/ 20.1	1.4/ 3.3	Sand	1.6	7.79	*Larrea tridentata*

[a] Measurements and samples collected at 5 cm depth
[b] Summer and winter values, respectively

Table 1.3 Effects of climate, land use, and season on soil respiration, temperature, volumetric water content, and organic matter in southern California, USA. Reported as ANOVA F-statistic and level of significance.

	Soil respiration		Soil temperature[a]		Soil volumetric water content[a]		Soil organic matter[a]	
	Statistic(d.f.)	*P*-value	Statistic(d.f.)	*P*-value	Statistic(d.f.)	*P*-value	Statistic(d.f.)	*P*-value
Climate	$F_{2,1323} = 3.20$	0.041	$F_{2,1323} = 173.08$	<0.001	$F_{2,1323} = 71.41$	<0.001	$F_{2,1323} = 94.34$	<0.001
Land use	$F_{2,1323} = 466.56$	<0.001	$F_{2,1323} = 1058.71$	<0.001	$F_{2,1323} = 1044.92$	<0.001	$F_{2,1323} = 164.18$	<0.001
Season	$F_{1,1323} = 267.37$	<0.001	$F_{1,1323} = 13265.66$	<0.001	$F_{1,1323} = 355.47$	<0.001		
C X L	$F_{4,1323} = 5.91$	<0.001	$F_{4,1323} = 109.45$	<0.001	$F_{4,1323} = 24.02$	<0.001	$F_{4,1323} = 125.90$	<0.001
C X S	$F_{2,1323} = 13.07$	<0.001	$F_{2,1323} = 68.24$	<0.001	$F_{2,1323} = 52.76$	<0.001		
L X S	$F_{2,1323} = 292.58$	<0.001	$F_{2,1323} = 256.18$	<0.001	$F_{2,1323} = 62.02$	<0.001		
C X L X S	$F_{4,1323} = 2.37$	0.051	$F_{4,1323} = 127.93$	<0.001	$F_{4,1323} = 11.18$	<0.001		

[a]Samples collected at 5 cm soil depth

Table 1.4 Effects of climate and land use on soil respiration for both treatments of water and dextrose and water in a coastal to desert climate gradient in southern California, USA. Reported as ANOVA F-statistic and level of significance.

	Water		Dextrose and Water	
	Summer	Winter	Summer	Winter
Climate	2.96/ 0.064	3.88/ 0.030	4.32/ 0.021	11.30/ <0.001
Land use	23.61/ <0.001	12.20/ <0.001	20.53/ <0.001	6.89/ 0.003
Climate X Land use	1.55/ 0.209	2.49/ 0.060	1.35/ 0.272	4.25/ 0.006

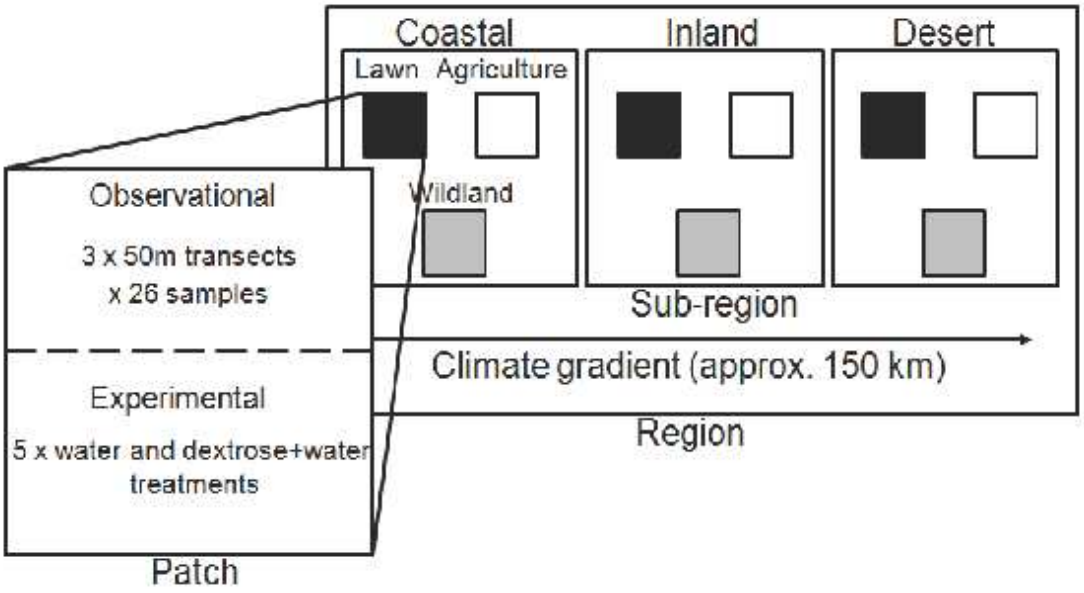

Figure 1.1 Diagram of the design used for this study. Both *in-situ* observational and experimental studies measured soil respiration within three land use types, spanning a coastal to desert regional climate gradient that encompasses three sub-regions. Spatially independent replicates were used for both observational (3 transects) and experimental studies (5 treatment triplets).

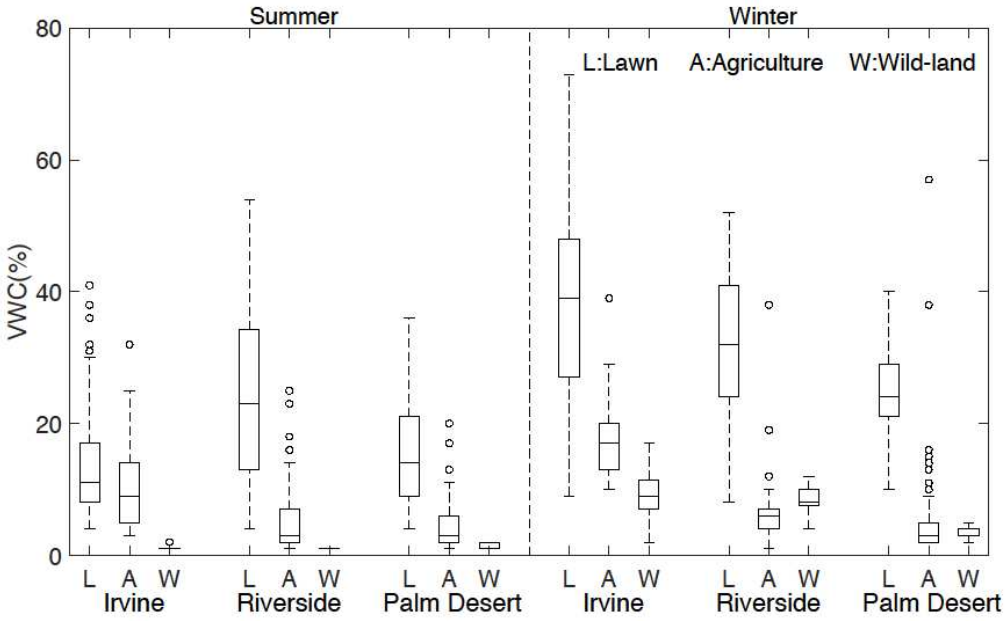

Figure 1.2 Box plots showing VWC for each site during the summer and winter months in 2012 to 2013 (n = 1323). Climate ($F_{2,1323} = 71.41$), land use ($F_{2,1323} = 1044.92$), and season ($F_{1,1323} = 355.47$) were significant ($p < 0.05$) in a three-way fixed-effect ANOVA.

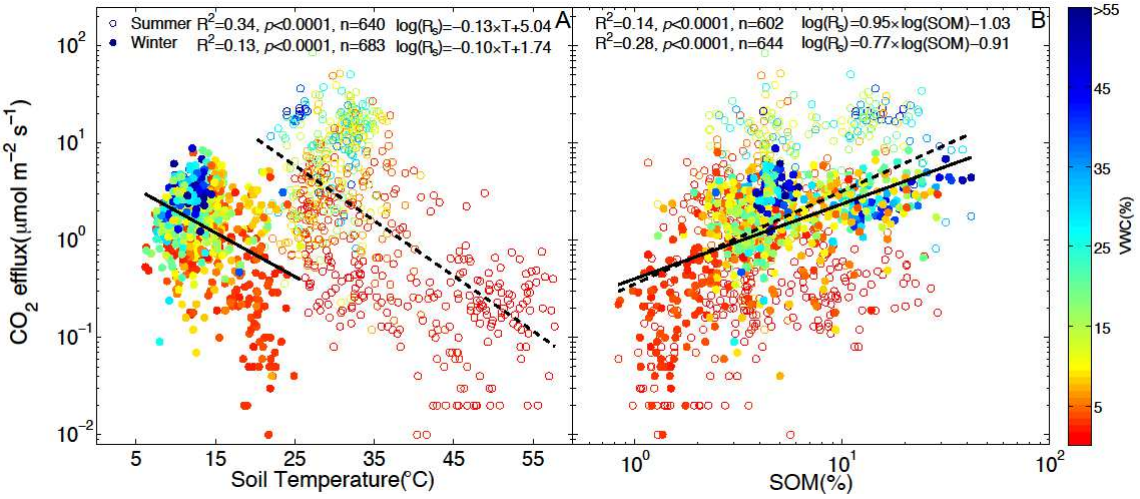

Figure 1.3 Over the entire study region, (a) R_s is negatively related to soil temperature (5 cm depth) and positively related to (b) percent SOM (5 cm depth) for both summer (dash line, $R^2 = 0.31$, $p < 0.0001$, and $R^2 = 0.14$, $p < 0.0001$, respectively) and winter (solid line, $R^2 = 0.13$, $p < 0.0001$, and $R^2 = 0.28$, $p < 0.0001$, respectively). Percent VWC (5 cm depth) is plotted using the color scale to the right. VWC is negatively correlated with temperature ($R^2 = 0.18$; $p < 0.0001$), and positively correlated with SOM ($R^2 = 0.13$; $p < 0.0001$). Each point represents a single chamber flux measurement.

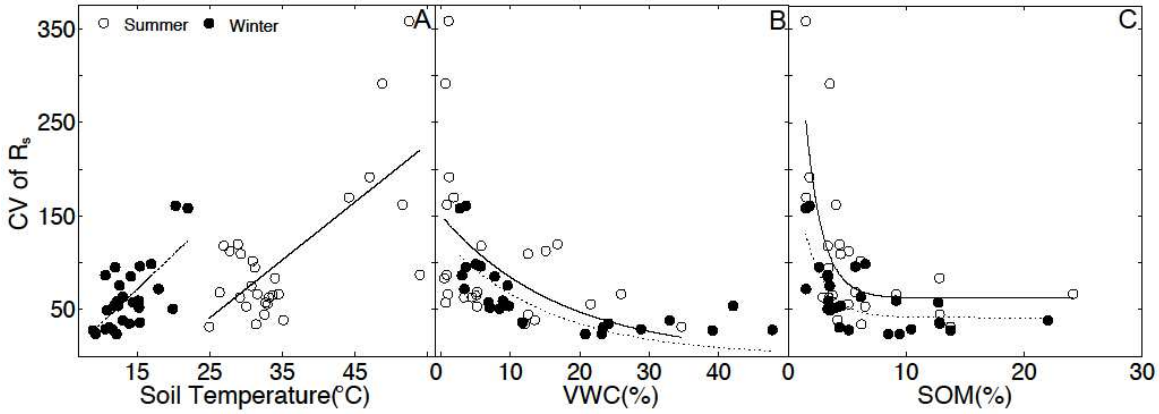

Figure 1.4 The mean coefficient of variation (CV) in R_s for each transect was positively related to (a) soil temperature (5 cm depth) for both summer (solid line, $R^2 = 0.48$, $p < 0.001$) and winter (dash line, $R^2 = 0.46$, $p < 0.001$). While the mean CV in R_s was negatively related to (b) percent VWC (5 cm depth) and (c) SOM (5 cm depth) for both summer ($R^2 = 0.21$, $p < 0.03$, $R^2 = 0.48$, $p < 0.01$, respectively) and winter ($R^2 = 0.56$, $p < 0.02$, $R^2 = 0.53$, $p < 0.001$, respectively).

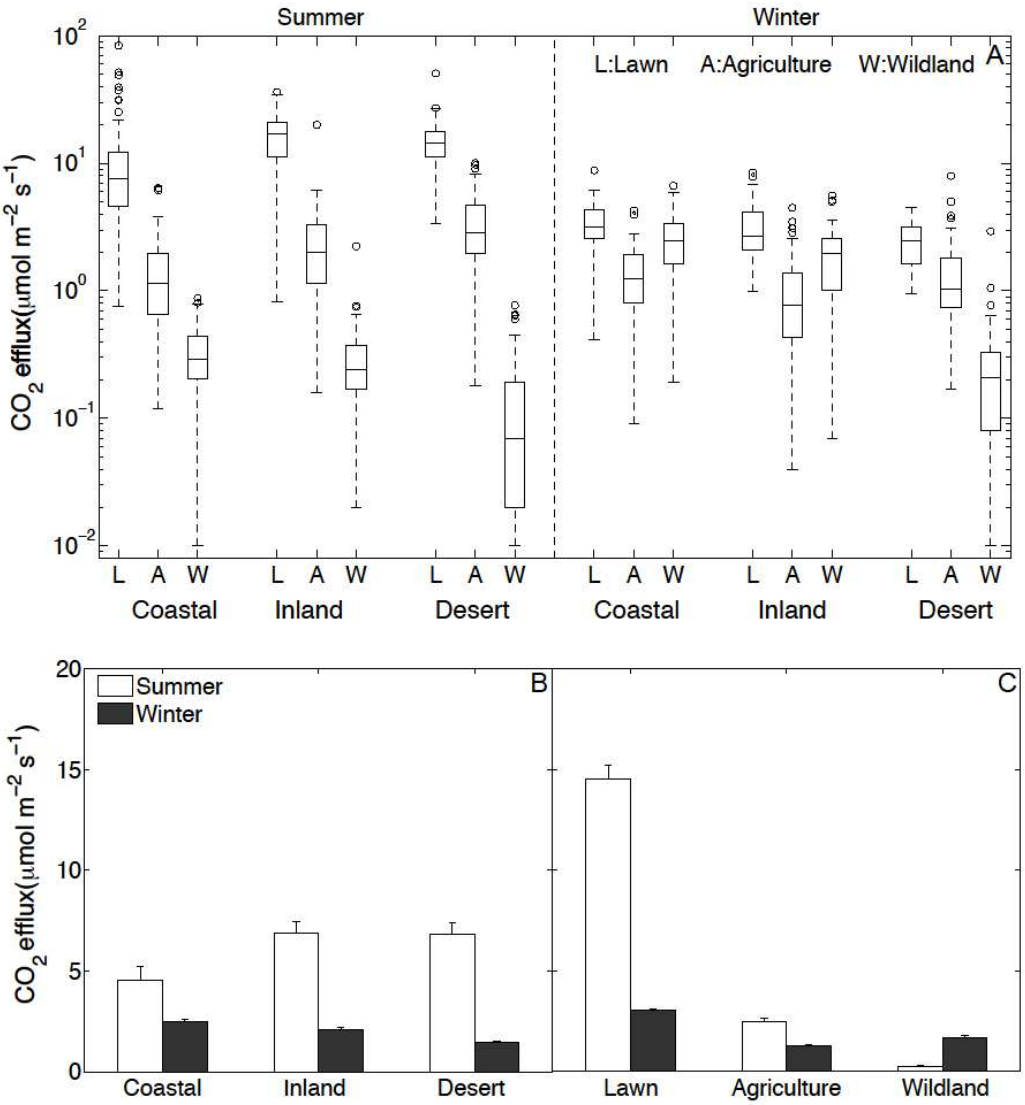

Figure 1.5 Box plots showing (a) R_s for each site during the summer and winter months in 2012 to 2013 (n=1323). (b) Mean R_s (±SE) deceased from summer to winter for all sub-regions. Wildland sites (c) experience the highest fluxes in the winter, contrasting that of lawn and agricultural land uses. The mean was measured using the jackknife method to assess the significance of the data. Climate ($F_{2,1323} = 3.20$), land use ($F_{2,1323} = 466.56$), and season ($F_{1,1323} = 267.37$) were significant ($p < 0.05$) in a three-way fixed-effect ANOVA. There were significant effects ($p < 0.001$) between each land use within each sub-region, and between each sub-region within each land use for both seasons for Tukey post-hoc comparisons.

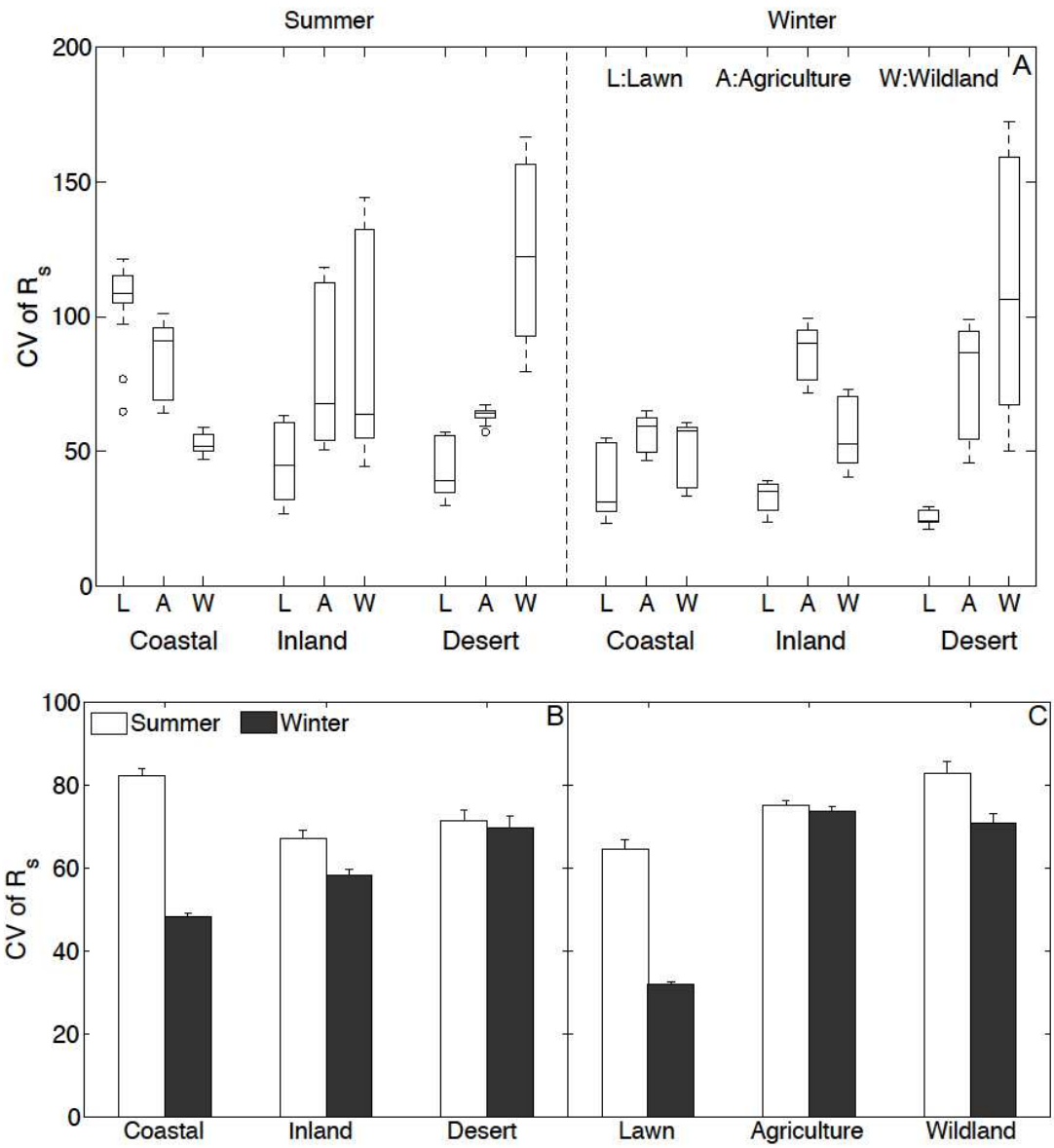

Figure 1.6 Box plots showing (a) coefficient of variation (CV) measured using the jackknife method to assess the significance of the data. Mean (± SE) CV in R_s for three (b) sub-regions and (c) land use types in summer and winter 2012 to 2013 showing climate and land use regulation (n = 1323). Climate ($F_{2,1323}$ = 15.08), land use ($F_{2,1323}$ = 812.01), and season ($F_{1,1323}$ = 503.30) were significant ($p < 0.001$) in a three-way fixed-effect ANOVA. There were significant effects ($p < 0.001$) between each land use within each sub-region, and between each sub-region within each land use for both seasons for Tukey post-hoc comparisons.

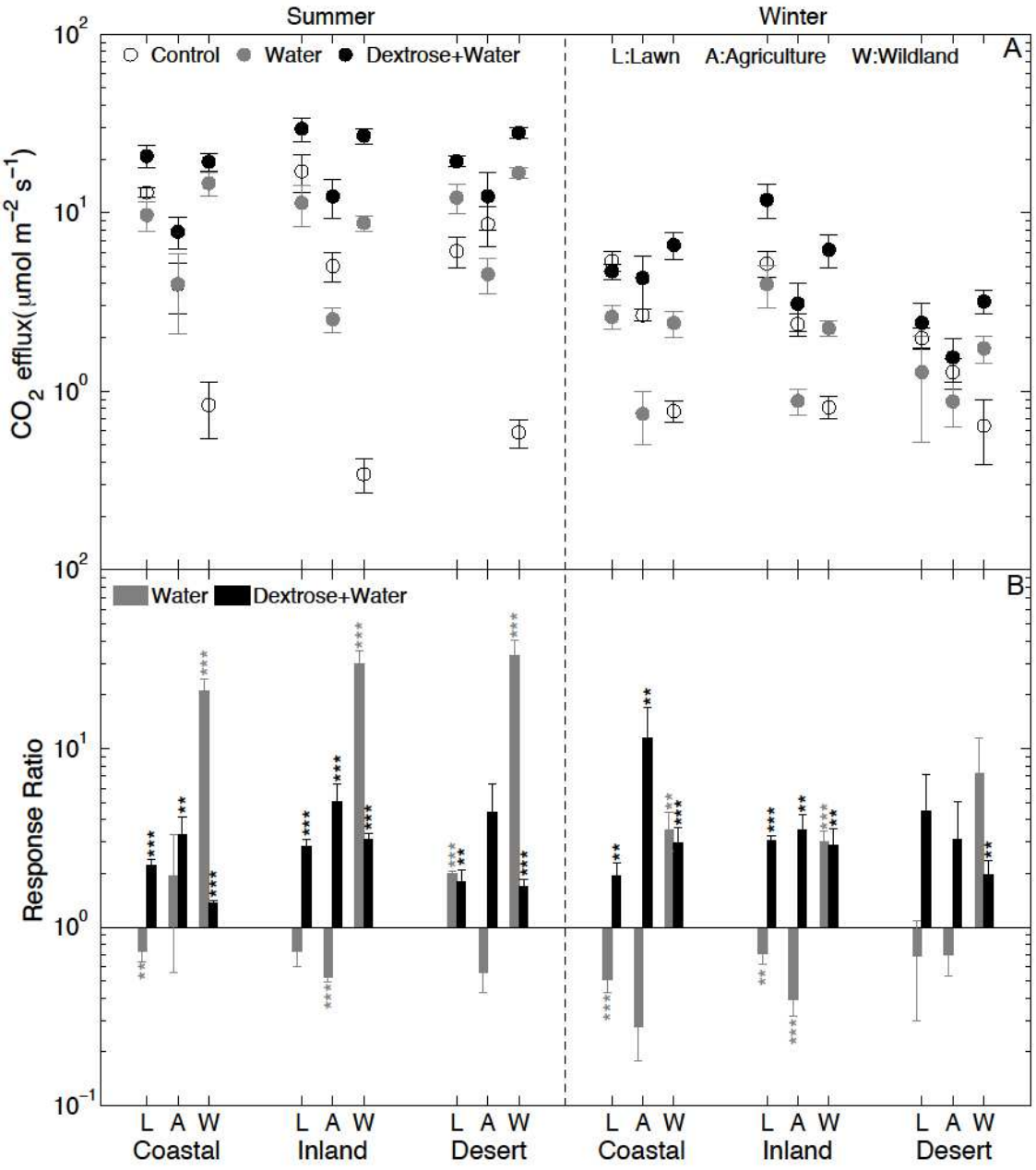

Figure 1.7 Mean R_s (±SE) (a) for each site and treatment during summer 2013 and winter 2012 (n = 270). Response ratios (b) were calculated using R_s for water divided by the control value, and R_s for the dextrose + water divided by the water value for each treatment. A log response ratio of zero indicates no treatment effect. * denotes treatment response *p*-value level of significance using Student's *t*-test, where **<0.05<***<0.01.

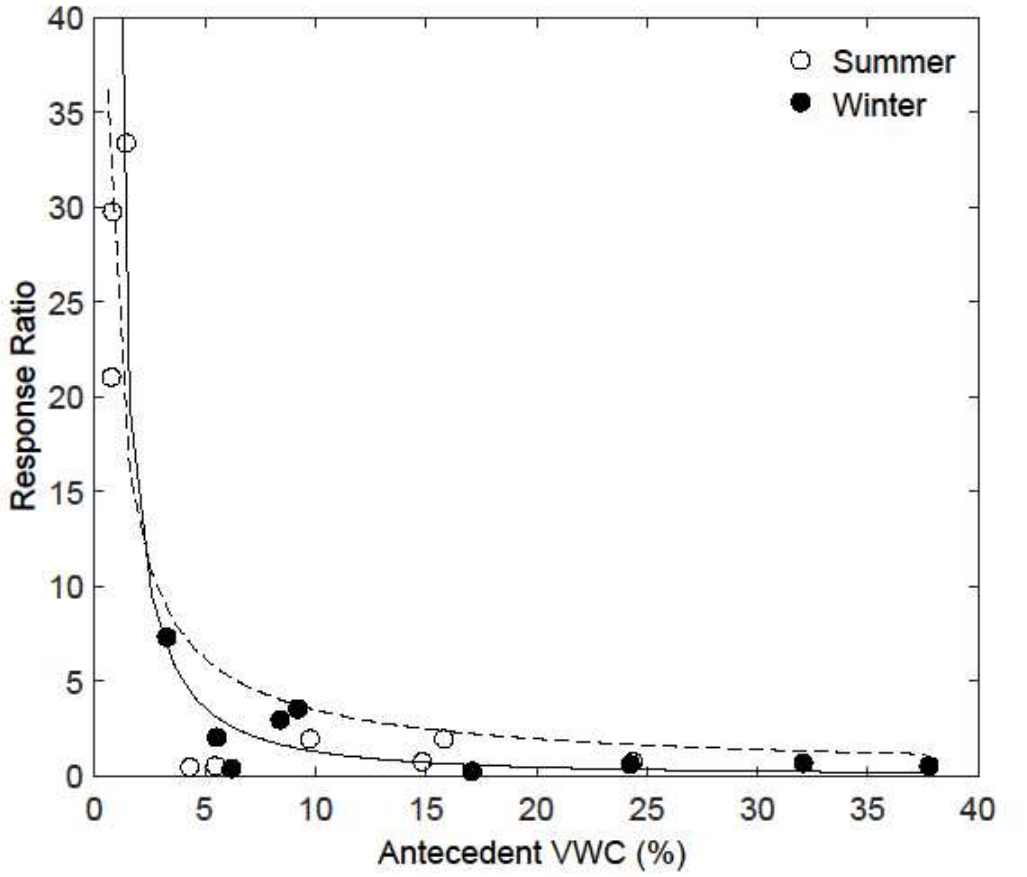

Figure 1.8 The mean response ratio of R_s for each transect was negatively related to antecedent soil VWC (5 cm depth) for both summer (solid line, $R^2 = 0.74$, $p < 0.01$) and winter (dash line, $R^2 = 0.70$, $p < 0.01$). Response ratios were calculated using R_s for water divided by the control value.

Chapter 2: The influence of vegetation, mesoclimate and meteorology on urban atmospheric microclimates across a coastal to desert climate gradient

Abstract

Many cities are increasing vegetation in part due to the potential microclimate cooling. However, the magnitude of vegetation cooling and sensitivity to mesoclimate and meteorology are uncertain. To improve understanding of the variation in vegetation's influence on urban microclimates I asked: how do meso- and regional-scale drivers influence the magnitude and timing of vegetation-based moderation on summertime air temperature (T_a), relative humidity (RH) and heat index (HI) across dryland cities? To answer this question I deployed a network of 180 temperature sensors in summer 2015 over 30 high- and 30 low-vegetated plots in three cities across a coastal to inland to desert climate gradient in southern California, USA. In a followup study, I deployed a network of temperature and humidity sensors in the inland city. I found negative T_a and HI and positive RH correlations with vegetation intensity. Furthermore, vegetation effects were highest in evening hours, increasing across the climate gradient, with reductions in T_a and increases in RH in low-vegetated plots. Vegetation increased temporal variability of T_a, which correspondes with increased nighttime cooling. Increasing mean T_a was associated with higher spatial variation in T_a in coastal cities and lower variation in inland and desert cities, suggesting a climate dependent switch in vegetation sensitivity. These results show that urban vegetation increases spatiotemporal patterns of microclimate with greater cooling in warmer environments and during nighttime hours. Understanding urban

microclimate variation will help city planners identify potential risk reductions associated with vegetation and target at-risk populations and develop effective strategies ameliorating urban microclimate.

Introduction

Metropolitan areas contain a mosaic of land covers that include contrasting patches of high- and low-vegetation intensity, and consequently have highly variable ecosystem structures and functions (Grimm et al. 2000). Patterns in vegetation intensity are directly linked to urbanization and mesoclimate distributions (Brazel et al. 2007, Jenerette et al. 2007). Since the mid-20th century, large cities in the United States are warming twice as fast as surrounding rural and wildland areas (Stone et al. 2012), especially in the dry southwestern United States (Brazel et al. 2000). Regional urban warming, commonly described as the urban heat island (UHI), is created by increasing impervious surfaces and decreasing vegetation cover, which warms temperatures in the urban core compared to surrounding rural and wildland areas (Oke 1973, Santamouris 2015). However, at finer scales vegetation may create heterogeneous cool refugia within cityscapes (Jenerette et al. 2011, Imhoff et al. 2010, Davis et al. 2016). Vegetation increases latent heat flux via transpiration and decreases sensible heat flux via shading, which cools local microclimates (Yang et al. 2011, Jenerette et al. 2011, Chakraborty et al. 2015). Regionally, the magnitude of vegetation cooling is influenced by climate

patterns, where, particularly in dryland regions, urbanization may increase vegetation intensity compared to rural and wildland areas. In these regions higher vegetation intensity creates an "oasis effect" and, as a result, reduces summer temperatures within some neighborhoods (Brazel et al. 2000, Jenerette et al. 2007, Buyantuyev and Wu 2010, Imhoff et al. 2010, Lazzarini et al. 2013, Jenerette et al. 2013). Locally, the distribution of urban vegetation may magnify temperature inequities within a city, resulting in unequal benefits and health consequences for residents (Jenerette et al. 2016). Within cities vegetation cooling is strongest in neighborhoods that are near parks or have high-vegetation cover and water consumption (Shashua-Bar and Hoffman 2000, Harlan et al. 2009, Cao et al. 2010, Jenerette et al. 2011, Declet-Barreto et al. 2013). Increases in relative humidity (RH) associated with highly-vegetated residential ecosystems of arid and semi-arid regions may counter this cooling effect through increases in human-perceived temperatures, or heat index (HI, Steadman 1979, Hall et al. 2016). HIs are used to combine T_a and RH into a single model that approximates human-perceived equivalent temperature in shaded areas (Rothfusz 1990). The spatiotemporal distributions of temperature and humidity create an "urban heat riskscape" where microclimates create varying levels of human exposure to heat hazards (Jenerette et al. 2011). Characterizing interactions between vegetation and T_a and RH in urban ecosystems may be used to predict urban responses to future climate change scenarios.

Patterns and influences of vegetation and landscape factors on fine-scale urban air temperature (T_a) within cities have been primarily analyzed using limited weather station data (e.g. Davis et al. 2016), with a small number of studies utilizing a distributed

network of sensors (e.g. Feyisa et al. 2014, Hall et al. 2016, Shiflett et al. 2017). These studies have found the greatest T_a differences are typically observed at night and morning hours (Landsberg 1981, Coseo and Larson 2014). Increased nighttime T_a variation likely arises as a consequence of differences in heat flux from urban covers. Impervious surfaces have high heat storage capacity, and thus absorb heat during the day and release it at night, creating contrasting responses in air and surface temperatures (Roth et al. 1989, Gallo et al. 1993, Grimmond 2007, Chakraborty et al. 2015, Hall et al. 2016, Davis et al. 2016). Some studies indicate that urban vegetation at the block or neighborhood scale (<250 m) may be highly influencial on T_a (Skelhorn et al. 2014, Feyisa et al. 2014), greater than a comparible volume of built cover (Davis et al. 2016). If local vegetation patterns modulate daily changes in T_a, then the greatest difference between high- and low-vegetated locations should occur at night, because vegetation reduces heat storage and sensible heat flux from urban land covers (Chow et al. 2011). This reduced heat flux is predicted to result in a greater range and temporal variation in T_a for highly vegetated locations. Alternatively, urban vegetation may increase nighttime T_a by providing insulation from high wind velocities (Gillner et al. 2015). Investigations into how urban landscapes affect T_a is essential to uncovering sources of inequities in cooling benefits and developing urban management policies for reducing heat vulnerabilities.

Important drivers of the influence of vegetation on T_a may be distributions of mesoclimate and meteorological conditions (Zhao et al. 2014). Mesoclimates, or city-scale climates, with high mean daily temperatures, or heat wave conditions in moderate climates may enhance vegetation cooling and UHI effects by increasing the effect of

shading and increasing potential transpiration rates (Jenerette et al. 2011, Jenerette et al. 2016, Tayyebi and Jenerette 2016, Ramamurthy and Bou-Zeid 2017). The negative feedback of vegetation cooling leads to a mean temperature-temperature variability hypothesis (the $\overline{T}_a$ -T_a variability hypothesis), that predicts warmer mesoclimates and warmer meteorology will lead to greater T_a spatial variation. Countering mean temperature effects within cities, there is some evidence that precipitation reduces urban heating effects on variation due to increases in air convection and reductions in surface heating (Imhoff 2010, Zhao et al. 2014, Chow et al. 2014). Wind is also predicted to minimize vegetation microenvironment effects through increased air mixing that reduces plant canopy insulating effects and temperature inequities (Grimmond 2007).

To assess the role of hypothesized drivers of variation in urban T_a, I asked: (1) what are the spatiotemporal patterns of summertime vegetation T_a cooling in dryland urban landscapes and (2) if patterns in vegetation intensity are correlated to spatial and temporal variation in T_a, how are these variables related to mesoclimate drivers of mean daily temperature, wind, and precipitation? I then expanded this question of microclimate climate variation by asking: how does vegetation distribution within a dryland city influence the spatiotemporal patterns of summertime RH and HI? To address these questions of variation in vegetation induced microclimate effects, I analyzed the patterns of T_a and RH in response to vegetation, climate, and meteorological sources of variation at three cities along a coastal to inland to desert climate gradient in urban landscapes of the greater Los Angeles metropolitan region of southern Califonia, USA. The combination of a prominent climate gradient of increasing T_a and airdity and

generally similar pattern of urbanizatzion provide a unique opportunity to study the effects of mesoclimate on urban microclimate. Understanding spatial and temporal variations in T_a and RH across urban landscapes will expand the urban heat "riskscape" concept to include micro-, meso- and regional-scale dynamics of urban microclimates, allowing city planners to better identify effectiveness of vegetation for urban cooling and reduce heat vulnerabilities, especially in areas of high heat risk.

Methods

Study sites and design

My study region is situated in the Los Angeles megacity of 18 million residents within southern California, USA, an area characterized by a Mediterranean climate with hot-dry summers and cool-wet winters. I distributed an T_a sensor network in mature street-side trees in three cities within this region along an approximately 150 km transect from mild coastal Irvine to inland Riverside to hot desert Palm Desert. These cities were selected to test hypotheses of mesoclimate effects on microclimate. Elevation of sensor plots ranged from 4 to 60 m in Irvine, 238 to 331 m in Riverside, and 0 to 144 m in Palm Desert. The surrounding native vegetation community for Irvine and Riverside is Coastal Sage Scrub and Sonoran Desert Scrub for Palm Desert. Across sites, mean annual precipitation (MAP) varies between 300 mm at the coast to 103 mm in the desert. Mean annual temperature (MAT) varies between 17.0 °C at the coast and 23.9 °C in the desert.

The climate gradient is more pronounced in summer, when average maximum temperatures in August are 28.4 °C and 41.2 °C in the coastal and desert cities, respectively.

In each of the three cities I established a network of twenty observational pairs, consisting of ten high and ten low vegetation density plots (Figure 2.1). Each high- and low-vegetation paired plot was positioned 1 to 1.5 km apart to quantify local-scale effects of vegetation while accounting for large-scale gradients in T_a related to geography and topography. Sites were selected using initial selection from high resolution imagery and later confirmed on the ground. I subsequently quantified vegetation differences as differences in the Normalized Difference Vegetation Index (NDVI, Tucker 1979, Turner et al. 1999), a proxy for vegetation patterns and readily obtained from remotely sensed imagery (van Leeuwen et al. 2006) commonly used for characterizing urban vegetation (Gallo et al. 1993, Shiflett et al. 2017). I chose NDVI over other indices because of the global availability and high repeat frequency of these data and its association with LST and T_a in prior studies (Jenerette et al. 2016, Shiflett et al. 2017). Average paired-plot level difference in NDVI between all paired high- and low-vegetated plots was 0.22±0.08, 0.31±0.12, and 0.28±0.12 at Coastal, Inland, and Desert cities, respectively (Student's *t*-test $P<0.05$; Figure 2.1e).

Using this design, the average changes in microclimate across paired-plots and correlations of NDVI with microclimate were quantified. All temperature measurements were collected in a 61-day time period in 2015 from July 18th to September 16th (corresponding to Julian day of year (DOY) 199 and 259), encompassing the warmest

months of the year. Subsequently, the following summer, relative humidity measurements were collected in the inland city in a 17-day time period from August 17th to September 13th 2016 (DOY 230 to 257) using the same sampling locations as the T_a measurements.

Micrometeorlogical sensors

Ten high- and ten low-vegetated plots consisted of three replicate temperature sensors (iButton Thermocron DS1922L, Maxim Integrated Products, Inc., San Jose, California, USA) with an accuracy of ±0.5°C and range from -10 to 65°C mounted on the trunks of three neighboring trees within 10 m of each other 2 m from the ground (n=180). To explore RH effects, in a follow-up study in 2016 one temperature and humidity sensor (iButton Hydrocron DS1923, Maxim Integrated Products, Inc., San Jose, California, USA) with a temperature accuracy of ±0.5°C from -10 to 65°C and RH accuracy of ±0.5% from 0 to 100% was mounted on the same trees 2 m from the ground at each plot in the inland city (n=20). The added cost of these temperature and humidity sensors limited this addition to one replicate per plot in the inland city. The iButton sensors are small, self-contained units with onboard memory, measuring 15 mm in diameter and 5 mm high. Readings were collected hourly throughout the study period. To shield each sensor from direct solar radiation, they were housed in custom polystyrene cylindrical white cups. Additionally, each sensor was mounted on the north side of the trees to avoid any remaining direct effects of solar radiation.

Since these sensors are mounted under the tree canopies, T_a and RH may be different than that of open spaces. Prior studies have found that individual tree canopies may increase (Gillner et al. 2015), decrease (Streiling and Matarakis 2003, Lin and Lin 2010), or have no effect on T_a (Armson et al. 2013). Furthermore, both increases and decreases in canopy level RH have been observed (Souch and Souch 1993, Gillner 2015). While these effects may influence my results, trees were generally pruned, which may minimize their effects at my sensor heights, and my design is a practical solution for embedding sensors within a populated urban environment. To test the accuracy of the custom made radiation shield systems I hung three sensors less than a meter away from a research-grade temperature sensor (HMP-60, Viasala, Helsinki, Finland) housed in a non-aspirated gilled radiation shield underneath an orange tree at the University of California Riverside's Agricultural Operations facility for seven days. Temperature differences between the iButton and the HMP-60 sensors were not observed (2-sample t-test, $P=0.64$). Furthermore, most iButton measurements fell within two standard deviations of the mean difference ($SD=0.42$ °C), with only 2% of measurements below and 2% above this indicator, with no outliers ($SD\geq3$, Osborne and Overbay 2004).

Reference T_a, wind velocity, and precipitation data were obtained from California Irrigation Management Information System (CIMIS) using stations at University of California Irvine's South Coast Research and Extension Center, University of California Riverside's Agricultural Experiment Station, and the Shadow Hills Golf Club in Indio, California (http://cimis.water.ca.gov/WSNReportCriteria.aspx Accessed Feb/4/2016). These stations were 10.6 to 26.4, 0.6 to 11.3, and 4.9 to 27 km away from iButton plots in

Irvine, Riverside, and Palm Desert, respectively. During the study period the average diurnal range in T_a was 10.96±3.52, 13.32±2.95, and 13.64±2.48 °C at Coastal, Inland, and Desert cities, respectively. Furthermore, the average diurnal range during sustained wind periods was 2.40±0.32, 3.71±0.58, and 2.83±0.58 m s^{-1} at Coastal, Inland, and Desert cities, respectively. Although wintertime precipitation was predominant, the summer 2015 study period was unusually wet for coastal and inland regions, following three years of drought. Precipitation from July to September was 65 and 57 mm at the coastal and inland cities, respectively. There were unseasonable rain events at the beginning (DOY 199 to 201) and end (DOY 259) of the study period. For comparison, the average precipitation from July to September is 13 and 10 mm at the coastal and inland cities, respectively. The desert city did not experience above average precipitation with 10 mm of rain, 6 mm below average. Characteristic of summer in this region, no precipitation occurred during the 2016 sampling period.

Remote sensing of vegetation

NDVI was derived from the Airborne Visible / Infrared Imaging Spectrometer (AVIRIS) data from the August, 2014 Hyperspectral Infrared Imager (HyspIRI) preparatory mission on a cloud free day. These data were obtained prior to my 2015 and 2016 study periods but provide a recent and relative consistency was confirmed visually. In a subsequent study in Riverside, California, reductions in NDVI between 2014 and 2015 were identified but these changes were proportional to 2014 values (Liang et al. *In Revisions*). The AVIRIS data collection consists of calibrated images with spectral

radiance in 224 10 nm contiguous spectral bands with wavelengths from 400 to 2500 nm (Roberts et al. 2015). Using a scanning mirror, AVIRIS produces 677 pixels for each of the 224 bands on each scan and at the altitude of data collection resulted in a spatial resolution of 20 m pixels. Level 2B post-processed data were used for analysis, which included atmospheric correction using Atmospheric CORection Now (ACORN) software (Roberts et al. 2015). We processed AVIRIS data to obtain NDVI using Eq. 1, where B29 and B51 correspond to AVIRIS spectral channels 29 and 51 with wavelengths 0.64 μm and 0.83 μm.

$$NDVI = B29\text{-}B51/B29+B51 \quad (1)$$

NDVI was analyzed at each sample plot in post processing using a single pixel and 90 m radius circular buffer.

Analysis

T_a, RH, and HI spatial heterogeneity and vegetation effects were quantified with four measures that compared variation in sensor measurements to local land cover distributions. In a preliminary comparison of the individual pixel and 90 m radius buffers, the land cover signal was more pronounced at the 90 m scale, likely in part due to noise at the individual pixel scale, and I chose the 90 m scale for subsequent analyses. My choice of buffer size agrees with prior research that has found urban microclimate vegetation effects on T_a strongest at scales of 50 to 500 m (Sashua-Bar and Hoffman

2000, Feyisa et al. 2014, Davis et al. 2016, Shiflett et al. 2017). First, as a direct measure of vegetation intensity on microclimate, the slope of the linear regression between NDVI and T_a was calculated hourly within each city. Additionally, the slope of the linear regression between NDVI, and RH and HI was calculated hourly within the inland city for 2016. HI was calculated using the Rothfusz (1990) model (EQ 2), which has been adopted by the United States National Weather Service (Steadman 1979).

$$HI=-42.379+2.049(T_a)+10.143(RH)-0.225(T_a)(RH)-0.007(T_a)(T_a)-0.055(RH)(RH) +0.001(T_a)(T_a)(RH)+0.0008(T_a)(RH)(RH)-0.000002(T_a)(T_a)(RH)(RH) \quad (2)$$

HI is a subjective index of human perceived temperatures and contains assumptions about human physiology, clothing, solar radiation exposure, and wind velocity (Rothfusz 1990). Second, the difference between low- and high-vegetated paired plots, expressed as ΔT_a and ΔRH, was used to evaluate vegetation effects on T_a and RH, respectively. These measures capture the mean T_a and RH difference between paired plots, while accounting for regional sources of climate variation. To obtain plot-level T_a an average was calculated using all three replicates from the 2015 study. Third, the mean T_a and RH difference between high- and low-vegetated plots was expressed as the mean percent change in T_a and RH, calculated by dividing ΔT_a and ΔRH by mean T_a and RH and expressed as a whole number percent, to show a normalized average. Fourth, the coefficient of variation (CV) was used to quantify spatial and temporal variations. The CV is a dimensionless quantity of variation normalized by the sample mean; commonly

expressed as a whole number percent frequently used to assess spatiotemporal landscape variation (Crum et al. 2016). Temporal heterogeneity in vegetation effects on T_a was analyzed at both daily and seasonal scales using correlation between NDVI and temporal CV of T_a. Daily-scale spatial averages were analyzed using the slope of correlation in NDVI and T_a, percent change in T_a, and the slope of correlation in mean T_a and spatial CV of T_a. Daily scale temporal variation is the average hourly data using all days of the study period. Seasonal variation includes data from all days of the study period, from DOY 199 to 259.

Results

Daily patterns in cooling intensity

Vegetation cooling effects, measured as the slope of NDVI and T_a, had a strong daily pattern throughout the climate gradient (Figure 2.2). Slopes were generally negative; increases in NDVI tended to decrease T_a, although during mid-day hours slopes approached zero or were not significant ($P>0.05$). Furthermore, slopes decreased along the climate gradient, with hourly average slopes ranging from -0.25 to -3.83 and -1.82 to -6.79, at the coastal and desert cities, respectively. Despite steeper relationships in the desert at night, there were fewer significant correlations compared to coastal and inland cities ($P<0.05$). Daily changes in the strength of the relationship, measured using the Pearson correlation coefficient, mirrored that of the slope, with the exception of the desert city where I observed weaker nighttime correlations than the other cities (Figure

2.3). Correlations decreased in the daytime more at the coast than the desert, with r-values reducing 0.67 at the coast and 0.33 at the desert.

In my follow-up study, vegetation effects on RH, measured as the slope of NDVI and RH, had a strong daily pattern in the inland city (Figure 2.4). Slopes were all positive with mean values ranging from 7.41 to 23.93, indicating that increases in NDVI consistently increased RH, with much lower slopes during the mid-day hours. During the evening the effects were driven by large differences in only some pairs. Two paired plots had unusually high nighttime ΔRH, with two hourly values greater than two standard deviations of the mean hourly difference (Figure 2.5). Unlike correlations found between temperature and NDVI, there was a less noticeable daily pattern in percentage of insignificant correlations for RH ($P>0.05$). Similar to 2015, slope of NDVI and T_a had a strong daily pattern in the inland city (Figure 2.4). This cooling effect was slightly reduced during the day where there were no significant correlations between 12:00 and 18:00 when factoring in heat index values (Figure 2.4).

The strength of vegetation effects varied throughout the study period, but generally vegetation cooling effects were greater at night for ΔT_a, the average of the local scale temperature change from low- to high-vegetated plots (Figure 2.6). ΔT_a was mostly positive with values as high as 4.07°C. There were some exceptions where there was a reversal in temperature differences, mostly in the daytime hours, with values as low as -0.14°C. When comparing ΔT_a during the rainiest day (DOY 259) with the hottest (DOY 252 at the coast and DOY 227 at the inland and desert cities) there are ΔT_a reductions ($P<0.001$) of 43% in coastal, 71% in inland, and 32% in desert cities. Along with reduced

vegetation effects, the coastal city had 20% reductions in spatial variation between local pairs, while there was increased variation between inland (132%) and desert (32%) cities. Daily averages of local scale vegetation cooling effects from the entire study period were measured as the average ΔT_a divided by mean T_a or percent change in T_a (Figure 2.7). A strong "U-shaped" daily pattern emerged throughout the climate gradient ranging from 1.12% to 8.11%. Furthermore, daily range in vegetation T_a effects increased along the climate gradient, with average percent change in T_a ranging from 1.12 to 4.82% and 1.43 to 8.11%, at the coastal and desert cities, respectively. Supporting findings from 2015, ΔT_a for the 2016 campaign for the inland city was the same (Figure 2.8, $P>0.05$, Student's *t*-test). There was no daily pattern in ΔRH in the inland city, but RH of low vegetated plots decreased by 4.93% ± 4.36 ($P<0.01$).

Vegetation and climate effects on air temperature variability

Temporal variation in T_a increased with NDVI at the 90 m radius scale in the coastal, inland, and desert cities, with consistent relationships along the climate gradient (Figure 2.9). These relationships have similar slopes across the climate gradient for both seasonal (Slope=5.3, 3.0, and 4.9, respectively) and daily (Slope=5.8, 4.2, and 6.0, respectively) scales, with differences in overall variation. For both temporal scales, there was higher overall variation in the inland city, with lower variation in the desert and coastal cities. Seasonal variation was higher than daily variation. The strength of these relationships was fairly consistent across the climate gradient at both seasonal (R^2=0.26,

0.25, and 0.21, respectively) and daily (R^2=0.29, 0.37, and 0.24, respectively) scales ($P<0.05$). There were no significant correlations at the individual pixel scale ($P>0.05$).

Spatial variation of air temperature (CV of T_a) is positively correlated to mean T_a for the coastal city, while negatively correlated in the inland and desert cities (Figure 2.10a, Slope=0.10, -0.07, and -0.26, respectively). Additionally, the strength of these relationships increased across the climate gradient (R^2=0.07, 0.09, and 0.40, respectively, $P<0.05$). These relationships were not consistent throughout the day, with large daily changes (Figure 2.10b). The coastal city had 12 significant positive relationships between T_a and CV of T_a from 9:00 to 21:00, with three negative relationships between 5:00 and 7:00. The inland city had both positive and negative relationships. There were five significant negative relationships between 12:00 to 18:00, and 12 positive relationships between 16:00 to 10:00. The desert city had mostly negative relationships with six between 13:00 to 19:00, with one positive relationship at 23:00. There was a strong daily pattern in slopes ranging from -0.35 to 1.99, -5.16 to 3.50, and -3.14 to 0.74 from coastal to inland to desert cities, respectively. Daily changes in the strength of the relationship mirrored that of the slope, with r-values ranging from -0.32 to 0.60, -0.52 to 0.66, and -0.59 to 0.34 from coastal to inland to desert cities, respectively.

Discussion

I found that vegetation reduces summer T_a primarily at night, or around the period when daily minimum temperatures occur. This finding supports the hypothesis that urban vegetation reduces T_a through reductions in heat fluxes from impervious surfaces that had been shaded during the daytime period. Importantly, this finding is in contrast with remotely sensed LST measurements, that show vegetation cooling of urban surfaces is largest during the daytime period (Buyantuyev and Wu 2010, Myint et al. 2013, Jenerette et al. 2016). During the daytime, urban vegetated surfaces may be directly cooled through increased evapotranspiration with large LST effects and relatively less T_a cooling. Consistent with the evapotranspiration hypothesis, I observed consistent increases in RH in more vegetated areas. Evapotranspiration is not a likely mechanism explaining the effects on nighttime microclimate variation, also consistent with limited nighttime LST cooling by vegetation, because it primarily occurs during active photosynthesis. However, relationships between vegetation and RH at night were stronger than the daytime, which could be attributed to nighttime irrigation associated with urban vegetation. Nevertheless, this finding has important implications for urban microclimates in that an increasing RH may counteract the human health benefits of vegetated T_a cooling at the local scale.

Across the coastal to desert climate gradient I found increasing local scale cooling effects (ΔT_a) positively correlated with NDVI, confirming studies that have found increased vegetation cooling intensity in hot arid regions, contributing to a negative

climate feedback effect (Imhoff et al. 2010, Tayyebi and Jenerette 2016). As the result of greater nighttime cooling effects, higher NDVI is associated with increased T_a temporal variability. This effect is reflected in seasonal scale variability, where changes in weather patterns, like heat waves, wind, and precipitation contribute to variation in addition to land cover drivers. Furthermore, supporting the $\overline{T}_a$ -T_a variability hypothesis I observed increased spatial variation with increasing mean temperature at the coast, however, wind may have played a larger role in inland and desert cities where there was a gradient toward decreased variation with increased mean temperature.

Mesoclimate and Meteorological influences on microclimate variation: mean temperature, wind, and precipitation

I found large differences in the $\overline{T}_a$ -T_a variability relationships among cities suggesting that mesoclimate may drive vegetation microclimate cooling effects. Mean T_a was positively correlated to variation of T_a at the coastal city, supporting the $\overline{T}_a$ -T_a variability hypothesis. Counter to this hypothesis, however, inland and desert cities exhibited reduced T_a variation with increased mean T_a at the city scale. These seemingly contradictory findings can be better understood by examining changes in the $\overline{T}_a$ -T_a variability relationship throughout the day. Negative relationships in inland and desert cities are consistent with daily patterns that show stronger negative correlations during the day, with an opposite pattern in the coastal city. Spatial variation in T_a was higher during warm summer nights and weakest during warm summer days for inland and desert cities, while the opposite daily trend occurred in the coastal city. Warm nights are more

variable in inland and desert cities resulting in increased nighttime T_a inequity between high- and low-vegetated neighborhood plots. This increased T_a variation on hot nights supports the $\overline{T}_a$ -T_a variability hypothesis, as urban surfaces re-emit absorbed heat in the evening (Roth et al. 1989).

There are two findings that do not support the $\overline{T}_a$ -T_a variability hypothesis. First, $\overline{T}_a$ -T_a variability relationships during the day for inland and desert cities were negative. Second, although both inland and desert cities exhibited positive nighttime slopes, relationships were stronger in the inland city than in the desert city, even though the desert city is hotter. These results were partially explained by examining patterns of wind and precipitation.

While wind may have little effect on patterns of surface heat storage and fluxes, T_a is influenced by air convection and mixing (Landsberg 1981, Imhoff 2010, Zhao et al. 2014). At whole city scales, temperature differences between rural and urban areas are driven by daily weather conditions and are reduced during windy days (Landsberg 1981, Gallo et al. 1993). Using a representative meteorological station for each city, I found the inverted daily relationships of mean T_a and spatial variation in inland and desert cities are partially explained by wind velocity. Wind velocity at each plot location would clarify relationships on the local dynamics of T_a and wind. Here, the lack of safe mounting locations and the cost associated with installing anemometers on street-side trees at each plot (n=60) precluded their deployment in my study – microclimate wind distributions remain an important research need (Vahmani and Ban-Weiss 2016). Among cities, wind velocity is highest during the day for coastal and inland cities, and warmer days are often

windier (R^2=0.51, P<0.001, Figure 2.11). Air mixing with increased wind velocity on warm days can result in lower T_a spatial variation. Furthermore, wind velocity is often reduced at night and there are weaker relationships between mean T_a and wind velocity (R^2=0.39, P<0.001, Figure 2.11). Thus at night, when wind velocity is lower, surface heat flux may more strongly drive spatial variation in T_a. Coastal regions, on the other hand, have different wind patterns, likely resulting in distinct diel $\overline{T}_a$ -T_a variability relationships. Coastal regions receive onshore wind in the daytime hours, since the land heats up faster than the neighboring ocean, which can interact with urban land cover influences on local climate (Ramamurthy and Bou-Zeid 2017). These onshore winds reduce T_a, thus the warmest days are often the *least* windy days. This unique coastal wind pattern would generate the least air mixing during warm days, which in combination with existing surface heat flux, would generate greater daytime T_a spatial variation.

For an initial evaluation of these predictions I compared the slope of wind velocity and variation of T_a (CV of T_a). Correlation was found for 8hrs of the day at the coastal city and 5 hrs of the day for the inland and desert cities (Figure 2.12). The inland city has faster winds in the day (2.37 m s^{-1} from 6:00 to 20:00) than at night (0.95 m s^{-1} from 20:00 to 6:00), while the desert city has similar average wind velocities both day (2.20 m s^{-1}) and night (2.26 m s^{-1}) over the entire study period. Greater daytime wind velocity in the inland city could help explain the larger daily range of correlations between wind velocity and CV of T_a, where higher daytime wind velocities were correlated with decreased spatial variation between 7:00 and 15:00 (Figure 2.12). Furthermore, similar average day and night wind velocities in the desert may help explain

the relatively consistent statistically significant correlations between NDVI and T_a in the daytime. Other weather events, particularly precipitation, may further drive daily patterns.

Like wind, rain also reduced vegetation effects along the climate gradient likely through reduced tree shading effects, direct cooling of impervious land surfaces, and homogenization of evapotranspiration (Landsberg 1981, Imhoff 2010, Zhao et al. 2014). Some rainy days had greater reductions in vegetation effects, which are a likely result of precipitation magnitude, timing, and duration. The largest reductions in ΔT_a were on the wettest day (DOY 259). Contrary to reduced vegetation effects, there were increases in spatial variation of T_a during rainy days for inland and desert cities. These increases in variation were less predictable since they were not correlated with increased vegetation effects. Examination of individual weather events on urban microclimate remains an important future research area.

Building on the "urban heat riskscape"

Understanding the spatiotemporal variation and drivers of vegetative cooling is important for reducing heat vulnerability (Demuzere et al. 2014, Vargo et al. 2016). I found at the local paired plot-scale (1 to 1.5 km) low vegetated areas have higher mean T_a and lower temporal variation in T_a primarily as a result of reduced nighttime vegetation cooling effects. Increases in temperatures that result from regional and global climate changes may reduce citywide T_a variation in arid and semi-arid cities. Although, urban environments typically have more intricate arrangements of land covers, so factors such

as changes in height-to-width ratio of the street, anthropogenic heat sources, surface albedo, tree canopy density, tree species, below tree ground cover, and tree age and vitality will likely add complexity to my findings (Taha 1997, Sashua-Bar and Hoffman 2000, Middle et al. 2014, Gillner et al. 2015). Furthermore, future work on the effects of buffer size when computing NDVI could refine vegetation effects on microclimate variation. My findings are in contrast with LST studies that have shown warming conditions may lead to greater urban vegetation cooling effects (Jenerette et al 2011, Jenerette et al. 2016, Tayyebi and Jenerette 2016). Nighttime vegetation cooling effects, important for mitigating urban warming, are driven by divergent processes across the region. While hotter nights are associated with increased spatial variation only in the inland city, exacerbating city-wide temperature inequities, there are reduced spatial effects of hotter nights in coastal and desert cities. Such regional climate considerations are important for designing geographically specific mitigation strategies.

Increasing urban vegetation is one strategy for mitigating urban warming (Larsen 2015), but there are confounding impediments. These include economic and resources costs associated with purchasing, planting and maintaining vegetation over its entire life cycle (Jenerette et al. 2011, Pataki et al. 2011, McPherson and Kendall 2014, Demuzere et al. 2014). Increasing vegetation offers greater nighttime cooling effects in inland and desert cities but may do little to reduce daytime T_a, especially on hotter days associated with higher wind velocity. Regardless, trees may decrease daytime human perceived temperatures through shading (Klemm et al. 2015, Taleghani et al. 2016). Furthermore, with increased irrigation and decreased wind velocity high-vegetated areas increase RH,

subsequently increasing the HI, potentially countering T_a cooling benefits (Potchter et al. 2006). Nevertheless, I found increases in HI are minimal compared to cooling benefits. More humid environments may be affected differently as high T_a was often associated with low RH in my study system. There are a wide range of mitigation strategies to reduce the effects of urban warming besides increasing urban vegetation; some of these include increasing albedo of building surfaces and spacing between buildings, and constructing a variety of different green infrastructures to increase evaporative cooling (Grimmond 2007, Demuzere et al. 2014, Wong and Jim 2015, Taleghani et al. 2016). Any mitigation strategy should consider trade-offs between geographic and temporally specific urban cooling benefits, and economic and resource costs.

Conclusions

I found the greatest vegetation cooling effects and T_a reductions in the evening hours, with minimal effects observed during midday. This effect increased in strength from coastal to desert cities. This "U-shaped" daily T_a vegetation cooling effect resulted in more daily and seasonal variation in high-vegetated areas which had a broader range of temperatures. Vegetation also increased RH and HI in the inland city, although these effects were limited. Furthermore, in the coastal city hotter days were correlated with increases in spatial variation in T_a while in inland and desert cities hotter days were correlated with reductions in spatial variation, and consequently areas of temperature refuge. Nighttime spatial variation in microclimate also differed among cities. In the

inland city, hotter nights were associated with increases in spatial variation in T_a, which likely increase inequities in urban temperatures. These patterns were partially explained by differences in wind velocity. Higher wind velocity was associated with reductions in spatial variation most in the inland areas, but this effect was not consistent across the climate gradient. Together these findings show that urban vegetation had consistent microclimate atmospheric cooling effects that primarily occur during the evening and are influenced by mesoclimate distributions and meteorological conditions.

Literature cited

Armson, D., M. A. Rahman, and A. R. Ennos. 2013. A comparison of the shading effectiveness of five street tree species in Manchester, UK. Arboriculture & Urban Forestry **39**:157-164.

Brazel, A., N. Selover, R. Vose, and G. Heisler. 2000. The tale of two climates—Baltimore and Phoenix urban LTER sites. Climate Research **15**:123-135.

Brazel, A., P. Gober, S. Lee, S. Grossman-Clark, J. Zehnder, B. Hedquist, and E. Comparri. 2007. Determinants of change in the regional urban heat island in metropolitan Phoenix (Arizona, USA) between 1990 and 2004. Climate Research **33**:171-182.

Buyantuyev, A., and J. G. Wu. 2010. Urban heat island and landscape heterogeneity: Linking spatiotemporal variations in surface temperature to land-cover and socioeconomic patterns. Landscape Ecology **25**:17-33.

Cao, X., A. Onishi, J. Chen, and H. Imura. 2010. Quantifying the cool island intensity of urban parks using ASTER and IKONOS data. Landscape and Urban Planning **96**:224-231.

Chakraborty, S. D., Y. Kant, and D. Mitra. 2015. Assessment of land surface temperature and heat fluxes over Delhi using remote sensing data. Journal of Environmental Management **148**:143-152.

Chow, W. T. L., A. Pope, C. A. Martin, and A. J. Brazel. 2011. Observing and modeling the nocturnal park cool island of an arid city: horizontal and vertical impacts. Theoretical and Applied Climatology **103**:197-211.

Chow, W. T. L., T. J. Volo, E. R. Vivoni, G. D. Jenerette, and B. L. Ruddell. 2014. Seasonal dynamics of energy balance in Phoenix, AZ. International Journal of Climatology **34**:3863-3880.

Coseo, P., and L. Larsen. 2014. How factors of land use/land cover, building configuration, and adjacent heat sources and sinks explain Urban Heat Islands in Chicago. Landscape and Urban Planning **125**:117-129.

Crum, S. M., L. L. Liang, and G. D. Jenerette. 2016. Landscape position influences soil respirations variability and sensitivity to physiological drivers in mixer-use lands of Southern California, USA. Journal of Geophysical Research: Biogeosciences **121**:2530-2543.

Davis, A. Y., J. Jung, B. C. Pijanowski, and E. S. Minor. 2016. Combined vegetation volume and "greenness" affect urban air temperature. Applied Geography **71**:106-114.

Declet-Barreto, J., A. J. Brazel, C. A. Martin, W. T. L. Chow, and S. L. Harlan. 2013. Creating the park cool island in an inner-city neighborhood: heat mitigation strategy for Phoenix, AZ. Urban Ecosystems **16**:617-635.

Demuzere, M., K. Orru, O. Heidrich, E. Olazabal, D. Geneletti, H. Orru, A. G. Bhave, N. Mittal, E. Feliu, and M. Faehnle. 2014. Mitigating and adapting to climate change: Multi-functional and multi-scale assessment of green urban infrastructure. Journal of Environmental Management **146**:107-115.

Feyisa, G. L., K. Dons, and H. Meilby. 2014. Efficiency of parks in mitigating urban heat island effect: An example from Addis Ababa. Landscape and Urban Planning **123**:87-95.

Gallo, K. P., A. L. McNab, T. R. Karl, J. F. Brown, J. J. Hood, and J. D. Tarpley. 1993. The use of a vegetation index for assessment of the urban heat island effect. International Journal of Remote Sensing **14**:2223-2230.

Gillner, S., J. Vogt, S. Dettman, and A. Roloff. 2015. Role of street trees in mitigating effects of heat and drought at highly sealed urban sites. Landscape and Urban Planning **143**:33-42.

Grimm, N. B., J. M. Grove, S. T. Pickett, and C. L. Redman. 2000. Integrated approaches to long-term studies of urban ecological systems. BioScience **50**:571-584.

Grimmond, S. 2007 Urbanization and global environmental change: local effects of urban warming. The Geographical Journal **173**:83-88.

Wong, G. K. L., and C. Y. Jim. 2015. Identifying keystone meteorological factors of green-roof stormwater retention to inform design and planning. Landscape and Urban Planning **143**:173-182.

Hall, S. J., J. Learned, B. Ruddell, K. L. Larson, J. Cavender-Bares, N. Bettez, P. M. Groffman, J. M. Grove, J. B. Heffernan, S. E. Hobbie, J. L. Morse, C. Neill, K. C. Nelson, J. P. M. O'Neil-Dunne, L. Ogden, D. E. Pataki, W. D. Pearse, C. Polsky, R. R. Chowdhury, M. K. Steele, and T. L. E. Trammell. 2016. Convergence of microclimate in residential landscapes across diverse cities in the United States. Landscape Ecology **31**:101-117.

Harlan, S. L., S. T. Yabiku, L. Larsen, and A. J. Brazel. 2009. Household water consumption in an arid city: affluence, affordance, and attitudes. Society & Natural Resources **22**:691-709.

Imhoff, M. L., P. Zhang, R. E. Wolfe, and L. Bounoua. 2010. Remote sensing of the urban heat island effect across biomes in the continental USA. Remote Sensing of Environment **114**:504-513.

Jenerette, G. D., S. L. Harlan, A. Brazel, N. Jones, L. Larsen, and W. L. Stefanov. 2007. Regional relationships between surface temperature, vegetation, and human settlement in a rapidly urbanizing ecosystem. Landscape Ecology **22**:353-365.

Jenerette, G. D., S. L. Harlan, W. L. Stefanov, and C. A. Martin. 2011. Ecosystem services and urban heat riskscape moderation: water, green spaces, and social inequality in Phoenix, USA. Ecological Applications **21**: 2637-2651.

Jenerette, G. D., G. Miller, A. Buyantuev, D. E. Pataki, T. W. Gillespie, and S. Pincetl. 2013. Urban vegetation and income segregation in drylands: a synthesis of seven metropolitan regions in the southwestern United States. Environmental Research Letters doi:10.1088./1748-9326/8/4/044001

Jenerette, G. D., S. L. Harlan, A. Buyantuev, W. L. Stefanov, J. Declet-Barreto, B. L. Ruddell, S. W. Myint, S. Kaplan, and X. Li. 2016. Micro-scale urban surface temperatures are related to land-cover features and residential heat related health impacts in Phoenix, AZ USA. Landscape Ecology **31**:745-760.

Klemm, W., B. G. Heusinkveld, S. Lenzholzer, and B. van Hove. 2015. Street greenery and its physical and psychological impact on thermal comfort. Landscape and Urban Planning **138**:87-98.

Landsberg, H. E. 1981. The urban climate. Academic Press, New York, NY, USA

Larsen, L. 2015. Urban climate and adaptation strategies. Frontiers in Ecology and the Environment **13**:486-492.

Lazzarini, M., P. R. Marpu, and H. Ghedira. 2013. Temperature-land cover interactions: The inversion of urban heat island phenomenon in desert city areas. Remote Sensing of Environment **130**:136-152.

Liang, L. L., R. G. Anderson, S. A. Shiflett, and G. D. Jenerette. *In Revisions*. Urban outdoor water use and response to drought assessed through mobile energy balance and vegetation greenness measurements. Environmental Research Letters. Revisions requested March 20, 2017.

Lin, B. S., and Y. J. Lin. 2010. Cooling effect of shade trees with different characteristics in a subtropical urban park. HortScience **45**:83-86.

McPherson, E. G., and A. Kendall. 2014. A life cycle carbon dioxide inventory of the Million Trees Los Angeles program. The International Journal of Life Cycle Assessment **19**:1653-1665.

Middle, A., K. Häb, A. J. Brazel, C. A. Martin, and S. Guhathakurta. 2014. Impact of urban form and design on mid-afternoon microclimate in Phoenix Local Climate Zones. Landscape and Urban Planning **122**:16-28.

Myint, S. W., E. A. Wentz, A. J. Brazel, and D. A. Quattrochi. 2013. The impact of distinct anthropogenic and vegetation features on urban warming. Landscape Ecology **28**:959-978.

Oke, T. R. 1973. City size and the urban heat island. Atmospheric Environment **7**:769-779.

Osborne, J. W., and A. Overbay. 2004. The power of outliers (and why researchers should ALWAYS check for them). Practical Assessment, Research & Evaluation **9** Available online: http://PAREonline.net/getvn.asp?v=9&n=6.

Pataki, D. E., C. G. Boone, T. S. Hogue, G. D. Jenerette, J. P. McFadden, and S. Pincetl. 2011. Ecohydrology bearings-invited commentary socio-ecohydrology and the urban water challenge. Ecohydrology **4**:341-347.

Potchter, O., P. Cohen, and A. Bitan. 2006. Climatic behavior of various urban parks during hot and humid summer in the mediterranean city of Tel Aviv, Israel. International Journal of Climatology **26**:1695-1711.

Ramamurthy, P., and E. Bou-Zeid. 2017. Heatwaves and urban heat islands: A comparative analysis of multiple cities. Journal of Geophysical Research: Atmospheres **122**:168-178.

Roberts, D. A., P. E. Dennison, K. L. Roth, K. Dudley, and G. Hully. 2015. Relationships between dominant plant species, fractional cover and land surface temperature in Mediterranean ecosystem. Remote Sensing and Environment **167**:152-167.

Roth, M., T. R. Oke, and W. J. Emery. 1989. Satellite-derived urban heat islands from three coastal cities and the utilization of such data in urban climatology. International Journal of Remote Sensing **10**:1699-1720.

Rothfusz, L. P. 1990. 'Heat index "equation" (or, more than you ever wanted to know about heat index)'. NWS technical attachment SR 90-23, National Weather Service, http://www.srh.noaa.gov/images/ffc/pdf/ta_htindx.PDF.

Santamouris, M. 2015. Analyzing the heat island magnitude and characteristics in one hundred Asian and Australian cities and regions. Science of the Total Environment **512**:582-598.

Shashua-Bar, I., and M. E. Hoffman. 2000. Vegetation as a climatic component in the design of an urban street: An empirical model for predicting the cooling effect of urban green areas with trees. Energy and Buildings **31**:221-235.

Shiflett, S. A., L. L. Liang, S. M. Crum, G. L. Feyisa, J. Wang, and G. D. Jenerette. 2017. Variation in the urban vegetation, surface temperature, air temperature nexus. Science of the Total Environment **579**:495-505.

Skelhorn, C., S. Lindley, and G. Levermore. 2014. The impact of vegetation types on air and surface temperatures in a temperate city: A fine scale assessment in Manchester, UK. Landscape and Urban Planning **121**:129-140.

Souch, C. A., and C. Souch. 1993. The effect of trees on summertime below canopy urban climates: A case study Bloomington, Indiana. Journal of Arboriculture **19**:303-312.

Steadman, R. G. 1979. The assessment of sultriness. Part I: A temperature-humidity index based on human physiology and clothing science. American Meteorological Society **18**:861-873.

Stone, B., J. Vargo, and D. Habeeb. 2012. Managing climate change in cities: Will climate action plans work? Landscape and Urban Planning **107**:263-271.

Streiling, S., and A. Matzarakis. 2003. Influence of single and small clusters of trees on the bioclimate of a city: A case study. Journal of Arboriculture **29**:309-316.

Taha, H. 1997. Urban climates and heat islands: Albedo, evapotranspiration, and anthropogenic heat. Energy and Buildings **25**:99-103.

Taleghani, M., D. Sailor, and G. A. Ban-Weiss. 2016. Micrometeorological simulations to predict the impacts of heat mitigation stratagies on pedestrian thermal comfort in a Los Angeles neighborhood. Environemntal Research Letters doi:10.1088/1748-9326/11/2/024003.

Tayyebi, A., and G. D. Jenerette. 2016. Increases in the climate change adaptation effectiveness and availability of vegetation across a coastal to desert climate gradient in metropolitan Los Angeles, CA, USA. Science of the Total Environment **548-549**:60-71.

Tucker, C. J. 1979 Red and photographic infrared linear combinations for monitoring vegetation. Remote Sensing of Environment **8**:127-150.

Turner, D. P., W. B. Cohen, R. E. Kennedy, K. S. Fassnacht, and J. M. Briggs. 1999. Relationships between leaf area index and Landsat TM spectral vegetation indices across three temperate zone sites. Remote Sensing of Environment **70**:52-68.

Vahmani, P., and G. A. Ban-Weiss. 2016. Climatic consequences of adopting drought-tolerant vegetation over Los Angeles as a response to California drought. Geophysical Research Letters **43**:8240-8249.

van Leeuwen, W. J. D., B. J. Orr, S. E. Marsh, and S. M. Herrmann. 2006. Multi-sensor NDVI data continuity: uncertainties and implications for vegetation monitoring applications. Remote Sensing of Environment **100**:67-81.

Vargo, J., B. Stone, D. Habeeb, P. Liu, and A. Russell. 2016. The social and spatial distribution of temperature-related health impacts from urban heat island reduction policies. Environmental Science & Policy **66**:366-374.

Yang, F., S. S. Y. Lau, and F. Qian. 2011 Urban design to lower summertime outdoor temperatures: an empirical study on high-rise housing in Shanghai. Building and Environment **46**:769-785.

Zhao, L., X. Lee, R. B. Smith, and K. Oleson. 2014. Strong contributions of local background climate to urban heat islands. Nature **511**:216-219.

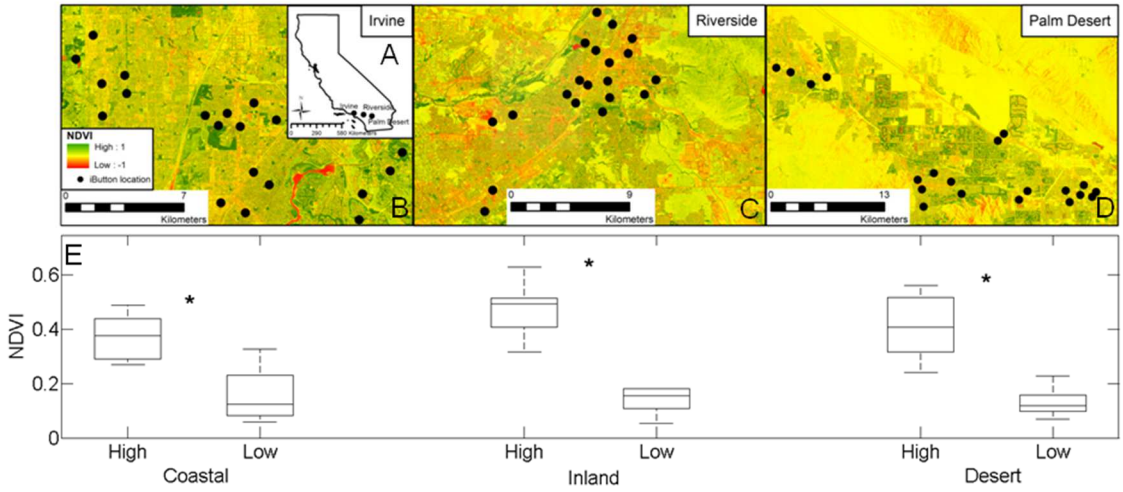

Figure 2.1 Site description for summer 2015 and 2016 study periods. (a) Coastal to desert transect in southern California including the three study cities Irvine, Riverside, and Palm Desert. (b,c,d) NDVI of each city with iButton air temperature sensor locations. Relative humidity and air temperature iButton sensors were placed in the same locations in Riverside during the 2016 study period. All sensors were mounted in street side trees. (e) Boxplot of NDVI in high- and low-vegetated locations at 90m radius resolution along the climate gradient. In all cases high-vegetated sites had greater NDVI than low-vegetated sites using Student's *t*-test ($P<0.05$).

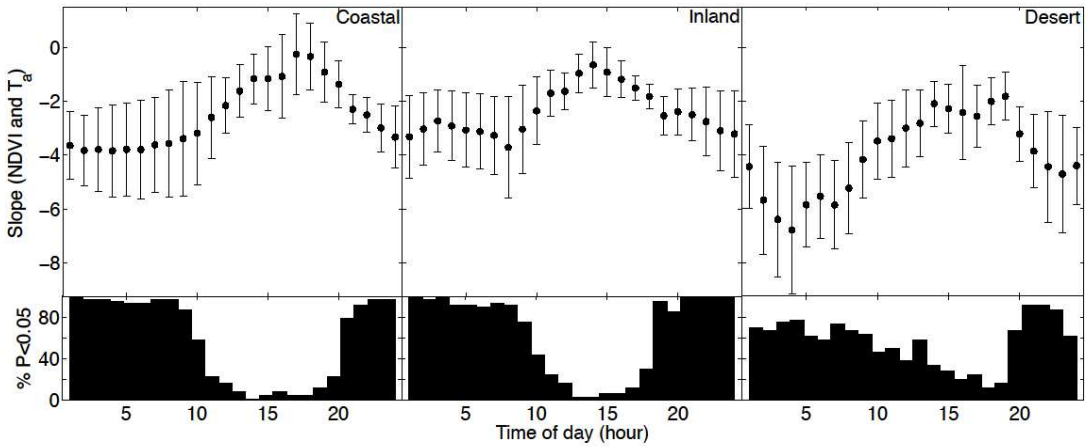

Figure 2.2 Daily changes in slope of NDVI at 90m radius resolution and air temperature (±SD), with frequency of P<0.05 along the climate gradient in 2015.

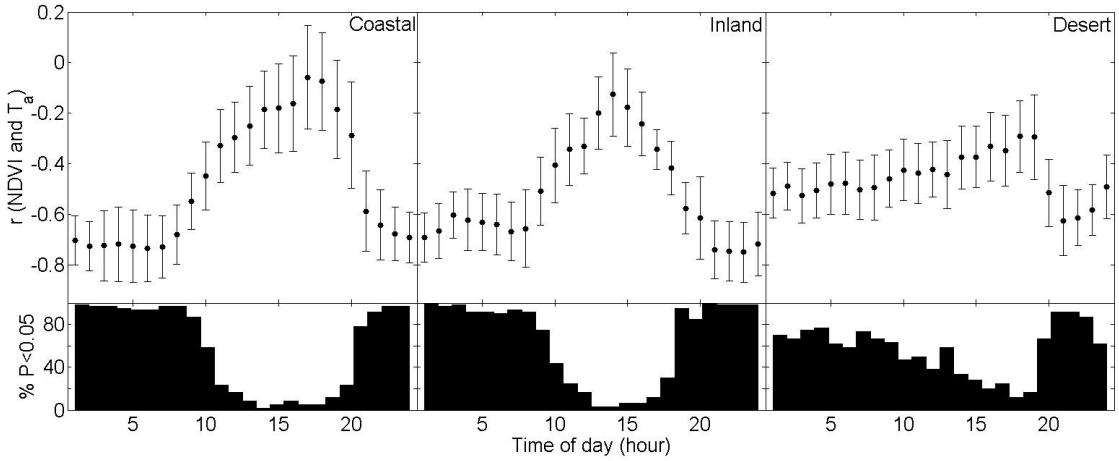

Figure 2.3 Daily changes in the Pearson correlation coefficient (r) of NDVI at 90m radius resolution and air temperature (±SD), with frequency of $P<0.05$ along the climate gradient. Equivalent relationships were found at 30m radius resolution.

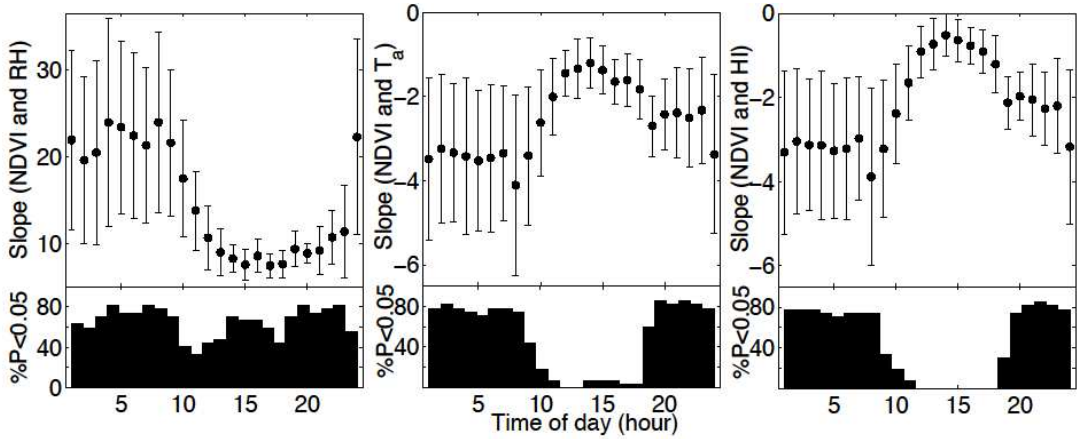

Figure 2.4 Daily changes in slope of NDVI at 90m radius resolution and relative humidity, air temperature, and heat index (±SD) with frequency of P<0.05 in the inland city in 2016. Plots were in the same locations as the 2015 study (n=20).

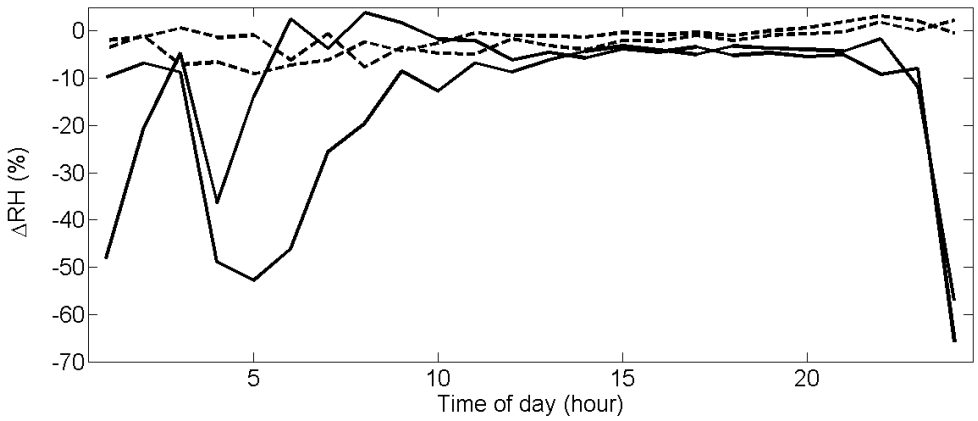

Figure 2.5 Percent change in relative humidity (ΔRH) for four representative paired plots in the inland city for 2016 (DOY 230). Some paired plots diverged radically in nighttime hours (solid lines), while others had consistent relationships throughout the day (dash lines). Two paired plots had unusually high nighttime ΔRH, with two hourly values greater than two standard deviations of the mean hourly difference. This indicates that the strong relationships between NDVI and RH at night may be driven by irrigation, which occurs primarily during the evening.

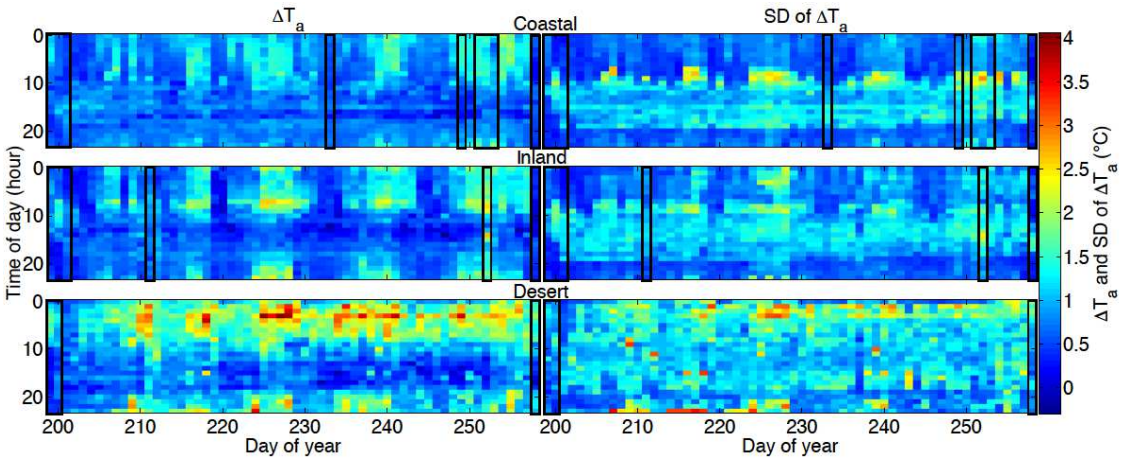

Figure 2.6 Heat map of the local vegetation temperature effects throughout the study period, low-vegetated minus high-vegetated cover (ΔT_a), with spatial standard deviation along the climate gradient. Black boxes indicate days with measurable precipitation.

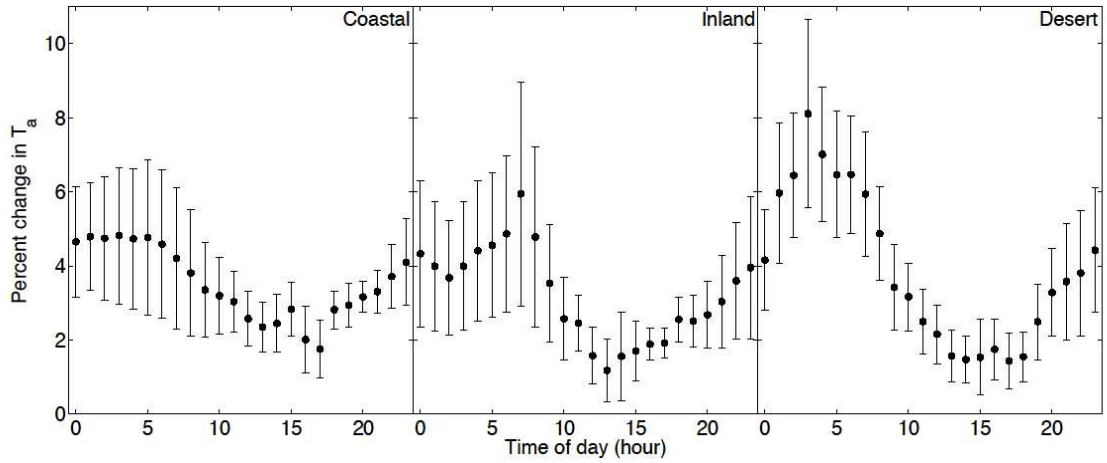

Figure 2.7 Normalized daily temperature effects (ΔT_a), or the percent change in air temperature between high- and low-vegetated plots (±SD), along the climate gradient. Low- and high-vegetated locations have little temperature difference in the day and greater difference at night. The effect is increased from coastal to desert cities.

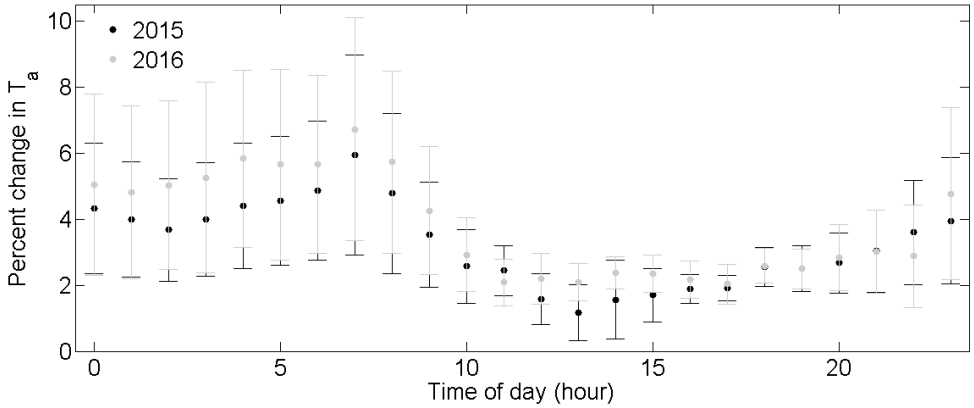

Figure 2.8 Normalized daily temperature effects (ΔT_a), or percent change in air temperature (±SD), for 2015 and 2016 campaigns in the inland city. Low- and high-vegetated locations have little temperature difference in the day and greater difference at night. ΔT_a was the same for both sampling periods ($P>0.05$, Student's *t*-test).

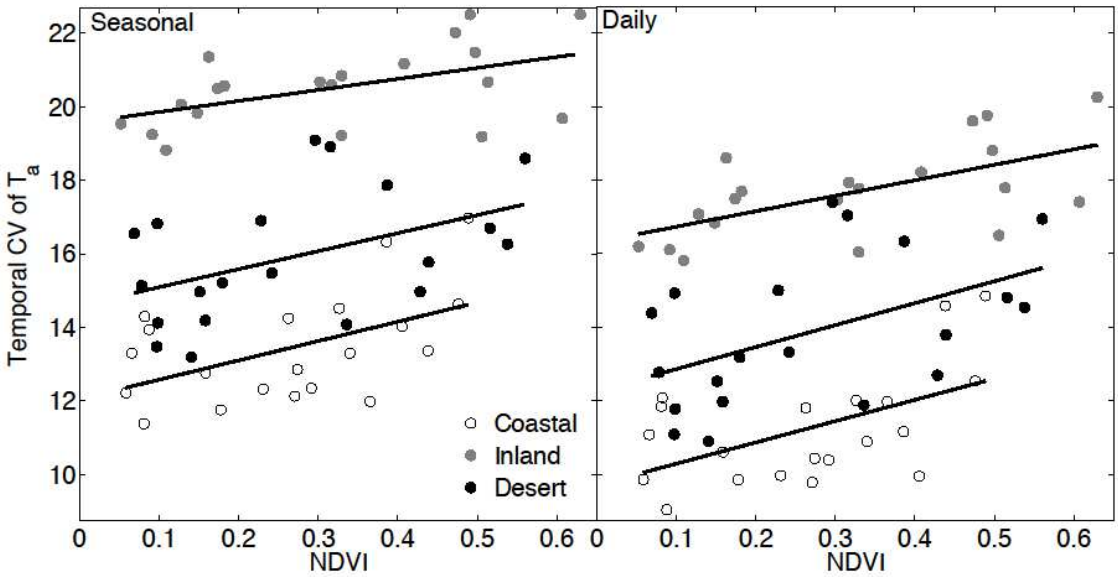

Figure 2.9 Temporal coefficient of variation of T_a is positively correlated to NDVI at 90m radius scale in the coastal, inland, and desert cities at both seasonal (R^2=0.26,0.25, and 0.21, respectively) and daily (R^2=0.29,0.37, and 0.24, respectively) scales (P<0.05). The relationships have similar slopes for both seasonal (Slope=5.3, 3.0, and 4.9, respectively) and daily (Slope=5.8, 4.2, and 6.0, respectively) scales across the climate gradient, with differences in overall variation. There are no significant correlations at 30 m radius scale.

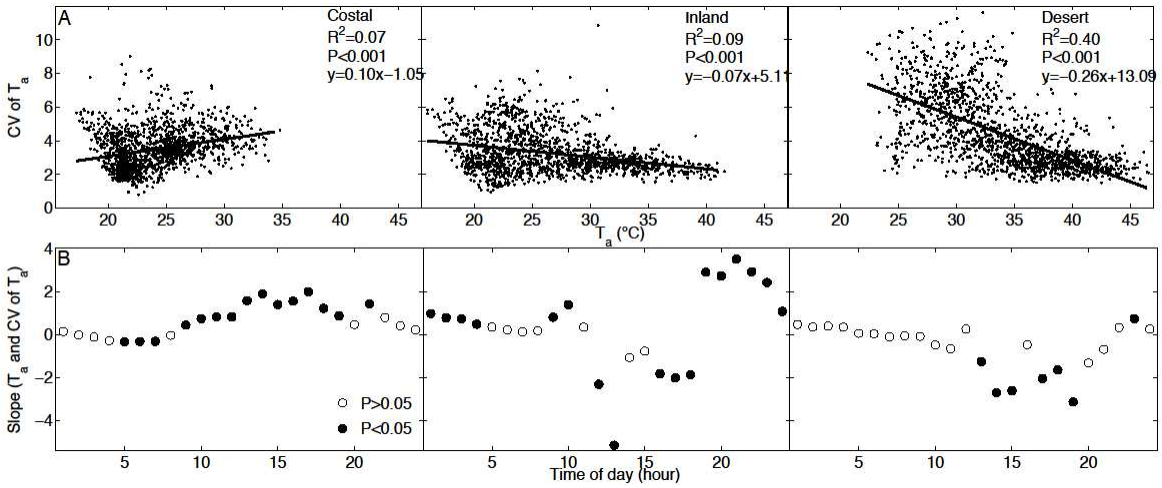

Figure 2.10 (a) Spatial variation of air temperature (CV of T_a) is positively correlated to mean air temperature (T_a) for the coastal city, while negatively correlated in the inland and desert cities. (b) In the day CV of T_a is positively correlated to T_a for the coastal city, while negatively correlated in the inland and desert cities, with reversed patterns at night. Each data point corresponds to the slope of the linear regression between citywide mean T_a and CV of T_a calculated hourly (n=60 per hour).

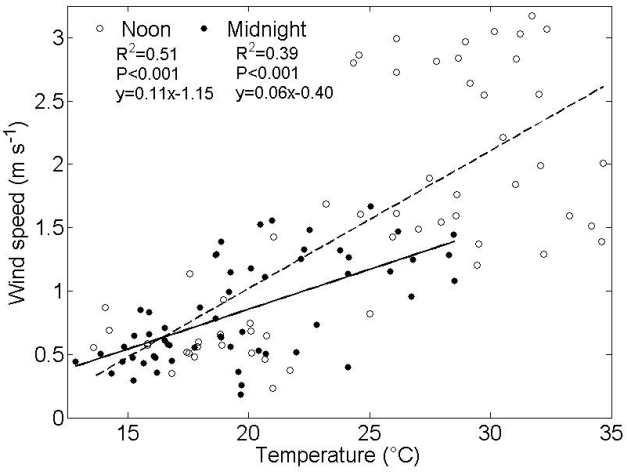

Figure 2.11 Mean air temperature is positively correlated to mean wind speed during both day and night in the inland city. Mean wind speed is generally higher during the day.

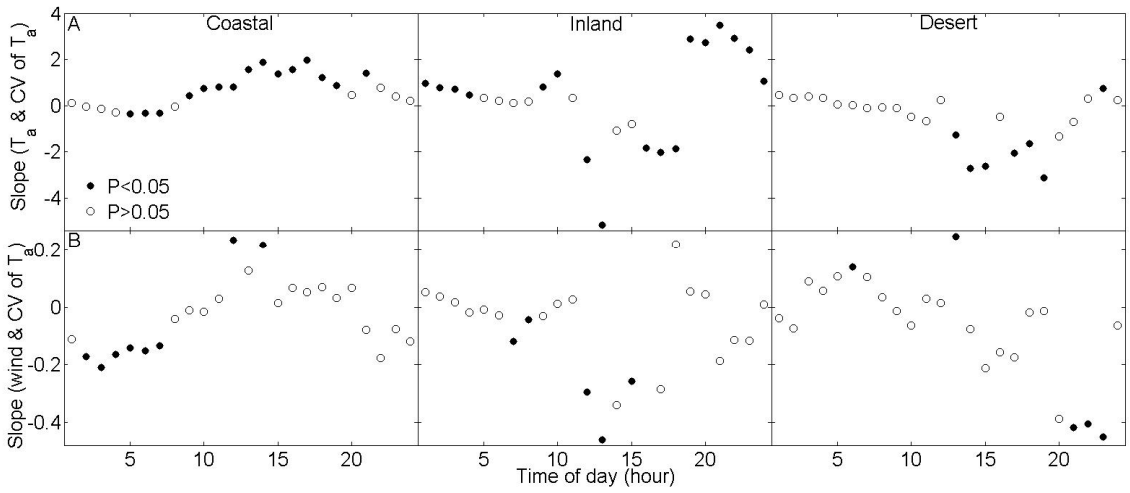

Figure 2.12 (a) Spatial variation of air temperature (CV of T_a) is positively correlated to mean air temperature (T_a) for the coastal city during the day, while negatively correlated in the inland and desert cities. (b) The correlations of CV of T_a and mean wind velocity explain some relationships found in the first panel. Each data point corresponds to the slope of the linear regression between citywide mean T_a and wind, and CV of T_a calculated hourly (n=60 per hour).

Chapter 3: Microclimate variation among urban land covers: The importance of vertical and horizontal structure in air and land surface temperature relationships

Abstract

Air and land surface warming effects from urbanization are of increasing concern due to expanding heat-related human health impacts in cities. While many studies have investigated land cover effects on air temperature (T_a) or land surface temperature (LST) individually, relatively few studies have examined the spatiotemporal relationships between these two heat indicators and other metrological variables. Here I asked: how does land cover influence local distributions of LST, T_a, and relative humidity (RH) and their interactions? I deployed a network of 30 air temperature and humidity sensors at two heights above the ground (0.1 and 1.5 m), along with a thermal camera and anemometer, during July 2016 over five common urban land covers—asphalt, bare surface, turf grass, short trees, and tall trees. Stronger T_a-LST relationships were observed at 0.1 m for asphalt (b=0.59), bare surface (b=0.63), and grass (b=1.08) land covers and, 1.5 m for short and tall tree covers (b=0.72, 0.89, respectively). Excluding the grass land cover, I found greater daytime than nighttime T_a-LST differences. Adding complexity to T_a-LST relationships, I found increasing spatial variation in LST during the day for short and tall tree land covers. Furthermore, both wind velocity and LST were correlated with T_a lapse rates. Finally, I found increased RH, and decreased LST, T_a, and VPD in vegetated covers. Through the use of thermal imagery and meteorological

measures I found that land cover affects patterns in microclimate, and that estimates of urban T_a using LST may improve with the use of land cover specific relationships.

Introduction

Urban microclimates are highly variable and respond in uncertain ways to characteristics of local land cover composition. Land cover may influence horizontal and vertical distributions of land surface temperature (LST), air temperature (T_a), and relative humidity (RH). Each of these microclimate components can impact human health and energy demand (Taha 1997, Harlan et al. 2006, Parris and Hazell 2005, Barreca and Schimshack 2012). At "human" scales of 1 to 100 meters vegetated and built land covers create heterogeneous patterns in air and land surface temperature that lead to cool refugia and warming hot spots within cities (Jenerette et al. 2016, Imhoff et al. 2010, Coseo and Larson 2014, Davis et al. 2016, Shiflett et al. 2017). Characterizing how vegetated and built land covers influence each of these microclimate components and their interrelationships remains an important research challenge.

T_a and LST are two distinct and complementary metrics of urban temperatures. Intraurban variation in T_a, associated with urban warming and cooling effects, is often greatest at night as surfaces re-emit heat at different rates and wind velocity is low (Oswald et al. 2012, Shiflett et al. 2017). However, LST variation is greatest during the day due to dynamic inputs in solar radiation (Buyantuyev and Wu 2010, Myint et al. 2013, Jenerette et al. 2016). Furthermore, maximum intraurban variation in T_a is

considerably less (e.g., 8 °C, Stabler et al. 2005) than that of LST (e.g., 25 °C, Jenerette et al. 2011). Thus, both the difference in timing and magnitude of variation contributes to a disconnect between T_a and LST. While land surfaces affect LST at micro-scales less than 10 m (Jenerette et al. 2016), land cover effects on T_a are frequently observed at larger scales of 20 to 500 m (Sashua-Bar and Hoffman 2000, Feyisa et al. 2014, Davis et al. 2016, Shiflett et al. 2017). These scaling differences in part are associated with lack of straightforward relationships between T_a and LST reflecting the complexities in the vertical and horizontal structure of urban land covers and its interaction with the local atmosphere (Hartz et al. 2006).

However, if relationships between T_a and LST can be identified, thermal imagery could then be used to model T_a—the standard metric of both regional and global climate warming. LST is typically measured from a relatively course spatial resolution, at 90m or larger scales (e.g., Roth et al. 1989, Imhoff et al. 2010, Zhao et al. 2014), a single time of day, and at varying heights both within and among pixels spanning tree canopies or roof tops to the ground. In contrast, most T_a measurements are recorded continuously at one height above the ground and over standardized land cover types—negating vertical and land cover variation in T_a. While fine-scale spatiotemporal variation in LST has begun to be studied in natural and built environments (Hartz et al. 2006, Tonolla et al. 2010, Gillner et al. 2015), little is known about land cover effects on fine-scale spatiotemporal variation of LST. Due to these potential sources of uncertainty, the T_a-LST linkage is rarely made and remains an important research challenge (Hartz et al. 2006, Schwarz et al. 2012). In support of this direction, some studies have identified significant

correlations between T_a and LST (e.g., Unger et al. 2009, Klock et al. 2012). When identified, the linkage between these two temperature metrics may vary throughout the day, with stronger relationships often observed at night (Kawashima et al. 2000, Schwarz et al. 2012, Shiflett et al. 2017). Stronger nighttime relationships between T_a and LST may potentially be due to lower wind velocities and reduced active heating of surfaces at night (Shiflett et al. 2017). While wind may have minimal effects on patterns of surface heat fluxes, T_a is influenced by air convection and mixing (Landsberg 1981, Imhoff 2010, Zhao et al. 2014, Stantamouris 2015). Thus, using LST to represent local atmospheric conditions can lead to uncertainties in cooling effectiveness of different urban management strategies.

In moderating urban heat, vegetation is frequently highlighted as a valuable urban management strategy. However, the effects of vegetation on microclimate are not well characterized at fine scales of human experience. Vegetation can decrease T_a and LST by increasing latent heat flux via evapotranspiration, increasing surface albedo relative to built surfaces, and decreasing sensible heat flux via shading (Yang et al. 2011, Jenerette et al. 2011, Chakraborty et al. 2015). Alternatively, vegetation may increase nighttime temperatures by providing insulation from high wind velocities which reduces the dissipation of surface radiation to the surrounding environment (Gillner et al. 2015). These microclimate effects may vary with the extent of canopy cover and vegetation type. Individual large tree canopies can reduce T_a from 1 to 2.5 °C (Streiling and Matarakis 2003, Lin and Lin 2010, Lee et al. 2013), while small-isolated tree canopies

may have no effect on T_a (Armson et al. 2013). Likewise, turf grass land cover may reduce both T_a (Chang et al. 2008) and LST (Jenerette et al. 2016) in urban areas.

In addition to influencing LST and T_a, vegetated land covers in arid and semi-arid environments are also associated with higher rates of evapotranspiration and lower wind velocity which may lead to higher RH (Souch and Souch 1993, Potchter et al. 2006, Gillner et al. 2015). Higher humidity associated with vegetation may counter the direct cooling benefits through greater human-perceived temperatures (Steadman 1979; Hall et al. 2016), heat related mortality (Barreca and Schimshack 2012), and incidents of respiratory system diseases (Gao et al. 2014). Increasing RH will also lower vapor pressure deficits (VPD, Chen et al. 2012, Litvak et al. 2013, Hall et al. 2016)—an important variable determining aridity and tree physiological performance (Chen et al. 2012). The changes in RH and VPD associated with vegetation may vary with height above the ground due to moisture inputs from crown-level transpiration and ground-level irrigation.

To address the uncertainties in the relationships among measures of microclimate and the influence of built and vegetated land covers on these relationships, I asked: how does land cover influence microscale distributions of LST, T_a, and RH and their interactions? To address these questions, I analyzed patterns of T_a and RH lapse rates using sensors at two heights (0.1 and 1.5 m) at five common urban land cover types—asphalt, bare surface, turf grass, small tree, and tall tree—in Riverside, California, USA. To investigate air and surface temperature linkages, I measured LST at each land cover using tower-mounted high resolution thermal imagery over a 24 hour period. I further

explored the potential role of wind velocity on T_a and RH lapse rates. At vegetated land covers I predicted lower T_a and higher RH at the height of transpiring vegetation. Furthermore, I predicted higher T_a and lower RH at 0.1 m at asphalt and bare surfaces, due to increased surface temperatures and heat fluxes. Reflecting the vertical height of sun exposed surfaces, stronger T_a-LST relationships were predicted at 0.1 m at asphalt, bare surface, and grass land covers, and 1.5 m at short and tall canopies land covers. T_a-LST differences and T_a lapse rates were predicted to be larger during the day due to increased evaporative cooling effects and surface heat fluxes. Finally, I predicted that intra-land cover variation in LST would increase in the morning hours due to differential heating of surfaces. Understanding these land cover drivers of microclimate is a necessary step in predicting and mitigating urban warming effects (Oswald et al. 2012, Coseo and Larson 2014, Gillner et al. 2015, Davis et al. 2016).

Methods

Study site

My study site is located at the Agricultural Experiment Station (33.965, -117.338) at the University of California Riverside, USA. Riverside is a part of the Los Angeles metropolitan region of 18 million residents. The region is characterized by a Mediterranean climate with hot-dry summers and cool-wet winters, and spans a semi-arid coastal to arid desert climate gradient. Riverside is situated at an intermediate position of this climate gradient, with mean annual precipitation of 262 mm and mean annual

temperature of 19.6 °C. Average maximum summer temperatures are warm at 35.0 °C in July. At neighborhood scales, vegetation in this region can have a prominent effect on both T_a and LST (Tayyebi and Jenerette 2016, Shiflett et al. 2017). Characteristic of summer in this region, there was no precipitation during the sampling period.

Five plots located within 650 m of each other, representing common land covers—asphalt parking lot, bare soil surface, turf grass (*Festuca arundinacea* and *Poa pratensis* mixture), short Valencia orange orchard (*Citrus x sinensis*), and tall Valencia orange orchard—were selected. The bare surface cover was unvegetated loam soil with low gravimetric water content (0.22±0.1% at 5 cm, n=3). Both tree height and canopy cover were greater at the tall (4 m and 62.5%, respectively) compared to the short orchard (3 m and 50%, respectively). Interspace widths were the same for both short and tall orchards (3 m), with different tree widths (3 and 5 m, respectively). Interspace soil gravimetric water content was similar for both short and tall orchard covers (3.4±2.5% and 2.8±2.9% at 5 cm, respectively, n=3). The land cover plots were similar in size, ranging from approximately 6000 to 8500 m^2. All temperature and humidity measurements were collected in a 17-day time period from July 15th to July 31st 2016 (corresponding to Julian day of year (DOY) 197 and 213), during the warmest period of the year. Sunrise, solar noon, and sunset mid-way through the study (DOY 204) were at 5:55, 12:56, and 19:57 Pacific Daylight Time (PDT; UTC -7 h), respectively. Simultaneous with temperature and humidity measurements infrared imagery and wind velocity were recorded for a 24 hr period at each land cover.

Data acquisition

In order to test the effect of land cover on T_a at each of the five plots, three replicate temperature sensors separated by approximately four meters (iButton Thermocron DS1922L, Maxim Integrated Products, Inc., San Jose, California, USA) with an accuracy of ±0.5 °C from -10 to 65 °C were mounted at two heights (0.1 and 1.5 m) from the ground on white PVC pipes near the center of each plot (n=30). To explore RH effects, in each plot one temperature and humidity sensor (iButton Hydrocron DS1923, Maxim Integrated Products, Inc., San Jose, California, USA) with a temperature accuracy of ±0.5 °C from -10 to 65 °C and RH accuracy of ±0.5% from 0 to 100% was mounted at two heights (0.1 and 1.5 m) from the ground (n=10). These sensors are small, self-contained units with onboard memory, measuring 15 mm in diameter and 5 mm high. Readings were collected every hour throughout the study period. To shield each sensor from direct solar radiation, they were housed in custom 0.2 mm thick rigid polystyrene cylindrical white cups measuring 47 mm in diameter and 30 mm high. The bottoms of the shields were exposed to air, allowing adequate ventilation, with an additional radiation shield hanging 20 mm below the sensor to preclude direct surface long-wave radiation. To test the accuracy of the custom made radiation shield systems I hung three iButton sensors less than a meter away from a research-grade temperature sensor (HMP-60, Viasala, Helsinki, Finland) housed in a non-aspirated gilled radiation shield at the Agricultural Experiment Station for seven days. Temperature differences between the iButton and the HMP-60 sensors were not observed (2-sample t-test, P=0.64). Furthermore, most iButton measurements fell within two standard deviations of the mean

difference (SD=0.42 °C), with only 2% of measurements below and 2% above this indicator (Altman and Bland 1983), with no outliers (SD≥3, Osborne and Overbay 2004), and good linear fit (R^2=0.995, b=0.993 P<0.001, RMSE=0.20 °C).

Alongside T_a and RH observations, tower mounted LST thermal imagery in the 7.5 to 13 μm spectral range (SC660, FLIR, Inc., Nashua, New Hampshire, USA) with an accuracy of ±1.0 °C from -40 to 1500 °C was recorded every 15 min for a 24 hr period at each land cover. All five 24 hr sequences were recorded in succession on cloud-free days with average maximum solar irradiance of 861.00±6.26 W/m^2 (http://cimis.water.ca.gov/WSNReportCriteria.aspx Accessed Dec/7/2016) from July 16th to July 21st 2016. The thermal camera was mounted on a mobile tower 6 m above each surface at a 55° angle capturing approximately 20 x 15 m of surface area. This was the highest allowable angle at this height since steeper angles capture the platform of the mobile tower. Each 640 x 480 pixel thermal image was corrected for surface emissivity, distance of camera to surface, atmospheric temperature and humidity, and estimated camera temperature (Figure 3.1). Surface emissivity was estimated using values from prior studies (Lo and Quattrochi 2003, Chen 2015, Gao et al. 2015). I used emissivity values of 0.95 for asphalt, and short and tall trees, 0.93 for bare surface, and 0.97 for grass. Continuous thermal imaging of urban (e.g., Gillner et al. 2015) and natural (e.g., Tonolla et al. 2010) surfaces is a recent development. The methods I used to measure LST have been demonstrated to correlate well with, generally-reliable, thermocouple-measured surface temperature (Aubrecht et al. 2016). Furthermore, wind velocity effects on microclimate lapse rate were measured using an anemometer (Anemometer #3002,

Young, Inc., Traverse city, Michigan, USA) with an accuracy of ±0.5 ms^{-1} from 0 to 50 ms^{-1}, data were recorded every 15 min for a 24 hr period at each land cover. The anemometer was mounted on a leveled tripod 2 m above the ground.

Analysis

T_a, RH, VPD, LST land cover effects were quantified using several measures. Lapse rates in T_a, RH, and VPD were quantified at each land cover using the average difference between high (1.5 m) and low (0.1 m) sensors over the change in vertical height.

Lapse rate = (value at 1.5m - value at 0.1 m)/(ΔHeight) (Eq. 1)

Daily variation in land cover effects on lapse rates and the slope of the linear regression between T_a and RH were calculated using hourly averages from the entire study period. Steep hourly slopes from T_a and RH relationships indicate that warmer periods have a larger effect on RH. To quantify wind and LST effects on lapse rates of T_a and RH, linear regressions between T_a lapse rate and wind velocity, T_a lapse rate and LST, and RH lapse rate and wind velocity were analyzed. To quantify air and surface temperature relationships linear regressions between mean T_a at two heights and mean LST were calculated. Furthermore, differences between T_a and LST (ΔT) were calculated using hourly averages among T_a replicates over one representative 24 hr period. Finally, the coefficient of variation (CV) was used to quantify spatial variations in LST. The CV is a

dimensionless quantity of variation normalized by the sample mean; commonly expressed as a whole number percent, frequently used to assess spatiotemporal landscape variation (Crum et al. 2016). Unstandardized measures of variation (e.g., standard deviation) would not be suitable for this study since values change with the sample mean, obscuring relative changes in variation.

Results

There were differing land cover effects on microclimate, with greater cooling, RH, and lower VPD at vegetated compared to unvegetated land covers (Table 3.1). The cooling effect was largest between asphalt and grass land covers at 0.1 m with a mean T_a reduction of 5.54±2.97 °C. The largest mean T_a difference at 1.5 m was between asphalt and short tree land covers with a mean T_a reduction of 2.17±1.59 °C. RH varied among land covers, with the largest effect between grass and asphalt land covers with a mean reduction of 31.98±10.64 and 6.40±4.53 % at 0.1 and 1.5 m, respectively. Likewise, the largest land cover effect on mean VPD was between grass and asphalt with a mean increase of 1.21±0.55 and 0.23±0.14 kPa at 0.1 and 1.5 m, respectively. Correlations between T_a and RH at both heights over all land cover types were stronger during the night than the day, with weaker relationships at 0.1 m (Figure 3.2). There were no distinguishable changes in this relationship among land covers.

Microclimate lapse rates

T_a lapse rate, measured as the difference between T_a at 1.5 and 0.1 m over the change in vertical height, had strong daily patterns among land cover types (Figure 3.3). Lapse rates were generally negative for asphalt and bare surface land covers during the day (minimum lapse rate = -2.29±0.41 and -3.38±0.30 °C m^{-1} at 11:00 and 10:00, respectively) with values approaching zero at night. In contrast, lapse rates were generally positive for short and tall tree land covers during the day (maximum lapse rate = 2.52±1.57 and 1.47±0.42 °C m^{-1} at 14:00 and 13:00, respectively) with values approaching zero at night. The grass land cover had a different pattern, with positive lapse rates at night (maximum lapse rate = 3.02±0.91 °C m^{-1} at 21:00) and rapidly decreasing lapse rates during the day (minimum lapse rate = -1.92±1.40 °C m^{-1} at 10:00). Approximately one hour after sunrise (7:00) at the asphalt land cover there was an outlier in lapse rate. This outlier was >3 SD from the daily mean (-1.18±0.80 °C m^{-1}), and 6:00 and 8:00 values (-0.70±0.20 and -0.75±0.54 °C m^{-1}, respectively). After re-inspection of the site, solar reflection from nearby surfaces likely caused this unexpected value.

RH lapse rate had less noticeable daily patterns among land cover types than T_a lapse rates (Figure 3.3). RH lapse rates varied from positive (asphalt and bare surface) to negative (grass, and short and tall trees). There was a steep increase in lapse rates at 8:00 for both asphalt and bare surface land covers (maximum lapse rate = 6.57±2.37 and 7.74±3.92 % m^{-1} at 8:00 and 10:00, respectively), while grass had a steady decline starting at 11:00 (minimum lapse rate = -20.24±4.04 % m^{-1} at 14:00). There were

considerable differences in the range of lapse rates among land cover types from 2.47 % m^{-1} at the tall tree land cover to 13.38 % m^{-1} at the grass land cover.

VPD, which is derived from both T_a and RH data, had strong daily changes in lapse rate among land cover types that, excluding the grass land cover, reflected patterns in T_a lapse rate (Figure 3.4). Lapse rates were generally negative for asphalt and bare surface land covers during the day (minimum lapse rate = -0.95±0.17 and -1.40±0.15 kPa m^{-1} at 11:00 and 12:00, respectively) with values approaching zero at night. In contrast, lapse rates were generally positive for short and tall tree land covers during the day (maximum lapse rate = 1.02±0.73 and 0.65±0.37 kPa m^{-1} at 15:00 and 14:00, respectively) with values approaching zero at night. The grass land cover had a different pattern, with positive and increasing lapse rates during the day (maximum lapse rate = 1.70±0.67 kPa m^{-1} at 14:00).

For asphalt and bare surface land covers I observed a negative relationship between T_a lapse rate and wind velocity, with a stronger correlation at the asphalt land cover (Figure 3.5; R^2=0.41, P<0.001 and R^2=0.32, P<0.01, respectively). The counter-clockwise hysteresis-like effect at the bare surface plot may explain its weaker correlation. For short and tall tree land covers, I observed a positive relationship between T_a lapse rate and wind velocity, with a stronger correlation at the short tree land cover (R^2=0.71, P<0.001 and R^2=0.32, P<0.01, respectively). Conversely, I observed a negative relationship between RH lapse rate and wind velocity, with a stronger correlation at the short tree land cover (Figure 3.6; R^2=0.54, P<0.001 and R^2=0.52, P<0.001, respectively).

Land surface temperature variability

Land cover effects on LST differed in magnitude, variation, and timing (Figure 3.7a). The time of maximum LST varied between 12:00 and 14:00. The average maximum LST was at 13:00, near solar noon (12:55). The highest range in LST among land covers was 29.98 °C during the day at 14:00, and the lowest range was 7.77 °C before sunrise at 5:00. Asphalt was consistently the warmest surface throughout the day, while grass, and short and tall tree land covers were the coolest at different times.

Spatial CV of LST varied throughout the day among land covers (Figure 3.7b). There was increasing variation in both short and tall tree land covers during the day, with maximum values of 24.4 and 20.98 at 13:30 and 13:00, respectively. These increasing trends began shortly after sunrise around 6:30 and returned to nighttime levels shortly after sunset around 21:00. Asphalt, bare surface, and grass land covers have less noticeable patterns in variation of LST. Variation in the asphalt land cover was consistent throughout the day, except for a dip in variation shortly after sunrise and a spike in variation at 8:30. Variation of LST in the grass land cover was highest at night, before decreasing around sunrise with a steady increase in variation until topping out at 13:00. Furthermore, relative to bare and asphalt covers, vegetated covers had elevated variation at night.

Air and land surface temperature linkage

There were divergent T_a-LST relationships among land covers and heights (Table 3.2). The strongest correlation was between T_a at 0.1 m and LST in the asphalt land cover (R^2=0.97), while the weakest correlation was at 1.5 m in the grass land cover (R^2=0.84). For asphalt, bare surface, and grass land covers there were higher correlations at 0.1 m (R^2=0.97, 0.94, and 0.93, respectively) than 1.5 m (R^2=0.96, 0.92, and 0.84, respectively). Likewise, there were steeper slopes at 0.1 m (0.59, 0.63, and 1.08, respectively) than 1.5 m (0.53, 0.49, and 0.88, respectively). Conversely, for short and tall tree land covers there were higher correlations at 1.5 m (R^2=0.94 and 0.96, respectively) than 0.1 m (R^2=0.92 for both). Likewise, there were steeper slopes at 1.5 m (0.72 and 0.89, respectively) than 0.1 m (0.61 and 0.74, respectively).

Daily changes in the difference between T_a and LST (ΔT) at 1.5 and 0.1 m over five land covers show divergent relationships (Figure 3.8). While asphalt and bare surface land covers have the greatest ΔT at 1.5 m during the day (-24.82±0.34 and -18.74±0.60 °C at 13:00 and 12:00, respectively), grass, and short and tall tree land covers have the greatest ΔT at 0.1 m (11.19±0.94, -9.6±0.66, and -5.1±1.44 °C at 18:00, 12:00, and 12:00 respectively). ΔT was smallest for asphalt, grass, bare surface, and short and tall tree land covers during the night, morning, or late afternoon hours (-4.70±0.10, -0.5±0.28, and 0.39±0.45, 0.20±0.24, and -0.06±1.34 °C at 4:00, 4:00, 23:00, 7:00 and 17:00 respectively). Differences in ΔT between 1.5 and 0.1 m was greatest during the day for all land covers (3.64, 4.29, 5.31, 2.63, and 0.76 °C at 12:00, 13:00, 20:00, 13:00, and 14:00, respectively).

For asphalt, bare surface, and grass land covers I observed a negative relationship between T_a lapse rate and LST, with the strongest correlation at the bare surface land cover (Figure 3.9; R^2=0.65, 0.81, and 0.51 P<0.001, respectively). For short and tall tree land covers, I observed a positive relationship between T_a lapse rate and LST, with a stronger correlation at the short tree land cover (R^2=0.93 and 0.90, P<0.001, respectively).

Discussion

Important for human health and tree physiology (Jenerette et al. 2011, Barreca and Schimshack 2012, Litvak et al. 2013), I found vegetated land covers increased canopy level RH and decreased LST, T_a, and VPD. I further found relationships among wind velocity and micrometeorlogical lapse rates across contrasting land cover types. The resulting vertical profiles in micrometeorology were influenced by land cover specific LST relationships. The differences in surface and atmosphere temperatures among relatively homogeneous land covers likely explains the frequent uncertainties associated with LST data at coarse scales (<90 m) that include mixtures of land covers. Identifying how urban land covers differ in their surface-atmosphere temperature coupling has been noted as an important research challenge for predicting and reducing urban warming effects (Hartz et al. 2006, Schwarz et al. 2012, Shiflett et al. 2017) and this is the first study to quantify relationships between vertical T_a gradients and LST among common urban land covers. My single-patch evaluation provides direction for subsequent study of

T_a-LST relationships and other microclimate evaluations in more complex land cover configurations.

Relationships between vertical T_a gradients and T_a-LST relationships

I found that T_a lapse rates were coupled to T_a-LST relationships. Variation in lapse rates among land covers account in part for poor relationships between T_a and LST found previously in the literature where standard meteorological measurements generally do not characterize land cover effects on the vertical structure of T_a. In plots that have little three-dimensional structure, LST predominantly measures the ground surface. Supporting this hypothesis, in asphalt, bare surface, and grass plots I found stronger T_a-LST relationships at 0.1 m. While asphalt and bare surface land covers had higher T_a at 0.1 m, the grass land cover had lower temperatures at 0.1 m, indicating near-surface evaporative cooling by grass. Conversely, in plots that had greater three-dimensional structure, LST measures varying heights above ground level from the ground surface to the top of the canopy. Consistent with greater three-dimensional structure, at short and tall tree plots I found stronger T_a-LST relationships at 1.5 m. Additionally, positive T_a lapse rates at short and tall tree plots indicate canopy level warming or surface shading effects. Furthermore, indicating canopy size effects, I found stronger T_a-LST relationships at 1.5 m in the tall tree cover. Other micrometeorological factors, including wind velocity, may add complexity to the T_a-LST relationship.

While wind may have minimal effects on patterns of LST, T_a is strongly influenced by air convection and mixing (Landsberg 1981, Imhoff 2010, Zhao et al.

2014). At whole city scales, T_a differences between rural and urban areas are reduced during windy days (Landsberg 1981, Gallo et al. 1993, Santamouris 2015). Microadvection in the canopy layer, which mixes surface sensible and latent heat fluxes to the wider environment, is noted as a potential driver of T_a lapse rates and T_a-LST linkages (Roth et al. 1989, Schwarz et al. 2012, Shiflett et al. 2017). Using wind velocity data at each land cover plot, I found that as wind velocity approached zero so did T_a lapse rates for several land covers. Tree canopy sheltering effects from high daytime wind velocity are consistent with higher T_a lapse rates. Likewise, stronger nighttime T_a-LST linkages may have been driven by decreased nighttime wind velocity, creating less microadvection and a more direct connection between surface heat flux and T_a (Voogt and Oke 2003). Although, the three-dimensional structure of land cover surfaces, and associated canopy level warming or surface shading effects, may have been a stronger driver of T_a lapse rates and T_a-LST linkages (Kawashima et al. 2000, Schwarz et al. 2012, Shiflett et al. 2017). Both wind velocity and LST have similar daily patterns, while I did not find hysteresis, or lags, in their relationships with T_a lapse rate, isolating their individual effects remains an important research challenge. Investigating scaling effects on T_a lapse rate, and T_a-LST linkages, may further refine the role of wind velocity and LST drivers.

Implications of small-scale spatial variation in T_a and LST on their linkages

Due to differences in surface thermal properties and shading effects, there is typically greater daytime variability in LST between surfaces than within (Urger et al.

2009, Armson et al. 2012, Gillner et al. 2015). The short and tall tree land covers contain a mixture of surfaces, both canopy and bare soil interspace, and greater three-dimensional structure relative to the other land covers. Increased canopy shading effects and daytime differences in LST between canopy and interspace likely contributed to greater spatial variation I observed at short and tall tree land covers. The largest inter-land cover temperature range was observed at 14:00, near the time of highest intra-land cover spatial variation for short and tall trees. Also, there were lower levels of daytime LST variation in the tall tree land cover, likely due to the reduction of interspace area and increased ground level shading. These trends in variation may impact T_a-LST relationships, since land cover will contribute differently to near surface T_a (Oke 1982, Roth et al. 1989). Surfaces with higher daytime LST than T_a re-emit heat during the night as sensible heat flux (Landsberg 1981, Roth et al. 1989). Consistent with other urban warming studies, I found effects of small-scale surface thermal properties on LST, and cumulative-three dimensional thermal property and wind velocity effects on T_a (Voogt and Oke 2003, Lo and Quattrochi 2003, Stathopoulou and Cartalis 2007). In conjunction with resolving land cover effects on T_a and LST relationships, an important next step to my findings is a determination of the effects of spatial resolution on this linkage.

When quantifying land cover temperature effects, I further found important distinctions between LST and vertical gradients in T_a. As this study shows, LST does not have a consistent relationship with T_a across land cover types. Land use and land cover patches have irregular boundaries, contributing to mixed pixel error and poor T_a-LST linkage when using relatively course and spatially uniform units (Stone and Norman

2006, Schwarz et al. 2012). Furthermore, I found that vertical height and wind velocity impacted T_a-LST linkages. Slopes between T_a and LST among land covers at 1.5 m ranged from 0.49 to 0.89, consistent with prior estimates of urban T_a at 70% of LST warming (Klock et al. 2012). These findings suggest remote sensing studies that quantify urban warming effects through surface temperatures may over estimate (e.g., asphalt, bare surface, and tree land covers) or underestimate (e.g., grass land cover) the extent of T_a warming. Instead, a land cover specific approach of estimating urban T_a spatial variation using remotely sensed LST will likely be more useful especially for pixels with mixed land uses as typically acquired from satellite platforms.

Vegetation feedbacks to humidity and vapor pressure deficit

My results of higher canopy level RH at short and tall tree compared to asphalt land covers (6.2 and 6.1 %, respectively) were consistent with other studies that saw 0.5 to 6.4% (Gillner et al. 2015) and 9.0 to 20.0% (Souch and Souch 1993) increases beneath trees. I also observed higher RH in turf grass compared to other land covers (6.4 and 4.7 % increase over asphalt and bare surface, respectively). This finding, along with observed decreases in T_a at the grass land cover, is important since standardized weather measurements are typically made at 1.5 m over turf grass (WMO, 2008), thus studies that analyze urban microclimate using standardized meteorological stations may not capture upper range of T_a and lower range of RH in semi-arid environments. While I observed higher RH at short and tall tree land covers, there was not an increase in crown level (1.5 m) RH associated with transpiration compared to near surface (0.1 m) RH. This is

consistent with other studies that have found no effects, or a decrease, in crown level RH in urban trees, particularly at night when canopies provide shelter from dew (Gillner et al. 2015). Instead, I found increasing wind velocity minimizes RH lapse rates, indicating that wind may have larger effects on the upper canopy boundary layer. Despite no canopy level increases in RH, consistent with evapotranspiration feedbacks to reduced plant stress responses (Chen et al. 2012, Litvak et al. 2013) and increased irrigation effects on microclimate, I found both higher RH and lower VPD over vegetated land covers. This effect was most clear in the grass land cover where there were positive and increasing daytime VPD lapse rates despite a decreasing trend in T_a lapse rates.

Synthesis

I empirically evaluated vertical microscale atmospheric profiles and explicitly connected these to remotely sensed surface temperatures and show how land surface characteristics, from relatively simple bare surfaces to complex shading from trees, differ in their microclimate distributions. These findings empirically show that vertical variation can be as large as the differences between land covers as predicted from modeling studies (Taleghani et al. 2016). The large variation among land cover types in their vertical microclimate distributions is coupled to surface characteristics and is also influenced by larger scale meteorological variation. My findings help develop better assessments of urban heat risk and vulnerability that consider both surface and air characteristics. With the rapidly expanding use of surface temperature measurements to assess heat vulnerability (Jenerette et al. 2016), my results show how this remotely

sensed heat metric is connected to air temperature through land cover specific vertical functions. The vertical temperature profiles within the first 2 meters from the surface can have a strong influence on heat vulnerability, especially for children whose body core is closer to the ground (Vanos 2015, Vanos et al. 2016). Policy assessments of heat mitigation strategies that evaluate altered urban land cover patterns to reduce heat vulnerability currently do not factor the vertical temperature variation (Georgescu et al. 2014, Vahmani and Ban-Weiss 2016). Research directed to evaluating microclimate lapse rates and T_a-LST relationships in mixed urban land covers are important future directions to minimize potential urban heat vulnerability.

Literature cited

Altman, D. G., and J. M. Bland. 1983. Measurement in medicine: the analysis of method comparison studies. Statistician **32**:307-317.

Armson, D., P. Stringer, and A. R. Ennos. 2012. The effect of tree shade and grass on surface and globe temperatures in an urban area. Urban Forestry and Urban Greening **11**:245-255.

Armson, D., M. A. Rahman, and A. R. Ennos. 2013. A comparison of the shading effectiveness of five street tree species in Manchester, UK. Arboriculture and Urban Forestry **39**:157-164.

Aubrecht, D. M., B. R. Helliker, M. L. Goulden, D. A. Roberts, C. J. Still, and A. D. Richardson. 2016. Continuous, long-term, high-frequency thermal imaging of vegetation: Uncertainties and recommended best practices. Agricultural and Forest Meteorology **228**:315-326.

Barreca, A. I., and J. P. Schimshack. 2012. Absolute humidity, temperature, and influenza mortality: 30 years of country-level evidence from the United States. American Journal of Epidemiology **176**:114-122.

Buyantuyev, A., and J. G. Wu. 2010. Urban heat island and landscape heterogeneity: Linking spatiotemporal variations in surface temperature to land-cover and socioeconomic patterns. Landscape Ecology **25**:17-33.

Chakraborty, S. D., Y. Kant, and D. Mitra. 2015. Assessment of land surface temperature and heat fluxes over Delhi using remote sensing data. Journal of Environmental Management **148**:143-152.

Chen, L., Z. Zhang, and B. E. Ewers. 2012. Urban tree species show the same hydraulic response to vapor pressure deficit across varying tree size and environmental conditions. PLoS ONE doi:10.1371/journal.pone.0047882.

Chen, C. 2015. Determining the leaf emissivity of three crops by infrared thermometry. Sensors **15**:11387-11401.

Coseo, P., and L. Larsen. 2014. How factors of land use/land cover, building configuration, and adjacent heat sources and sinks explain urban heat islands in Chicago. Landscape and Urban Planning **125**:117-129.

Crum, S. M., L. L. Liang, and G. D. Jenerette. 2016. Landscape position influences soil respirations variability and sensitivity to physiological drivers in mixer-use lands of Southern California, USA. Journal of Geophysical Research: Biogeosciences **121**:2530-2543.

Davis, A. Y., J. Jung, B. C. Pijanowski, and E. S. Minor. 2016. Combined vegetation volume and "greenness" affect urban air temperature. Applied Geography **71**:106-114.

Demuzere, M., K. Orru, O. Heidrich, E. Olazabal, D. Geneletti, H. Orru, A. G. Bhave, N. Mittal, E. Feliu, and M. Faehnle. 2014. Mitigating and adapting to climate change: Multi-functional and multi-scale assessment of green urban infrastructure. Journal of Environmental Management **146**:107-115.

Feyisa, G. L., K. Dons, and H. Meilby. 2014. Efficiency of parks in mitigating urban heat island effect: An example from Addis Ababa. Landscape and Urban Planning **123**:87-95.

Gallo, K. P., A. L. McNab, T. R. Karl, J. F. Brown, J. J. Hood, and J. D. Tarpley. 1993. The use of a vegetation index for assessment of the urban heat island effect. International Journal of Remote Sensing **14**:2223-2230.

Gao, J., Y. Sun, Y. Lu, and L. Li. 2014. Impact of ambient humidity on child health: a systematic review. PLoS ONE doi:10.1371/journal.pone.0112508.

Gao, C. X., Y. G. Qian, N. Wang, L. L. Ma, and X. G. Jiang. 2015. Land surface emissivity retrieval from airborne hyperspectral scanner thermal infrared data over urban surfaces. International Conference on Intelligent Earth Observing and Applications 2015 doi:10.1117/12.2220606.

Georgescu, M., P. E. Morefield, B. G. Bierwagen, and C. P. Weaver. 2014. Urban adaptation can roll back warming of emerging megapolitan regions. Proceedings of the National Academy of Sciences U. S. A. **111**:2909-2914.

Gillner, S., J. Vogt, S. Dettman, and A. Roloff. 2015. Role of street trees in mitigating effects of heat and drought at highly sealed urban sites. Landscape and Urban Planning **143**:33-42.

Grimmond, S. 2007. Urbanization and global environmental change: local effects of urban warming. The Geographical Journal **173**:83-88.

Hall, S. J., J. Learned, B. Ruddell, K. L. Larson, J. Cavender-Bares, N. Bettez, P. M. Groffman, J. M. Grove, J. B. Heffernan, S. E. Hobbie, J. L. Morse, C. Neill, K. C. Nelson, J. P. M. O'Neil-Dunne, L. Ogden, D. E. Pataki, W. D. Pearse, C. Polsky, R. R. Chowdhury, M. K. Steele, and T. L. E. Trammell. 2016. Convergence of microclimate in residential landscapes across diverse cities in the United States. Landscape Ecology **31**:101-117.

Harlan, S. L., A. J. Brazel, L. Prashad, W. L. Stefanov, and L. Larsen. 2006. Neighborhood microclimates and vulnerability to heat stress. Social Science and Medicine **63**:2847-2863.

Hartz, D. A., L. Prashad, B. C. Hedquist, J. Golden, and A. J. Brazel. 2006. Linking satellite images and hand-held infrared thermography to observed neighborhood climate conditions. Remote Sensing of the Environment **104**:190-200.

Imhoff, M. L., P. Zhang, R. E. Wolfe, and L. Bounoua. 2010. Remote sensing of the urban heat island effect across biomes in the continental USA. Remote Sensing of the Environment **114**:504-513.

Jenerette, G. D., S. L. Harlan, W. L. Stefanov, and C. A. Martin. 2011. Ecosystem services and urban heat riskscape moderation: water, green spaces, and social inequality in Phoenix, USA. Ecological Applications **21**:2637-2651.

Jenerette, G. D., S. L. Harlan, A. Buyantuev, W. L. Stefanov, J. Declet-Barreto, B. L. Ruddell, S. W. Myint, S. Kaplan, and X. Li. 2016. Micro-scale urban surface temperatures are related to land-cover features and residential heat related health impacts in Phoenix, AZ USA. Landscape Ecology **31**:745-760.

Kawashima, S., T. Ishida, M. Minomura, and T. Miwa. 2000. Relations between surface temperature and air temperature on a local scale during winter nights. Journal of Applied Meteorology **39**:1570-1579.

Klock, L., S. Zwart, H. Verhagen, and E. Mauri. 2012. The surface heat island of Rotterdam and its relationship with urban surface characteristics. Resources, Conservation and Recycling **64**:23-29.

Landsberg, H. E. 1981. The urban climate. Academic Press, New York, NY, USA

Larsen, L. 2015. Urban climate and adaptation strategies. Frontiers in Ecology and the Environment **13**:486-492.

Lee, H., J. Holst, and H. Mayer. 2013. Modification of human-biometeorologically significant radiant flux densities by shading as local method to mitigate heat stress in summer within urban street canyons. Advances in Meteorology 2013.

Lin, B. S., and Y. J. Lin. 2010. Cooling effect of shade trees with different characteristics in a subtropical urban park. HortScience **45**:83-86.

Litvak, E., N. Bijoor, and D. E. Pataki. 2013. Adding trees to irrigated turfgrass lawns may be a water saving measure in semi-arid environments. Ecohydrology **7**:1314-1330.

Lo, C. P., and D. A. Quattrochi. 2003. Land-use and land-cover change, urban heat island phenomenon, and health implications: A remote sensing approach. Photogrammetric Engineering & Remote Sensing **69**:1053-1063.

Middle, A., K. Häb, A. J. Brazel, C. A. Martin, and S. Guhathakurta. 2014. Impact of urban form and design on mid-afternoon microclimates in Phoenix local climate zones. Landscape and Urban Planning **122**:16-28.

Myint, S. W., E. A. Wentz, A. J. Brazel, and D. A. Quattrochi. 2013. The impact of distinct anthropogenic and vegetation features on urban warming. Landscape Ecology **28**:959-978.

Oke, T. R. 1982. The energetic basis of the urban heat island. Quarterly Journal of the Royal Meteorological Society **108**:1-24.

Osborne, J. W., and A. Overbay. 2004. The power of outliers (and why researchers should ALWAYS check for them). Practical Assessment, Research and Evaluation **9** Available online: http://PAREonline.net/getvn.asp?v=9&n=6.

Oswald, E. M., R. B. Rood, K. Zhang, C. J. Gronlund, M. S. O'Neill, J. L. White-Newsome, S. J. Brines, and D. G. Brown. 2012. An investigation into the spatial variability of near-surface air temperatures in the Detroit, Michigan, Metropolitan region. Journal of Applied Meteorology and Climatology **51**:1290-1304.

Parris, K. M., and D. L. Hazell. 2005. Biotic effects of climate change in urban environments: The case of the grey-headed flying fox (*Pteropus poliocephalus*) in Melbourne, Australia. Biological Conservation **124**:267-276.

Potchter, O., P. Cohen, and A. Bitan. 2006. Climatic behavior of various urban parks during hot and humid summer in the Mediterranean city of Tel Aviv, Israel. International Journal of Climatology **26**:1695-1711.

Roth, M, T. R. Oke, and W. J. Emery. 1989. Satellite-derived urban heat islands from three coastal cities and the utilization of such data in urban climatology. International Journal of Remote Sensing **10**:1699-1720.

Santamouris, M. 2015. Analyzing the heat island magnitude and characteristics in one hundred Asian and Australian cities and regions. Science of the Total Environment **512**:582-598.

Schwarz, N., U. Schlink, U. Franck, and K. Großmann. 2012. Relationship of land surface and air temperatures and its implications for quantifying urban heat island indicators - An application for the city of Leipzig (Germany). Ecological Indicators **18**:693-704.

Shashua-Bar, I., and M. E. Hoffman. 2000. Vegetation as a climatic component in the design of an urban street: An empirical model for predicting the cooling effect of urban green areas with trees. Energy and Buildings **31**:221-235.

Shiflett, S. A., L. L. Liang, S. M. Crum, G. L. Feyisa, J. Wang, and G. D. Jenerette. 2017. Variation in the urban vegetation, surface temperature, air temperature nexus. Science of the Total Environment **579**:495-505.

Souch, C. A., and C. Souch. 1993. The effect of trees on summertime below canopy urban climates: A case study Bloomington, Indiana. Journal of Arboriculture **19**:303-312.

Stabler, L. B., C. A. Martin, and A. J. Brazel. 2005. Microclimates in a desert city were related to land use and vegetation index. Urban Forestry and Urban Greening **3**:137-147.

Stathopoulou, M., and C. Cartalis. 2007. Daytime urban heat islands from Landsat ETM+ and Corine land cover data: An application to major cities in Greece. Solar Energy **81**:358-368.

Steadman, R. G. 1979. The assessment of sultriness. Part I: A temperature-humidity index based on human physiology and clothing science. American Meteorological Society **18**:861-873.

Streiling, S., and A. Matzarakis. 2003. Influence of single and small clusters of trees on the bioclimate of a city: A case study. Journal of Arboriculture **29**:309-316.

Stone, B., and J. M. Norman. 2006. Land use planning and surface heat island formation: A parcel-based radiation flux approach. Atmospheric Environment **40**:3561-3573.

Taha, H. 1997. Urban climates and heat islands: Albedo, evapotranspiration, and anthropogenic heat. Energy and Buildings **25**:99-103.

Taleghani, M., D. Sailor, and G. A. Ban-Weiss. 2016. Micrometeorological simulations to predict the impacts of heat mitigation strategies on pedestrian thermal comfort in a Los Angeles neighborhood. Environmental Research Letters **11** doi:10.1088/1748-9326/11/2/024003.

Tonolla, D., V. Acuña, U. Uehlinger, T. Frank, and K. Tockner. 2010. Thermal heterogeneity in river floodplains. Ecosystems **13**:727-740.

Tayyebi, A., and G. D. Jenerette. 2016. Increases in the climate change adaptation effectiveness and availability of vegetation across a coastal to desert climate gradient in metropolitan Los Angeles, CA, USA. Science of the Total Environment **548**:60-71.

Unger, J., T. Gal, J. Rakonczai, L. Mucsi, J. Szatmári, Z. Tobak, B. van Leeuwen, and K. Fiala. 2009. Air temperature versus surface temperature in urban environment. The seventh International Conference on Urban Climate, Yokohama, Japan.

Vahmani, P., and G. A. Ban-Weiss. 2016. Climatic consequences of adopting drought-tolerant vegetation over Los Angeles as a response to California drought. Geophysical Research Letters **43**:8240-8249.

Vanos, J. K. 2015. Children's health and vulnerability in outdoor microclimates: A comprehensive review. Environment International **76**:1-15.

Vanos, J. K., A. Middle, G. R. Mckercher, E. R. Kuras, and B. L. Ruddell. 2016. Hot playgrounds and children's health: A multiscale analysis of surface temperatures in Arizona, USA. Landscape and Urban Planning **146**:29-42.

Voogt, J. A., and T. R. Oke. 2003. Thermal remote sensing of urban climates. Remote Sensing of the Environment **86**:370-384.

WMO, 2008. Guide to Meteorological Instruments and Methods of Observation, 7th ED. WMO-No. 8

Wong, G. K. L., and C. Y. Jim. 2015. Identifying keystone meteorological factors of green-roof stormwater retention to inform design and planning. Landscape and Urban Planning **143**:173-182.

Yang, F., S. S. Y. Lau, and F. Qian. 2011. Urban design to lower summertime outdoor temperatures: an empirical study on high-rise housing in Shanghai. Building and Environment **46**:769-785.

Zhao, L., X. Lee, R. B. Smith, and K. Oleson. 2014. Strong contributions of local background climate to urban heat islands. Nature **511**:216-219.

Table 3.1 Mean (±SD) for land surface temperature (LST) over 24-hr study period and air temperature (T_a), relative humidity (RH), and vapor pressure deficit (VPD) at two heights above the ground over a 17-day study period for five land covers

	LST (°C)	T_a (°C)	RH (%)	VPD (kPa)
Asphalt	39.24±13.92			
0.1 m		31.81±8.32	36.08±21.64	3.75±2.62
1.5 m		30.10±7.59	40.09±22.38	2.53±1.66
Bare surface	31.98±13.70			
0.1 m		30.92±9.17	38.02±23.98	3.64±2.77
1.5 m		29.25±7.53	41.75±23.25	2.48±1.66
Grass	22.31±7.74			
0.1 m		26.27±7.89	68.06±22.86	1.53±1.42
1.5 m		28.48±7.25	46.49±23.96	2.30±1.62
Short trees	25.33±8.88			
0.1 m		26.46±5.83	53.75±20.37	1.91±1.39
1.5 m		27.94±6.80	46.33±22.18	2.30±1.60
Tall trees	24.39±6.96			
0.1 m		27.13±6.15	49.74±21.46	2.18±1.57
1.5 m		28.10±6.91	46.19±22.28	2.31±1.62

Table 3.2 Linear regression statistics between air temperature at two heights above ground level and land surface temperature for five land covers. P<0.001 for all regressions.

	R^2	F-value	Slope	Intercept
Asphalt				
0.1 m	0.97	618.56	0.59	5.79
1.5 m	0.96	539.08	0.53	6.11
Bare surface				
0.1 m	0.94	339.00	0.63	8.63
1.5 m	0.92	267.61	0.49	11.09
Grass				
0.1 m	0.93	294.12	1.08	0.48
1.5 m	0.84	118.80	0.88	7.81
Short trees				
0.1 m	0.92	257.54	0.61	8.36
1.5 m	0.94	325.07	0.72	6.21
Tall trees				
0.1 m	0.92	244.83	0.74	5.51
1.5 m	0.96	487.16	0.89	2.70

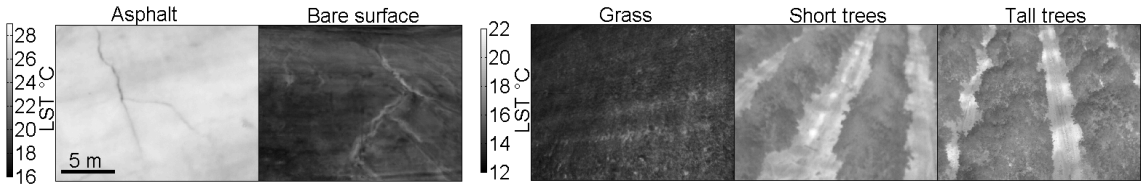

Figure 3.1 Representative infrared images from asphalt, bare surface, grass, short tree, and tall tree land covers at midnight used to assess land surface temperature (LST) relationships.

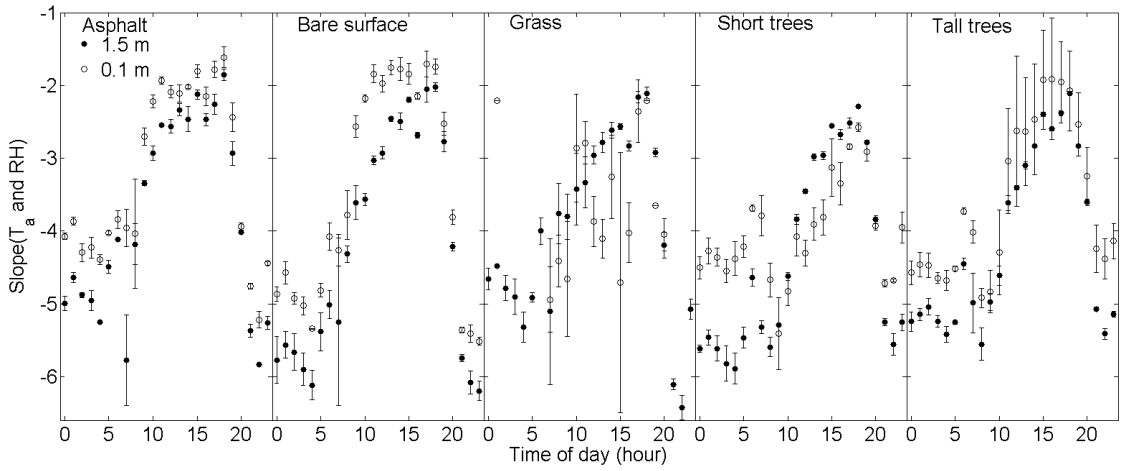

Figure 3.2 Daily changes in slope of air temperature (T_a) and relative humidity (RH) at 1.5 and 0.1 m over five land cover types (±SD) were stronger during the night than the day, with weaker relationships at 0.1 m. Each data point corresponds to the slope of the linear regression between mean T_a and RH ($P<0.05$) calculated hourly (n=17 per hour).

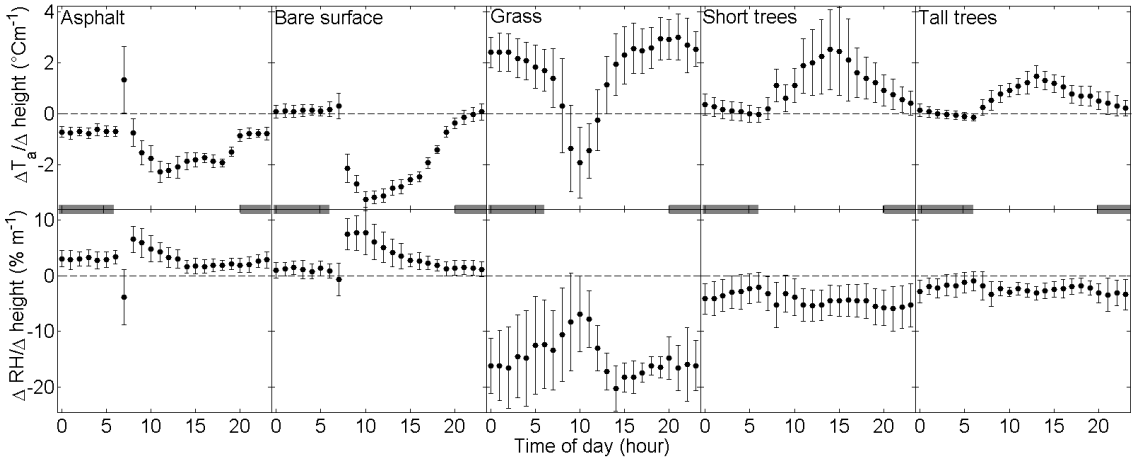

Figure 3.3 Divergent daily changes in air temperature lapse rate (ΔT_a / Δsensor height, ±SD) over five land cover types varied from decreasing daytime lapse rates to increasing daytime lapse rates. Relative humidity lapse rate (ΔRH / Δsensor height, ±SD) over five land cover types varied from positive lapse rates (asphalt and bare surface) to negative lapse rates (grass, and short and tall trees) with little daily trends. Gray bars indicate approximate nighttime hours after sunset and before sunrise.

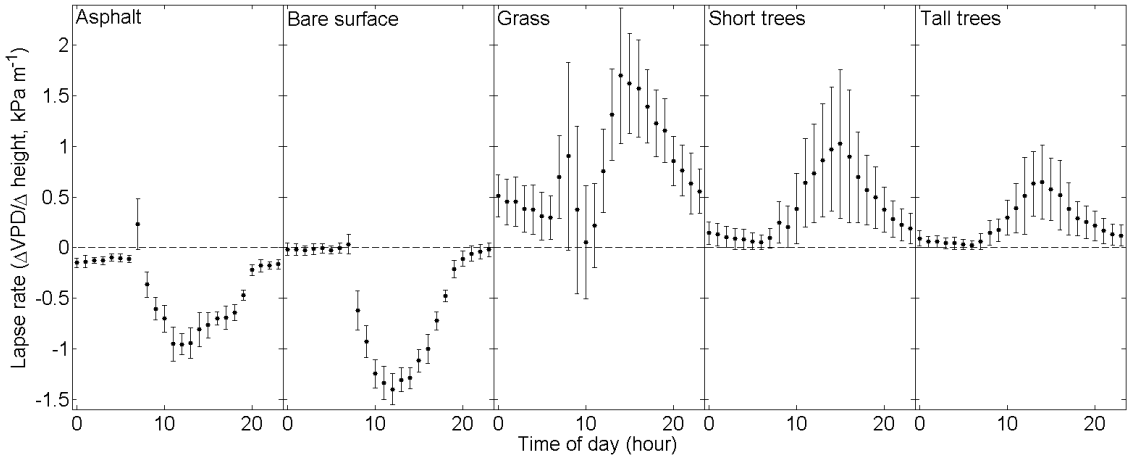

Firgure 3.4 Divergent daily changes in vapor pressure deficit lapse rate (ΔVPD/ Δsensor height, ±SD) over five land cover types varied from decreasing daytime lapse rates (asphalt and bare surface) to increasing daytime lapse rates (grass, and short and tall trees). Land cover effects on lapse rate were significant ($F=2141.24$, $P<0.001$) in a one-way ANOVA.

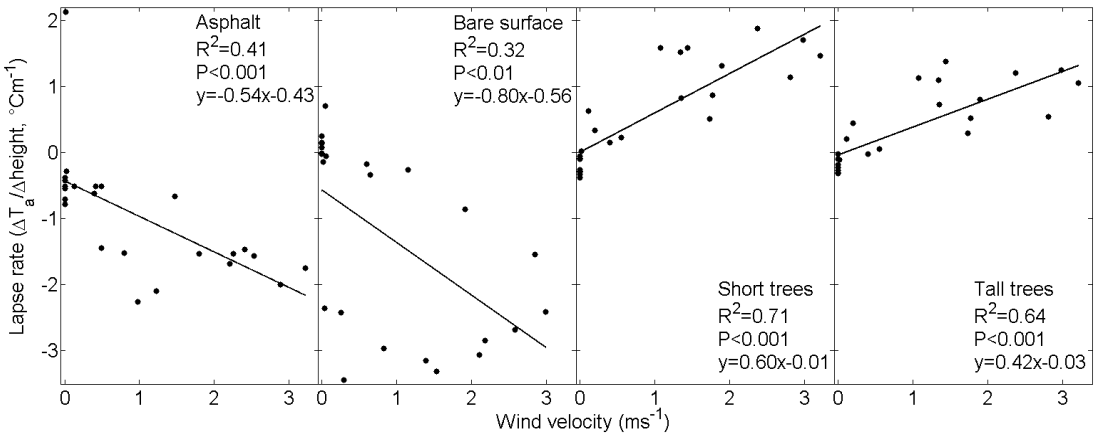

Figure 3.5 Air temperature lapse rate (ΔT_a / Δsensor height) is negatively correlated to wind velocity for asphalt (R^2=0.41, P<0.001) and bare surface (R^2=0.32, P<0.01) land cover types, and positively related to wind velocity in short (R^2=0.71, P<0.001) and tall (R^2=0.64, P<0.001) tree land covers. There was not a significant relationship (P>0.05) for grass cover. Wind velocity was measured for a 24 hr period at each land cover (n=24).

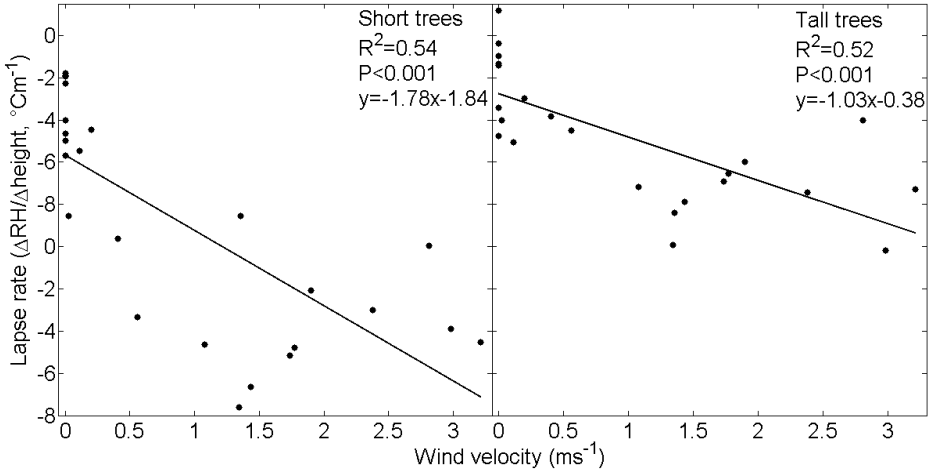

Figure 3.6 Relative humidity lapse rate (ΔRH / Δsensor height) is negatively correlated to wind velocity for short (R^2=0.54, P<0.001) and tall (R^2=0.52, P<0.001) tree land covers. There were no significant relationships (P>0.05) for asphalt, bare surface, and grass covers. Wind velocity was measured for a 24 hr period at each land cover (n=24).

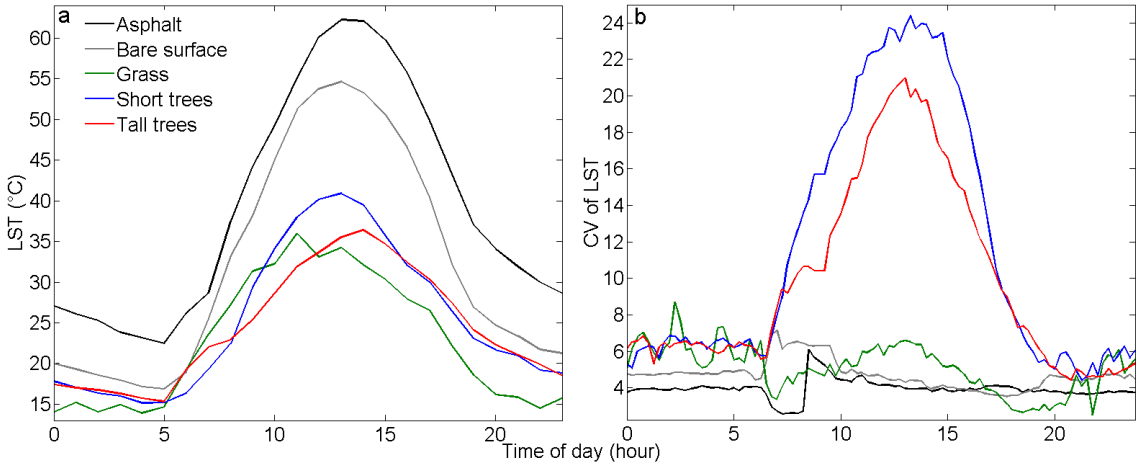

Figure 3.7 (a) Land surface temperature (LST) varied between land cover types, with the highest range in temperatures during mid-day. (b) Spatial coefficient of variation of land surface temperature (CV of LST) increased during the day for short and tall tree land covers, with relatively consistent levels for asphalt, bare surface, and grass land cover types.

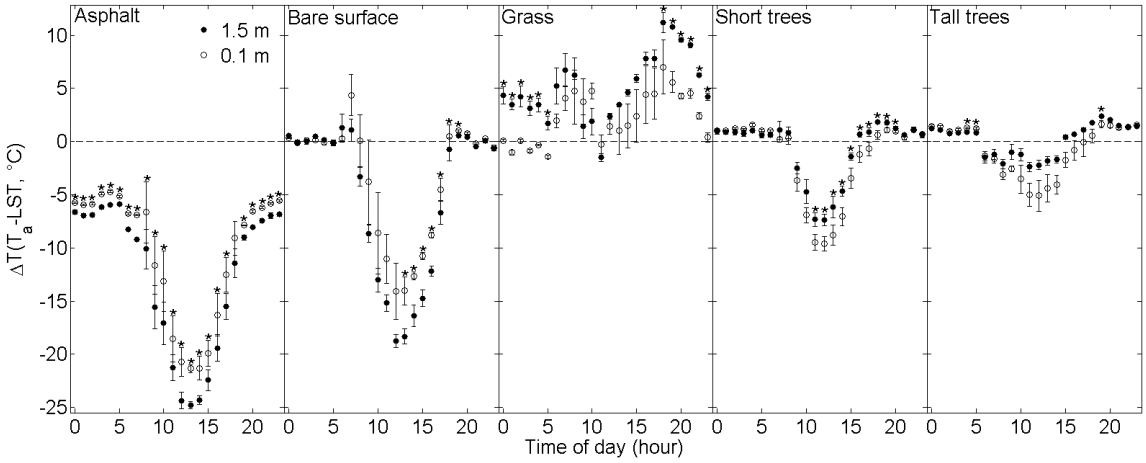

Figure 3.8 Daily changes in the difference between air and land surface temperature (ΔT, T_a-LST) at 1.5 and 0.1 m over five land cover types (±SD) show different relationships among land cover types. While asphalt and bare surfaces have the greatest ΔT at 1.5 m during the day, grass, and short and tall tree land covers have the greatest ΔT at 0.1 m. Each data point corresponds to the average difference between mean T_a and LST calculated hourly for one day. The asterisk denotes significant differences ($P<0.05$) between 1.5 and 0.1 m ΔT values using a paired Student's *t*-test.

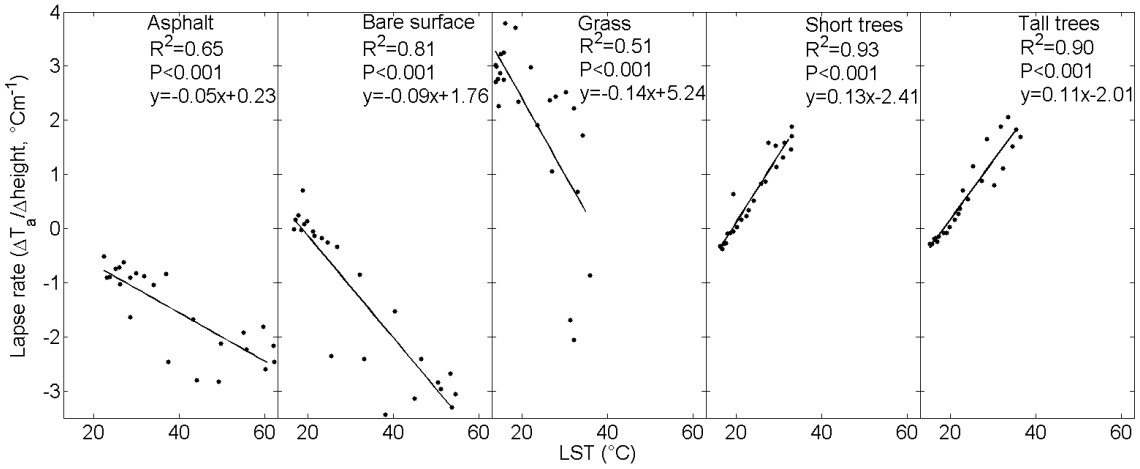

Figure 3.9 Air temperature lapse rate (ΔT_a / Δsensor height) is negatively related to land surface temperature (LST) for asphalt (R^2=0.65, P<0.001), bare surface (R^2=0.81, P<0.001), and grass (R^2=0.51, P<0.001) land cover types, and positively related to LST in short (R^2=0.93, P<0.001) and tall (R^2=0.90, P<0.001) tree land cover. LST was measured for a 24-hr period at each land cover (n=24).

Conclusions

The research presented in this dissertation found land use, land cover, vegetation composition and climate to be directly linked to biogeochemical cycles and microenvironmental conditions. At fine-scales I found R_s, an important measure of ecosystem functioning, was regulated by land use and seasonally specific organismal responses to microenvironmental conditions including temperature, moisture, and substrate levels. While at regional-scales, landscape position strongly regulated R_s. Bridging fine and regional-scale drivers of ecosystem functioning I found that heterogeneity in urban land cover drove patterns in vegetation cooling. Using a multi-scale approach this dissertation explored the effects of interactive global change drivers on urban ecosystem processes.

In chapter 1 I found, from a combination of observational surveys and manipulative experiments, variation in physiological drivers linked to meter- and regional-scale patterns of R_s. I further found R_s responded non-linearly to changes in drivers, which resulted in higher variability when conditions in general reduced rates. The importance of soil moisture and substrate levels was magnified in water and substrate limited environments. In resource scarce environments the greater relative importance of biogeochemical hot spots may have created greater resource discontinuity and spatial variation in R_s. Ecosystems with the highest responses to water and substrate additions also had the greatest spatial variability in surveyed R_s. Fine-scale spatial variation in soil physiological drivers did not correlate with variation or absolute levels of R_s. Instead,

sites with mean VWC and SOM high enough to be on the flat part of physiological saturating response functions had less variable R_s, regardless of microsite variation in these drivers. In contrast, when soil water and substrates are low enough to fall within the dynamic ranges of the response functions, then microsite differences become important in determining R_s. In these conditions, small changes in soil moisture and substrate levels may have large consequences on the sensitivity of R_s to other physiological drivers. This evidence supports the hypothesis that R_s spatial variability is a consequence of limitations in soil moisture or substrate supply (Xu and Qi 2001). This systematic evaluation of physiological and landscape variation provides a key framework for understanding the effects of interactive global change drivers of land use and climate to ecosystem metabolism.

In chapter 2 I found, from an extensive observational network of microclimate sensors imbedded in urban environments, the greatest vegetation T_a cooling effects in the evening hours and in warmer cities. Additionally, vegetation cooling effects resulted in more daily and seasonal variation in high-vegetated areas which had a broader range of temperatures. Potentially offsetting cooling benefits, vegetation also increased RH and HI, although these effects were limited. Furthermore, in the coastal city hotter days were correlated with increases in spatial variation in T_a, supporting a $\overline{T}_a$ -T_a variability hypothesis, while in inland and desert cities spatial variation was likely regulated by wind velocity. Nighttime spatial variation in microclimate also differed among cities. In the inland city, hotter nights were associated with increases in spatial variation in T_a, exacerbating inequities in urban temperatures and potentially human heat-risks (Vargo et

al. 2016). Together these findings show that urban vegetation had consistent microclimate atmospheric cooling effects that primarily occur during the evening and are influenced by mesoclimate distributions and meteorological conditions.

In chapter 3 I evaluated vertical micro-scale atmospheric profiles and explicitly connected these to remotely sensed LST. I found land surface characteristics, from relatively simple bare surfaces to complex shading from trees, differ in their microclimate distributions and interactions. These findings empirically show that vertical variation can be as large as the differences between land covers as predicted from modeling studies (Taleghani et al. 2016). The large variation among land cover types in their vertical microclimate distributions is coupled to surface characteristics and is influenced by larger scale meteorological variation. My findings help develop better assessments of urban heat risk that consider both surface and air characteristics. With the rapidly expanding use of surface temperature measurements to assess heat vulnerability (Jenerette et al. 2016), my results show how remotely sensed temperature is connected to T_a through land cover specific vertical functions.

This dissertation explored the effects of interactive global change drivers of climate and land cover on urban ecosystem processes. The research I presented in chapter 1 is important for improving biogeochemical models used at regional scales that increasingly rely on complex soil microbial and biophysical schemes (Zhang et al. 2012, Zhang et al. 2014). Furthermore, the research I presented in chapters 2 and 3 may be incorporated into policy assessments of heat vulnerabilities and mitigation strategies that

currently do not factor meteorological drivers of vegetation cooling, vertical T_a variation, and T_a-LST discrepancies (Georgescu et al. 2014, Vahmani and Ban-Weiss 2016).

Literature cited

Georgescu, M., P. E. Morefield, B. G. Bierwagen, and C. P. Weaver. 2014. Urban adaptation can roll back warming of emerging megapolitan regions. Proceedings of the National Academy of Sciences U. S. A. **111**:2909-2914.

Jenerette, G. D., S. L. Harlan, A. Buyantuev, W. L. Stefanov, J. Declet-Barreto, B. L. Ruddell, S. W. Myint, S. Kaplan, and X. Li. 2016. Micro-scale urban surface temperatures are related to land-cover features and residential heat related health impacts in Phoenix, AZ USA. Landscape Ecology **31**:745-760.

Taleghani, M., D. Sailor, and G. A. Ban-Weiss. 2016. Micrometeorological simulations to predict the impacts of heat mitigation stratagies on pedestrian thermal comfort in a Los Angeles neighborhood. Environemntal Research Letters doi:10.1088/1748-9326/11/2/024003.

Vahmani, P., and G. A. Ban-Weiss. 2016. Climatic consequences of adopting drought-tolerant vegetation over Los Angeles as a response to California drought. Geophysical Research Letters **43**:8240-8249.

Vargo, J., B. Stone, D. Habeeb, P. Liu, and A. Russell. 2016. The social and spatial distribution of temperature-related health impacts from urban heat island reduction policies. Environmental Science & Policy **66**:366-374.

Xu, M., and Y. Qi. 2001. Soil-surface CO_2 efflux and its spatial and temporal variations in a young ponderosa pine plantation in northern California. Global Change Biology **7**:667-677.

Zhang, C., H. Tian, G. Chen, A. Chappelka, X. Xu, W. Ren, D. Hui, M. Lui, C. Lu, S. Pan, and G. Lockaby. 2012. Impacts of urbanization on carbon balance in terrestrial ecosystems of the Southern United States. Environmental Pollution **164**:89-101.

Zhang, X., G. Niu, A. S. Elshall, M. Ye, G. A. Barron-Gafford, and M. Pavo-Zuckerman. 2014. Assessing five evolving mirobial enzyme models against field measurements from a semiarid savannah—What are the mechanisms of soil respiration pulses? Geophysical Research Letters **41**:6428-6434.